12-17-2004

Mechanistic Study of Pollutant Degradation

Weixi Zheng
University of New Orleans

MECHANISTIC STUDY OF POLLUTANT DEGRADATION

A Dissertation

Submitted to the Graduate Faculty of the
University of New Orleans
in partial fulfillment of the
requirements for the degree of

Doctor of Philosophy
in
The Department of Chemsitry

by

Weixi Zheng

B.S. Beijing Normal University, 1995
M.S. Chinese Academy of Sciences, 1998

December 2004

To my parents, for their love and support

Acknowledgments

I would like to express my gratitude to my adviser, Professor Matthew A. Tarr. He guided me through my five years of work. Many thanks for his patience, confidence and the opportunity he offered for me to gain professional experience and maturity.

I would like to thank my committee members Professor Richard B. Cole, Professor Ronald F. Evilia, Professor Steven W. Rick and Professor Zeev Rosenzweig. They gave me suggestions and fresh ideas in many valuable discussions.

I would also like to thank Corinne Gibb for her great help in my NMR work. She made a great effort to make all my intended measurements possible.

I must thank all my coworkers and friends for sharing their knowledge and experience with me. Not only did I learn a lot from them but I found my work much easier with their help.

Last, but not the least, I would like to thank my husband, Hongbo Ding, who gives me love and support all the time.

Table of Contents

Abstract vi
Chapter 1. Introduction 1
1.1 Environmental pollution and certain pollutants 1
1.2 Environmental remediation methods 4
1.3 Fenton and sonochemical degradation 7
1.4 Purpose of this study 11
1.5 References 11
Chapter 2. Modified Fenton degradation of some chemical warfare analogues and herbicides 17
2.1 Introduction 17
2.1.1 Fenton Chemistry 18
2.1.2 Cyclodextrin 19
2.2 Experimental 23
2.3 Results and discussion 24
2.4 References 28
Chapter 3. Investigation of ternary complexes of iron, carboxymethyl-β-cyclodextrin and hydrophobic pollutants in Fenton degradation system 31
3.1 Introduction 31
3.1.1 Continuous variation method— measuring binding stoichiometry 32
3.1.2 NMR titration – measuring binding constant 32
3.1.3 Fluorescence quenching 34
3.1.4 NMR measurements in the presence of paramagnetic species 36
3.1.5 Fluorescence resonance energy transfer (FRET) 37
3.2 Experimental 39
3.2.1 Temptation in preparation of crystal of βCD with iron ions, and βCD with both iron ions and hydrophobic compounds 39
3.2.2 UV, fluorescence and NMR measurements 39
3.3 Results and discussion 41
3.3.1 Temptation to grow crystal of binary complexes: βCD-iron ions, and ternary complexes: βCD-iron ions-hydrophobic compounds 41
3.3.2 Binding stoichiometry between Fe^{2+} and CMCD 43
3.3.3 Fluorescence quenching of anthracene and 2-naphthol by Fe^{2+}, Br^- and Eu^{3+} 45
3.3.3.1 Different quenching effect of Fe^{2+} and Br^- 45
3.3.3.2 pH effect 49
3.3.3.3 Fluorescence quenching by Eu^{3+} 51
3.3.4 Ca^{2+} and Cd^{2+} substitution of Fe^{2+} in fluorescence quenching experiment 52
3.3.5 NMR study of interactions among 2-naphthol, CMCD and Fe^{2+} 54

3.3.5.1 NMR measurement of binding constant between 2-naphthol and CMCD 54
3.3.5.2 NMR spectra in the presence of Fe^{2+} 57
3.3.5.3 Cd^{2+} and Ca^{2+} substitution of Fe^{2+} in NMR measurement 60
3.3.5.4 2D NMR ─ NOESY and ROESY experiments 62
3.3.6 Intended FRET experiment 64
3.3.7 More discussion on degradation results observed in Chapter 2 65
3.4 References 68
Chapter 4. Assessment of ternary complexes of iron, hydrophobic pollutants and several other cyclodextrins in aqueous solution 70
4.1 Introduction 70
4.2 Experimental 71
4.3 Results and discussion 72
4.3.1 Hydroxypropyl-β-cyclodextrin 72
4.3.2 Sulfated-β-cyclodextrin 77
4.3.3 β-cyclodextrin 79
4.3.4 α-cyclodextrin 83
4.4 References 85
Chapter 5. Enhancement of sonochemical degradation of phenol using hydrogen atom scavengers 87
5.1 Introduction 87
5.1.1 Cavitation phenomenon 88
5.1.2 Chemical processes in transient cavitation 90
5.1.3 Some effects that influence the cavitaion and chemical processes 90
5.1.4 Drawback and possible improvement of the method in application of pollutant degradation 91
5.2 Experimental 93
5.3 Results and discussion 95
5.3.1 Phenol degradation in the presence and absence of CCl_4 95
5.3.2 Measurement of H_2O_2 produced in the sonolysis process 99
5.3.3 Phenol degradation in the presence of perfluorohexane 101
5.3.4 Phenol degradation in the presence of iodate 103
5.4 References 104
Conclusions 106
Vita 108

Abstract

Environmental pollution has been a serious concern worldwide. Many degradation methods have been developed to clean sites contaminated with pollutants. More knowledge and better understanding in this field will help to protect our environment. The goal of the research in this thesis is to gain a better understanding of the mechanism of organic pollutant degradation in Fenton reactions and sonochemical reactions.

Fenton degradation uses hydroxyl radical to oxidize organic compounds. The radical is produced by catalytic decomposition of hydrogen peroxide with Fe(II). Further research has found that addition of cyclodextrins can enhance degradation efficiency of hydrophobic organic pollutants. To study the mechanism of the enhancement, pollutant-cyclodextrin-Fe(II) aqueous systems were studied by fluorescence and NMR techniques. The results indicated the formation of pollutant/carboxymethyl-β-cyclodextrin/Fe(II) ternary complexes in the solution. With the ternary complex, the catalyst Fe(II) becomes closer to the pollutant, therefore leading to more efficient hydroxyl radical attack on the pollutant. Additional studies showed that hydropropyl-β-cyclodextrin, β-cyclodextrin and α-cyclodextrin bound pollutant well, but bound Fe(II) poorly. Sulfated-β-cyclodextrin did not bind well with pollutant although it bound Fe(II) well.

Sonochemical degradation is another important pollutant treatment method in practice. It was found that phenol sonolysis can be enhanced by volatile hydrogen atom scavengers such as carbon tetrachloride and perfluorohexane. The non-volatile hydrogen atom scavenger iodate did not enhance phenol degradation. The first order rate constant for aqueous phenol degradation increased by about 2.2-2.8 times in the presence of 150 μM carbon tetrachloride. In the presence

of less than 1.5 μM perfluorohexane the first order rate constant increased by about 2.3 times. Hydroquinone was the major observed reaction intermediate both in the presence and absence of hydrogen atom scavengers. Hydroquinone yields were substantially higher in the presence of hydrogen atom scavengers, suggesting that hydroxyl radical pathways for phenol degradation were enhanced by the hydrogen atom scavengers.

The additives investigated in this study have potential to improve pollutant degradation efficiency. Other fields may also benefit from the information gained in this study. For example the improvement could be achieved in synthetic processes that rely on hydroxyl radical as a key intermediate.

Chapter 1. Introduction

1.1 Environmental pollution and certain pollutants

Modern technology has greatly changed our way of life, and unfortunately also our environment for the worth. Many serious environmental problems have emerged such as the greenhouse effect, depletion of ozone layer, acid rain, rapid shrinking of clean drinking water sources… the facts are shocking. The worst result of deterioration of the environment could be the extinction of living species in this planet including human beings. It was found that a lot of environmental damages were caused by improper use or release of chemicals. While we enjoy the benefits of modern science and technology ranging from the important development of new medicines to the convenience of detergents for dish washing, we also expose ourselves and our environment to possibly dangerous chemical pollution.

Both inorganic and organic chemicals can cause severe damage to people and the environment. The inorganic pollutants mainly include heavy metals as well as their complexes, and small molecules such as carbon monoxide, sulfur dioxide, nitrogen dioxide, etc. Carbon dioxide was not considered as a pollutant decades ago, but now it is a major contribution to the greenhouse effect. The known organic contaminants have exceeded 20,000 species.[1] PAHs (polycyclic aromatic hydrocarbons) are among these chemicals. They have serious environment pollution and carcinogenic potential and they are also major pollutant examples used in this research.

PAHs are a family of more than 200 structurally similar compounds. Some examples of PAHs are shown in Figure 1.1.

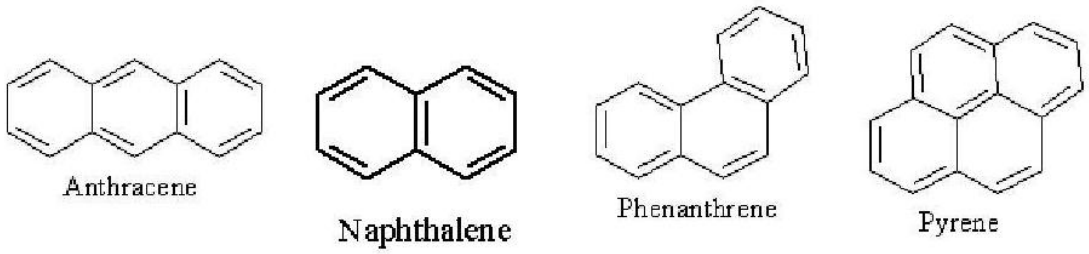

Figure 1.1 Molecular structures of anthracene, naphthalene, phenanthrene and pyrene.

PAHs are produced generally from heating or burning of organic materials. Some natural processes such as forest fires, eruption of volcanoes and biosynthesis by certain species of bacteria are also sources of PAHs.[2] Since the energy for industrial processes and everyday life comes largely from combustion of organic fuel such as coal and petroleum, we produce a great amount of PAHs. It was found that 36% of total PAH emission in America came from automobiles. Residential heating contributed about 12% and power generation 7% in the 1980's.[3] From the survey by Bjorseth and Ramdahl in 1985,[4] it was estimated that the largest industrial PAH releasers were aluminum producers. About 235g of PAH can be released for each ton of aluminum. Iron works, ferroalloy and carbon black industries were all among the major PAHs polluters.

The first correlation between PAHs and cancer was proposed in 1775 by Pott who attributed the formation of malignant human tumors to a long time contact with carbon soot.[5] In 1930, Kennaway found that tumors could be induced in mouse skin by dibenz[a,h]anthracene, a member of the PAH family.[6] Three years later, Cook and co-workers established the relationship between PAH and cancer with isolation of the

carcinogen benzo[a]pyrene from coal tar extract.[7] From then on, a great amount of effort has been devoted to investigate the PAH-cancer linkage and the mechanisms of PAHs carcinogenicity.

The practical use of PAHs is rather limited. Only several species are used in the dye, photoconductor and semiconductor industries. Once released into atmosphere, water systems or lands, some species of PAHs can be absorbed by plants and even animals. It was shown that grain samples from industrial areas contained higher PAH levels than those from nonindustrial areas.[8] The food, therefore, was contaminated. Due to their extensive conjugation structure, PAHs are photochemically reactive in soils and water suspension, which sugguests they are able to be photodegraded in nature.[9] Several low weight PAHs were also reported to be oxidized by soil and marine bacteria.[10-12]

Apart from PAHs, phenol (monohydroxyl benzene) was also used as an example pollutant in this study. The phenolic group of compounds contains species that have one or more hydroxyl groups attached to an aromatic ring. Phenol is largely used in modern industry. The most important commercial usage is its condensation with formaldehyde to produce phenolic resins.[13] Except for the great amount produced by human beings, phenol could also be formed in random reactions in nature or from biosynthesis. It is known that phenol can be absorbed readily by people or animals through digestion, respiratory passage and skin. If exposed to the lethal concentration of phenol, people can have symptoms such as muscle weakness, convulsion and coma.[13] Although a clear connection between phenol and cancer is not available right now, researchers did find that phenol can promote tumor activity when large concentrations of its solution was

painted on the skin of certain kinds of mice.[13] Therefore, both phenol and PAHs are listed as priority pollutants.

1.2 Environmental remediation methods [14]

Knowing that we have produced and released a large amount of health hazards to the environment, people are now making big efforts to clean them up and develop new technologies to prevent or reduce further pollution. The widely used remediation methods are biodegradation and chemical degradation. Biodegradation depends on bacteria to decompose organic compounds, while chemical degradation applies physical and chemical processes to remove or destroy inorganic and organic pollutants. Biodegradation is usually more selective and less expensive. However, the bacteria are sensitive to the ambient conditions and the transformation rate is relatively low. Chemical degradation, on the other hand, is less selective but faster. It can treat highly and multiply contaminated systems while requiring no strict ambient conditions. The energy and labor are consumed more in chemical methods, so the cost is generally greater. Nevertheless, both methods are successful in cleaning up the pollutions under appropriate conditions.

To date more than ten chemical degradation methods have been developed using various kinds of oxidation-reduction processes, many of which involve different energy sources. These methods include photon assisted degradations, electrochemical degradations, electron beam radiation degradation, supercritical water degradation, enzyme degradation, sonochemical degradation and direct redox degradations by addition of redox reagents. The main oxidizing reagents involved in these methods are ozone, oxygen and hydrogen peroxide. These reagents, and sometimes water, can produce highly

reactive radicals such as hydroxyl radical and $^1O_2$ under proper conditions. The main reducing reagents involved are electrons or zero valent metals such as iron. These species can be introduced by addition or by in situ reactions.

In photon assisted degradations, UV radiation is used as an energy source to directly decompose ozone, hydrogen peroxide or through a photosensitizer to degrade oxygen or water to create reactive radicals. UV radiation itself sometimes can be used to directly photolyze pollutants. Combinations between the UV and oxidizing reagents are flexible. This kind of method is very suitable for water and air treatment and some have already been extensively used in water treatment plants.

Electrochemical degradation uses electrode reactions to directly electrolyze pollutants or to produce reactive species such as ozone or hydrogen peroxide that will further react with pollutants. This method is also used for the phase separation that is required for the treatment of wastewaters containing colloidal particles or heavy metals. It has a versatile ability to deal with solid, liquid or gaseous pollutants, but the cost is relatively high.

Electron beam radiation degradation is a method that uses electron beam obtained from an accelerator to produce reactive species — hydroxyl radical, aqueous electrons, hydrogen atoms and others from water. This method is particularly suitable for flowing stream treatment because it can continuously produce reactive species, and the degradation processes with the reactive species are very fast.

Supercritical water degradation uses supercritical water as a medium to oxidize organic pollutants. When water transfers to supercritical condition under high temperature (647 K) and pressure (218 atm), the viscosity of water decreased to a gas-

like value and the solubility of organic compounds increased. These properties allow the contact of organic pollutants with oxygen in one phase where the oxidation reactions take place. This method is ideal for degradation of aqueous hazards. With a high degradation efficiency (> 99.99%), the process produces relatively environmentally tolerable products: water and carbon dioxide.

Enzyme degradation is a recently developed technique. Different from biodegradation, this method employs enzymes instead of living bacteria to degrade organic pollutants. It inherits the high selectivity of biodegradation while avoids certain rate-limiting factors in biodegradation. The cell-free enzyme is easier to handle and store. The operation conditions are mild. Sometimes, even species that may resist biodegradation or chemical degradation can be degraded by enzyme reactions. Despite the above, the method has not been applied on a large scale. The availability of enzymes is limited and the cost is rather high. Sometimes an enzyme loses its activity in a system that has relatively extreme conditions or interfering species. In some cases, the final product can be even more toxic.

Sonochemical degradation uses ultrasonic irradiation to introduce extreme physical conditions (3000-5000 K, 500-10000 atm in a small spatial range) and reactive species to the system. No redox reagents need to be added. It sometimes offers alternative reaction pathways which may be faster and environmentally safer due to the unique character of sonochemical processes. This method is mainly applied to aqueous systems.

There are several different degradation systems in direct redox methods. Fenton degradation is one of them. In this technique, hydrogen peroxide is used to produce hydroxyl radicals under the catalysis of iron ion. Another method uses solvated electrons

to reduce pollutants. The electrons are produced by interaction of metals (group I or II) with liquid ammonia. A third method uses zero valent metals such as iron to reduce organic and inorganic contaminants. While the first method is good for both water and soil treatment, the second one is good for soil treatment and the third one for water treatment.

Each of these methods, with its advantages and disadvantages, is suitable for degrading pollutants under certain conditions. New technology tends to combine two or more of the above methods to clean up complicated contaminations and make the degradation more efficient.

1.3 Fenton and sonochemical degradation

Among all the techniques introduced above, Fenton and sonochemical degradations were selected as two focuses in this study.

Fenton reaction was first reported by Fenton in 1876.[15] He obtained a colored product by mixing tartaric acid with hydrogen peroxide and a low concentration of a ferrous salt. In 1932-1934, Harber and Weiss[16] proposed free hydroxyl radicals in the decomposition of H_2O_2 catalyzed by iron salts. Around 1950, Baxendale and colleagues suggested that superoxide reduces Fe(III) formed on reaction, explaining the catalytic role of iron in the reaction.[17] After that, many other transition metal ions in their lower oxidation states (e.g. Cu(I), Co(II)) were found to have a similar catalytic effect as Fe(II) in decomposing H_2O_2. The reactions of these metal ions or complexes with H_2O_2 are called "Fenton-like" reactions.[18-21] Apart from hydroxyl radical, Fe(IV) was proposed as an alternative intermediate in Fenton reaction.[22] The debate between the two mechanisms

continued to today.[23-30] The most study on this subject favored the opinion of hydroxyl radical mechanism.

Hydroxyl radical is not selective in reacting with organic compounds. This makes Fenton reaction very useful in pollutant degradation. Great efforts have been devoted into the study of application of the method to environmental remediation. Sato C. et al. used the method to decompose perchloroethylene (PCE) and polychlorinated biphenyls (PCB) that are absorbed on sand.[31] Koyama O. et al. studied the degradation of chlorinated aromatics by Fenton oxidation in digester sludge.[32] Li Z.M. and colleagues evaluated the feasibility of Fenton reaction in remediation of TNT contaminated water, soil and water-soil slurries.[33] Fenton degradation of inorganic pollutants such as cyanides was investigated by Aronstein B.N. and colleagues.[34] There are many more research in this field other than the examples listed above. In these studies, the degradation conditions (e.g. pH, temperature, the initial concentration of Fe(II) and H_2O_2) and kinetics and products of the reactions were investigated. The results offered very useful information for real applications.

In Fenton degradation, the matrix of the system plays an important role in the chemical processes occurring. The matrix effects have been widely studied too. Lindsey M.E. and Tarr M.A. found that the dissolved natural organic matter (NOM) could inhibit the hydroxyl radical reaction with aromatics.[35-36] They attributed the inhibition to the separated sites of hydroxyl radical production and appearance of aromatic compounds in the presence of NOM. Lipczynska-Kochany E. and colleagues found that some anions such as ClO_4^-, NO_3^-, SO_4^{2-} and Cl^- that existed in groundwater and surface waters could decrease the reaction rate of 4-chlorophenol by Fenton reaction. They explained the

observation as a result of hydroxyl radical scavenging by those anions and slower oxidation rates of Fe(II)-anion complex.[37] Puppo A. reported an enhanced Fenton degradation which uses Fe(III)-EDTA as the catalyst by myricetin, quercetin, catechin, morin and kaempferol, members of flavoids (commonly found in plants).[38] The researcher drew the conclusion that the enhancement was due to the ability of flavoids to reduce Fe(III) to Fe(II). In another study conducted by Cheng I. and Breen K., it was found that flavenoids inhibit hydroxyl radical formation in the presence of adenosine triphosphate.[39] The conflicting results indicate that the individual effects of each species are interrelated, which makes the matrix effects complicated. The thorough study of the matrix effect for in situ application is important for efficient degradation.

Combining Fenton degradation with other degradation methods to enhance the degradation efficiency is a new research direction in pollutant remediation field. Photo-Fenton combination has been studied by many researchers.[40-44] In the method, Fe(III) is convert back to Fe(II) by absorbing a photon. At the same time, a hydroxyl radical is produced. Both processes increase the formation of hydroxyl radical, which in turn enhances the degradation efficiency. Electrochemical techniques are also used in association with Fenton reaction.[45-49] In this combination, H_2O_2 is produced in situ by reduction of O_2 at the cathode. At the anode, hydroxyl radical is generated by oxidation of water. Biodegradation has been operated with Fenton method too.[50-54] It was found that pretreatment with Fenton reaction makes biodegradation easier or faster in some cases. Combination of more than two methods is also under investigation.[45]

Based on the extensive studies, Fenton reaction has been widely used for in situ remediation of water system and soil system.[14]

Compared to Fenton degradation, sonochemical degradation is a relatively new technique employed in the environmental protection field. It has been investigated for the past decade on the laboratory scale. The attractiveness of sonochemical degradation lies in the facts that firstly, it triggers chemical processes without adding any chemical reagents; secondly, it is often conducted at ambient temperatures and pressures. However, the cost of the method is high and reactor design for the scale up applications has not been quite successful.[14]

Sonochemical degradation has been studied in decomposing chlorinated organic compounds, aromatic compounds, surfactants etc. Cheung H.M. et al. studied the sonolysis of methylene cloride, carbon tetrachloride, 1,1,1-trichloroethane and trichloroethylene.[55] They found that HCl was one of the major degradation products and calculated the first order rate constant of HCl formation. Petrier C. and Francony A. studied the effect of ultrasound frequencies on sono-degradation of tetrachloride and phenol.[56] They reported that under all the frequencies being used, carbon tetrachloride was always degraded faster than phenol. The degradation efficiency of carbon tetrachloride increased with the increase of frequency while that of phenol reaches maxim at 200 kHz. Hua I. and Hoffmann M.R. examined the kinetics and mechanism of sonolytic degradation of carbon tetrachloride.[57] They proposed a radical- reaction mechanism after thermolysis of the compound. Wheat P.E. and Tumeo evaluated the ability of ultrasonic radiation in degrading phenanthrene and biphenyl, two members of PAH.[58] They found that the extent of degradation is proportional to the sonicaiton time. Several intermediates were detected by GC/MS. They suggest that the method is promising in PAH remediation in tandem with other techniques. Laughrey Z. et al.

investigated the sonolytic decomposition of PAH in the presence of additional dissolved species.[59] They found that certain organic compounds including humic acid, benzoic acid, and sodium dodecyl sulfate could decrease degradation rate of PAH while dissolved oxygen could enhance the degradation. Destaillats et al. studied the sonolysis of nonionic surfactants, tert-octylphenoxypolyethoxyethanol and tert-octylphenol.[60] Their results showed that the concentration of the surfactant has a dramatic effect in degradation rate. When the initial concentration was above the critical micelle concentration (CMC), the rate constant became very small. They attribute the observation to the isolation effect of the micelle which separate the free surfactant monomer from being in the liquid-gas interface. By-products of the degradation were also identified in their study.

The combination of sonochemical technique with other degradation techniques such Fenton, photo, electro methods has also been conducted.[61-64] Other methods seem to benefit from sonication not only by the chemical processes it causes, but also by its physical processes which enhance the solubility of pollutants or catalysts and accelerate mass transfer. All these studies illustrate sonochemistry is promising in environmental remediation.

1.4 Purpose of this study

One of the important degradation pathways in both Fenton and sonochemical methods is hydroxyl radical oxidation. It is well known that hydroxyl radical is a very reactive species. The reaction rate constants of hydroxyl radical with organic substances is generally in the range of $10^7 - 10^9$ $M^{-1}S^{-1}$.[65] Therefore, a large amount of hydroxyl radicals are consumed by nontoxic materials which are the main composition of most

degradation systems. Recently, methods were found to improve the efficiency of hydroxyl radical's reaction with certain pollutants such as polycyclic aromatic hydrocarbons and phenol.[66-67] In the present study, the improved Fenton reaction has been extended to degrade other classes of pollutants. The mechanisms underlying the improved degradation efficiencies of both methods have been investigated. The knowledge obtained in the research enables a better understanding about the interactions among certain organic pollutants, degradation reagents and other species in the aqueous systems. The information can help to improve the efficiency of the degradation techniques and lower their costs as well. At the same time, this study also offers some insights to the fields where certain radicals or the geometry of different species are involved as the main issues.

1.5 References

1. Harrison, R.M., Ed. *Understanding Our Environment*, third edition, The Royal Society of Chemistry, 1999, p215.
2. Gelbion, H. V.; Paul O.P. TS'O, Ed. *Polycyclic Hydrocarbons and Cancer* Academic Press, New York, San Francisco, London, 1978, Vol. 1, 47-54.
3. Ivan Gutman and Sven J. Cyvin, *Introduction to the Theory of Benzenoid Hydrocarbons* Springer-Verlag, Berlin Heidelberg, New York, London, Paris, Tokyo, Hong Kong, 1989, p10.
4. Bjørseth, A. and Ramdahl, T., Ed. *Handbook of Polycyclic Aromatic Hydrocarbons* Marcel Decker, New York, 1985, p1.

5. Pott, P. in "Chirurgical Observations Relative to the Cataract, the Polypus of the Nose, the Cancer of the Scrotum, the Different Kinds of Ruptures, and the Mortification of the Toes and Feet", Hawes, L.; Clarke, W. and Collins, R.; London, p63.
6. Kubota, H.; Griest, W. H.; and Guerin, M.R. "Determination of carcinogens in tabacco smoke and coal-derived samples-trace polynuclear aromatic hydrocarbons." From "Trace Substances in Environmental Health-IX. A Symposium" Edited by Hemphill, D.D., 1975.
7. Freudenthal, R.I.; Lutz, G.A.; and Mitchell, R.I. "Carcinogenic Potential of Coal and Coal Conversion Products." A Battelle Energy Program Report, battelle Pacific Northwest Laboratories, Richland, Washington.
8. Grimmer, G.; and Hildebradt, A. *Chem. Ind.* 1967, 2000.
9. Fatiadi, A.J. *Environ. Sci. Technol.* 1967, 1, 570.
10. White, C.M.; and Newman, J.O.H. "Chromatographic and Spectrometric Investigation of a Light Oil Produced by the Symthoil Process" PERC/RI-76/3. Pittsburgh Energy Res. Cent., Pittsburgh, Pennsylvania, 1976.
11. Mazumdar, S.; Redmond, C.; Sollecito, W.; and Sussman, N. *J. air Pollut. Control Assoc.* 1975, 25, 382.
12. Reichert, J.; Kunte, H.; Engelhardt, K.; and Borneff, J. *Arch. Hyg. Bakteriol*. 1971, 155, 18.
13. *Summary Review of the Health Effects Associated with Phenol,* Research and Development, EPA/600/8-86/003 F, Jan. 1986, p1-6.

14. Tarr, M. A., Ed. *Chemical Degradation Methods for Wastes and Pollutants*, Marcel Dekker, New York, 2003.

15. Fenton HJH. *Chem. News* 1876, 33, 190.

16. Haber, F. and Weiss, J.J. *Proc. R. Soc. London [Biol.]* 1934, A147, 332-351.

17 Wardman, P. and Candeias, L.P. *Radiat. Res.* 1996,145, 523-531.

18. Zapski, G.; Samuni, A. and Meisel, D. *J. Phys. Chem.* 1971, 75, 3271-3280.

19. Davies, G.G.; Sutin, N.; Kay, O. and Walkins, O. *J. Am. Chem. Soc.* 1970, 92, 1892-1897.

20. Heckman, R.A. and Espenson, J.A. *Inorg. Chem.* 1979, 18, 38-43.

21. Pecht, I. and Anbar, M. *J. Chem. Soc.*1968, 1902-1904.

22. Bray, W.C. and Gorin, M.H. *J. Am. Chem. Soc.* 1934, 54, 2124-2125.

23 Shen, X.; Tian, J.; Li, J.; Li, X. and Chen, Y. *Free Radical Biology & Medicine* 1992, 13, 585-592.

24. Burkitt, M.J. *Free Rad. Res. Comms*. 2001, 18, 43-57.

25. Lloyd, R.V.; Hanna, P.M. and Mason, R.P. *Free Radical Biology & Medicine* 1997, 22, 885-888.

26. Pignatello, J.J.; Liu, D. and Huston, P. Environ. Sci. Technol. 1999, 33, 1832-1839.

27. Croft, S.; Gilbert, B.C.; Lindsay Smith, J.R. and Whitwood, A.C. *Free Rad. Res. Comms*.1992, 17, 21-39.

28. Pogozelski, W.K.; NcNeese T.J. and Tullius, T.D. *J. Am. Chem. Soc*. 1995, 117, 6428-6433.

29. Arasasingham, R.D.; Cornman, C.R. and Balch, A.L. *J. Am. Chem. Soc*. 1989, 111, 7800-7805.

30. Maskos, Z.; Rush, J.D. and Koppenol, W.H. *Free Radical Biol. Med*. 1990, 8, 153-162.

31. Sato, C.; Leung, S.W.; Bell, H.; Burkett, W.A. and Watt, R.J. *Emerging Technologies in Hazardous Waste Management III* ACS Symposium series, American Chemical Society, Washington, DC 1993, 343-355.

32. Koyama, O.; Kamagata, Y. and Nakamura K. *Wat. Res*. 1994, 28, 895-899.

33. Li, Z.M.; Comfort, S.D. and Shea, P.J. *J. Environ. Qual*. 1997, 26, 480-487.

34. Aronstein, B.N.; Lawal, R.A. and Maka A. *Environmental Toxicology and Chemistry* 1994, 13, 1719-1726.

35. Lindsey, M.E. and Tarr, M.A. *Environ. Sci. technol.* 2000, 34, 444-449.

36. Lindsey, M.E. and Tarr, M.A. *Wat. Res*. 2000, 34, 2385-2389.

37. Lipczynska-Kochany, E.; Sparah, G. and Harms S. *Chemosphere* 1995, 30, 9-20.

38. Puppo, A. *Photochemistry* 1992, 31, 85-88.

39. Cheng I. and Breen K. *BioMetals* 2000, 13, 77-82.

40. Ansari, A.; Peral, J.; Domenech, X.; Rodriguez-Clemente, R. and Casado, J. *Journal of Molecular Catalysis A: Chemical* 1996, 112, 269-276.

41. Torrades, F.; Garcia-Montano, J.; Garcia-Hortal, J.A.; Nunez, L.; Domenech, X. and Peral, J. *Coloration Technology* 2004, 120, 188-194.

42. Mogra, D.; Agarwal, R.; Punjabi, P.B. and Ameta, S.C. *Chemical & Environmental Research* 2003, 12, 227-235.

43. Lin, K.; Yuan, D.; Chen, M. and Deng, Y. *Journal of Agricultural and Food Chemistry* 2004, 52, 7614-7620.

44. Maciel, R.; Sant'Anna, G.L. and Dezotti, M. *Chemosphere* 2004, 57, 711-719.

45. Brillas, E.; Sauleda, R. and Casado, J. *J. Electrochem. Soc.* 1998, 145, 759-765.

46. Arias, C.; Brillas, E. Cabot, P.; Carrasco, J. Centellas, F.; Garrido, J.A. and Rodrigues, R.M. *Trends in Electrochemistry and Corrosion at the Beginning of the 21st Century* 2004, 359-382.

47. Friedman, C.L. and Lemley, A.T. *Abstracts of Papers, 228th ACS National Meeting*, Philadelphia, PA, USA, Aug. 22-26, 2004.

48. Moreno, A.D.; Frontana-Uribe, B.A. and Ramirez Zamora, R.M. *Water Science and Technology* 2004, 50, 83-90.

49. Hu, C.; Wang, G.; Wu, C.; Li, P. and Wei, C. *Huanjing Kexue* 2003, 24, 106-111.

50. Bittkau, A.; Geyer, R.; Bhatt, M. and Schlosser, D. *Toxicology* 2004, 205, 201-210.

51. Oviedo, C.; Contreras, D.; Freer, J. and Rodriguez, J. *Environmental technology* 2004, 25, 801-807.

52. Kim, Y-S; Kong, S-H; Bae, S-Y and Hwang, G-C *Kongop Hwahak* 2001, 12, 755-760.

53. Lee, B-D; Hosomi, M. and Murakami A. *Water Sci. Technol*. 1998, 38, 91-97.

54. Lee, B-D; Hosomi, M. *Chemosphere* 2001, 43, 1127-1132.

55. Cheung, H. M.; Bhatnagar, A. and Jansen G. *Environ. Sci. Technol*. 1991, 25, 1510-1512.

56. Petrier, C. and Francony A. *Ultrosonics Sonochemistry* 1997, 4, 295-300.

57. Hua, I. and Hoffmann, M.R. *Environ. Sci. Technol.* 1996, 30, 864-871.

58. Wheat, P.E. and Tumeo, M.A. *Ultrosonics Sonochemistry* 1997, 4, 55-59.

59. Laughrey, Z.; Bear, E.; Jones, R. and Tarr, M.A. *Ultrosonics Sonochemistry* 2001, 8, 353-357.

60. Destaillats, H.; Hung, H.M. and Hoffmann, M.R. *Environ. Sci. Technol.* 2000, 34, 311-317.

61. Hirano, K.; Nitta, H. and Sawada, K. *Ultrosonics Sonochemistry* 2005, 12, 271-276.

62. Entezari, M.H. and Petrier, C. *Applied Catalysis, B: Environmental* 2004, 53, 257-263.

63. Stavarache, C.; Nishimura, R.; Maeda, Y. and Vinatoru, M. *Central European Journal of Chemistry* 2003, 1, 339-355.

64. Mrowetz, M.; Pirola, C. and Selli, E. *Ultrosonics Sonochemistry* 2003, 10, 247-254.

65. Dorfman, L.F. and Adams, G.E. *National Bureau of Standards Report* No. NSRDS-NBS-46. Government Printing Office; Washington, DC, 1973.

66. Lindsey, M.E.; Xu, G.; Lu, J.; Tarr, M.A. *Sci. Tot. Environ,* 2003, 307, 215-229.

67. Zheng, W.; Maurin, M. and Tarr, M.A.; *Ultrasonics Sonochemistry*, in press.

Chapter 2. Modified Fenton degradation of some chemical warfare analogues and herbicides

2.1 Introduction

It was found that the Fenton degradation efficiencies of many harmful compounds such as polycyclic aromatic hydrocarbons (PAHs), polychlorinated biphenyls (PCBs) and 2,4,6-trinitrotoluene (TNT) are increased by addition of carboxymethyl-β-cyclodextrins (CMCD).[1] In this chapter, the method has been applied to degrade some chemical warfare analogues — malathion and demeton-S, and some herbicides — linuron, monuron and diuron. The molecular structures of these compounds are shown in Figure 2.1 and some of their physical properties are listed in Table 2.1. Afterwards,the detailed information about Fenton chemistry and cyclodextrins are introduced.

Table 2.1 Some physical properties of the five compounds under investigation

Compounds	M.W.	Aqueous Solubility (mg/L)	Vapor Pressure (mmHg)
Malathion	330.36	143.1	4×10^{-5}
Demeton-S	258.34	2000	2.6×10^{-4}
Linuron	249.10	75	1.5×10^{-5}
Monuron	198.65	Very slight	5×10^{-7}
Diuron	233.10	42	3.1×10^{-6}

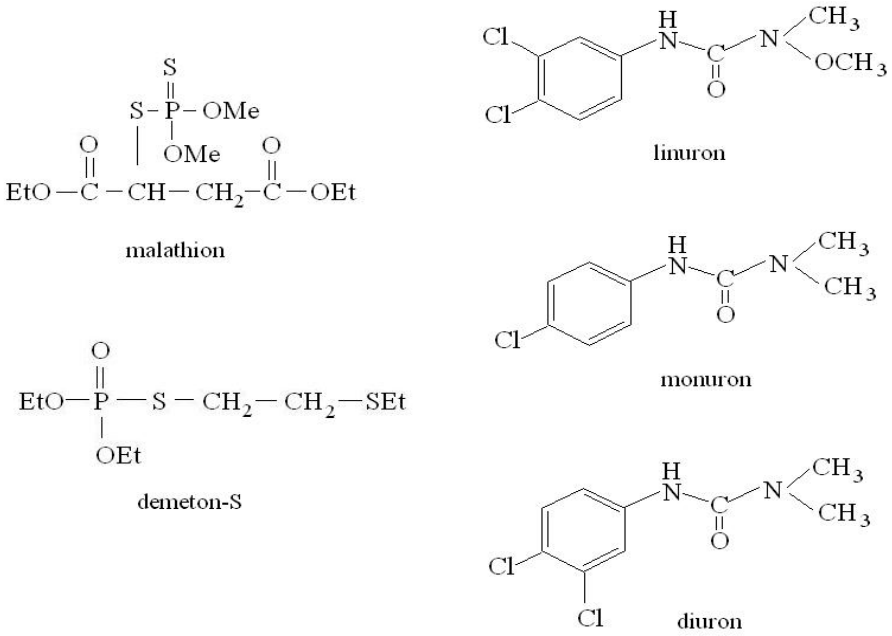

Figure 2.1 Molecular structures of malathion, demeton-S, linuron, monuron and diuron.

2.1.1 Fenton Chemistry[2,3]

In Fenton degradation, the main reaction that takes place is:

$$H_2O_2 + Fe^{2+} \rightarrow HO\cdot + OH^- + Fe^{3+} \qquad (2.1)$$

H_2O_2 and Fe^{2+} are referred to as Fenton reagents. Actually, the Fenton system is a very complicated one. In addition to the above main reaction, there are many other important reactions that also take place:

$$Fe^{3+} + H_2O_2 \rightarrow Fe^{2+} + H^+ + HO_2\cdot \qquad (2.2)$$

$$Fe^{3+} + HO_2\cdot \rightarrow Fe^{2+} + H^+ + O_2 \qquad (2.3)$$

$$Fe^{2+} + HO_2\cdot \rightarrow Fe^{3+} + HO_2^- \qquad (2.4)$$

$$Fe^{2+} + HO\cdot \rightarrow Fe^{3+} + OH^- \qquad (2.5)$$

$$H_2O_2 + HO\cdot \rightarrow H_2O + HO_2\cdot \qquad (2.6)$$

Fe^{2+} ions are recycled between reaction 2.1 and 2.2 or 2.3. So Fe^{2+} acts as a catalyst in the reactions. All above reactions are connected with one another in some way. Therefore, the overall process in a Fenton system is largely dependent on reaction conditions such as pH, initial concentrations of various reagents and non-Fenton species that exist in the solution. The more fundamental mechanism of reaction (2.1) has been proposed as:

$$Fe^{2+} + HOOH \rightarrow Fe(OH)^{2+} + HO\cdot \qquad (2.7)$$

$$Fe(OH)^{2+} \rightarrow Fe^{3+} + OH^{-} \qquad (2.8)$$

where reaction (2.7) is the rate limiting step.

Hydroxyl radical produced in the reaction is the main species that degrades the pollutants. However, since it is very reactive, it is scavenged by nearly everything on its way. Thus, the opportunity for a pollutant to be attacked by hydroxyl radical is rather small. On the other hand, a big category of pollutants is hydrophobic organic compounds. They are likely to avoid the aqueous environment in which hydroxyl radical is produced. Therefore, using Fenton reactions to degrade hydrophobic organic pollutants seems less efficient. To solve the problem, cyclodextrins were used as intermediates in the Fenton system.

2.1.2 Cyclodextrin

Cyclodextrins are cyclic oligosaccharides with α-1,4-type glycosidic linkages that contain six, seven or eight glucose units (Figure 2.2a). Such components and structure make them non-reducing species. They can be produced by a relatively simple technology by fermentation of starch.[4] Cyclodextrins have doughnut-like shape (Figure 2.2b). The internal cavity is built up by carbon-carbon, carbon-oxygen and carbon-hydrogen bonds which are slightly nonpolar. The surface of the outer ring contains several hydroxyl groups which are relatively polar. The names and physical properties of the natural cylcodextrins are listed in Table 2.2.[5]

(a)

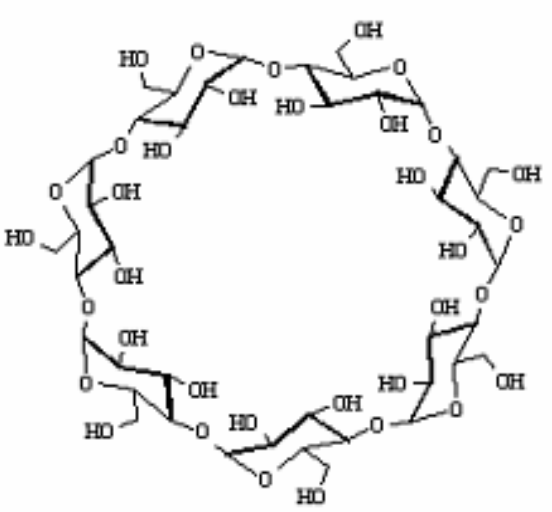

(b)

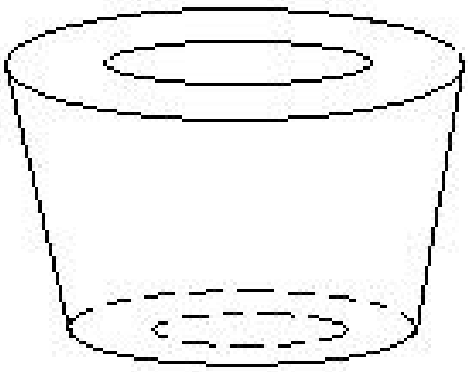

Figure 2.2. (a) The chemical structure of β-cyclodextrin and (b) the steric structure of β-cyclodextrin.

Table 2.2. Some physical properties of natural cyclodextrins

Cyclodextrin	Number of glucose unit	Molecular weight (calculated)	Water solubility (g/100ml)	Specific rotation $[\alpha]_D^{25}$	Cavity dimension (1) internal diameter (Å)	Cavity dimension (2) depth (Å)
α-cyclodextrin	6	972	14.5	150.5 ± 0.5	4.5	6.7
β-cyclodextrin	7	1135	1.85	162.5 ± 0.5	~ 7.0	~ 7.0
γ-cyclodextrin	8	1297	23.2	177.4 ± 0.5	~ 8.5	~7.0

Due to the hydrophilic property of the hydroxyl groups, cyclodextrins are water soluble. At the same time, the hydrophobic internal cavity is capable of encapsulating appropriately sized nonpolar organic molecules.[5-8] The inclusion is totally or in part by physical forces, that is without covalent bonding. The driving forces of the formation of such complexes are based on several facts: 1) nonpolar/nonpolar (guest/CD) interaction are preferred over the polar/nonpolar (water/CD) interaction; 2) substitution of water by the less polar guest molecules can release the strain of the CD ring; 3)Van der Waals and hydrogen bonding interactions help to bind guest/host molecules together; 4) the formation of the inclusion complexes decreases the free energy of the system. For the potential guest molecules, its size must be compatible with the dimension of the cavity. However, for larger molecules, certain sub-groups or side chains could enter the cavity. Apart from the 'size' requirement, the 'polarity' is another important characteristic to decide if the complex could be formed. Species that are less polar than water are more likely to be encapsulated. Strong hydrophilic molecules, highly hydrated or ionized groups have very weak complexation ability if there is any. Hydrogen bonding between the guest and the host could increase the stability of the complex. For the cyclodextrins, the cavity size is

crucial in complex formation. With bigger cavities, such as those that occur in δ-cyclodextrin (having 9 glucose units) or higher homologues, the cavity is able to accommodate so many water molecules that the properties of the internal solvent resemble those of the bulk solvent. Under such circumstances the driving forces for complex formation drop substantially.[4]

By encapsulation, many easily oxidized species could be protected from oxidation reagents like oxygen. Volatile substances may be stabilized by forming crystalline complexes with CDs. In the aqueous solution, such complexes are usually stable at room temperature for quite a long time. In some cases, specific catalytic effects could be induced by the interaction of the guest and host molecules. The well size-defined cavities also have certain applications in separation processes. Under many circumstances, natural CDs could be modified to better achieve the specific goals by substituting the hydroxyl groups with other groups such as carboxymethyl groups. Due to above phenomena cyclodextrins have been widely used as vessels for reaction, model system of enzymes, and solubilizers of water-insoluble species.[4,9,10] The formation of host-guest binary complexes with natural or modified cyclodextrins has been extensively studied.[11-15]

Another noteworthy property of the CDs is their chirality. The cavities of CDs are non-symmetric and this gives rise to different binding ability of CDs to enantiomers. Due to this fact, CDs and modified CDs have been widely used in chiral separation[16-23].

The prospective industrial fields for the application of CDs include food, pharmaceutical, agriculture, cosmetics, chemical production and environmental protection industries, etc.

2.2 Experimental

Malathion (98.2%) and demeton-S (99%) were obtained from Chem Service. Linuron (99%), monuron (99.9%) and diuron (99%) were obtained from Riedel-deHaën. Hydrogen peroxide (wt. 35%) and iron (II) perchlorate hydrate (98%) were obtained from Aldrich. Carboxymethyl-β-cyclodextrin (average substitution degree = 3) was obtained from Cerestar. Propanol was obtained from EM Science. Hexane (pesticide grade) was obtained from Fisher. All reagents were used as received. Purified water for the preparation of aqueous solutions was obtained from a Barnstead NanopureUV water treatment system.

Due to the low aqueous solubility of the five compounds, a more concentrated stock solution of each compound was first prepared in hexane or methanol. A small aliquot of the stock solution was transferred into a clean dry volumetric flask and the solvent was evaporated. Water (pH adjusted with $HClO_4$) was then used to fill the flask to the mark. The solute was dissolved by vigorously shaking. Typically, 50-100mL aqueous solutions were prepared each time. To make one degradation sample, 2mL of the solution was transferred into a 20mL vial. Solid CMCD was added with the desired concentrations when needed. The solutions were shaken on an orbital shaker for about one hour. Afterwards, iron(II) perchlorate and sometimes propanol as well were added with the desired concentrations. Then one dose of hydrogen peroxide was added. The solution was allowed to shake for 20-30min before further treatment. The reactions of malathion and demeton-S were quenched by 2mL hexane which also served as an extraction solvent. The extracted solution was then analyzed by GC. The reactions of linuron, monuron and diuron were quenched by 100uL propanol and the solution was analyzed by HPLC.

GC analysis was carried out on a HP 6890 series with a fused silica capillary column (30m×0.32mm×0.25um). GC conditions were as follows: split injection at 200 or 275°C for 1uL

or 2uL injection; oven temperature programmed from 150°C to 220°C at 10°C /min and hold 2min at 220°C; detector for malathion was ECD, for demeton-s was FID. HPLC analysis was carried out on a HP (Hewlett Packard) 1090 series. An Allsphere ODS-2 column (250mm×4.6mm×5um) was used. The mobile phase was a mixture of 60:40 acetonitrile:water. The eluent was delivered at a rate of 1.0mL/min. The wavelength for absorbance detection was 254nm.

The concentration of hydrogen peroxide was determined by classic iodometric titration. The reactions used in this method are:

$$H_2O_2 + 3I^- + 2H^+ \rightarrow 2H_2O + I_3^- \qquad (2.9)$$

$$I_3^- + 2S_2O_3^{2-} \rightarrow 3I^- + S_4O_6^{2-} \qquad (2.10)$$

And the concentration of $Na_2S_2O_3$ was determined by reactions:

$$IO_3^- + 8I^- + 6H^+ \rightarrow 3I_3^- + 3H_2O \qquad (2.11)$$

$$I_3^- + 2S_2O_3^{2-} \rightarrow 3I^- + S_4O_6^{2-} \qquad (2.12)$$

2.3 Results and discussion

Fenton degradation of malathion in the absence and presence of CMCD is shown in Figure 2.3. In the figure (and following figures), control group means the malathion samples that were not degraded and reaction group means the malathion samples that had been degraded. Under the given conditions (listed in the figure captions), more than 90% of malathion was degraded in the absence of CMCD while only about 30% was degraded in the presence of CMCD. Obviously, degradation efficiency is higher without CMCD.

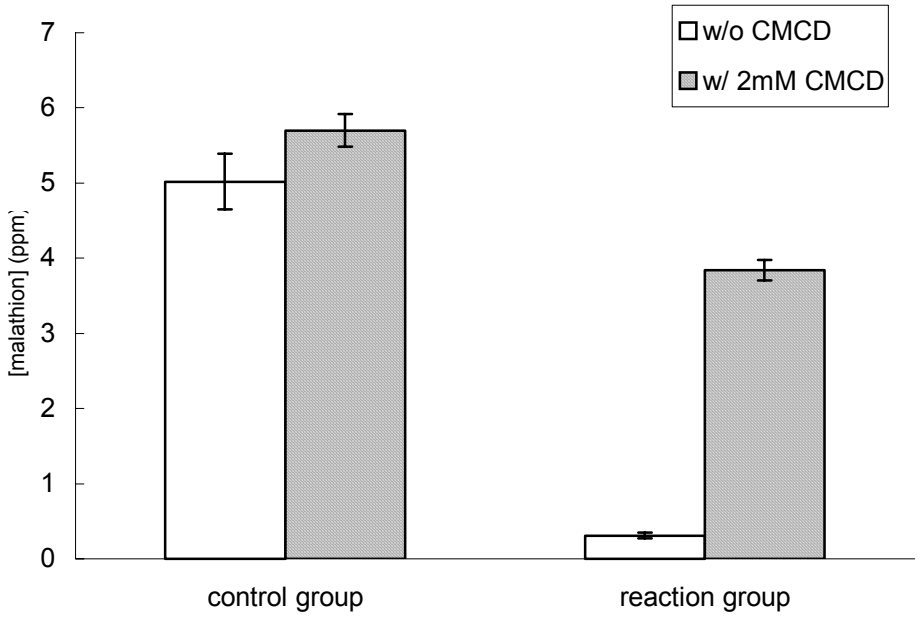

Figure 2.3 Degradation of malathion in the absence and presence of CMCD. Degradation conditions were: $[Fe^{2+}]$=2mM, $[H_2O_2]$=0.5mM, [CMCD]= 2mM and pH=2.5.

Figure 2.4 shows the degradation of malathion under the similar conditions but with extra scavenger—propanol in the solution. The results indicate that in the presence of extra scavenger the degradation of malathion with or without CMCD was comparable. Malathion degradation in the absence of extra scavenger was repeated at near neutral pH condition (Figure 2.5). The pH of the samples was about 5-6. The small acidity was due to the acidity of nanopure water. Compared to Figure 2.3, results in Figure 2.5 showed that the degradation efficiency in the presence of CMCD was lower at near neutral pH while the degradation efficiency in the absence of CMCD was not influenced.

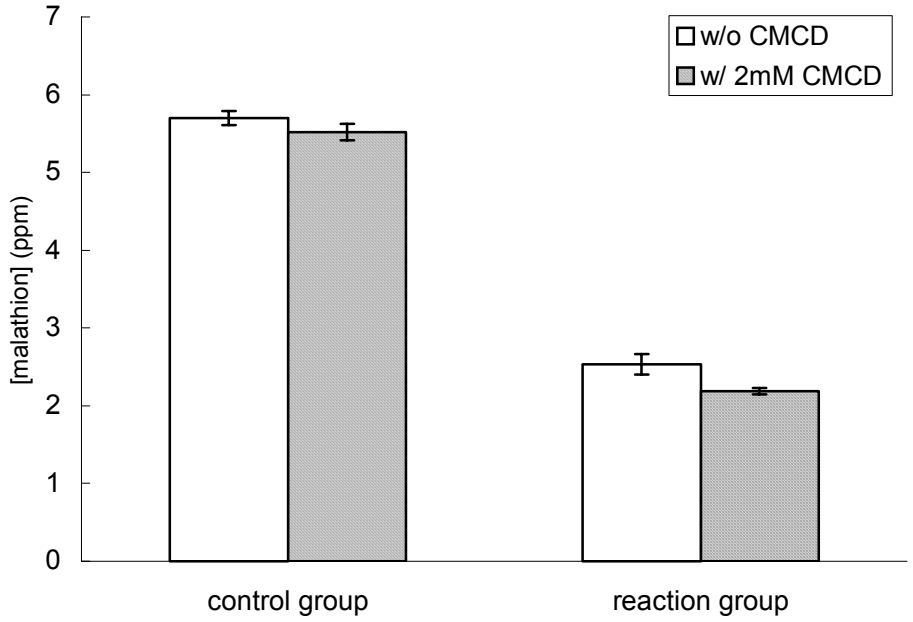

Figure 2.4 Degradation of malathion in the absence and presence of CMCD with extra scavenger-propanol in the solution. Degradation conditions were: $[Fe^{2+}]$=4mM, $[H_2O_2]$=10mM, [CMCD]= 2mM, [propanol]=10mM and pH=2.5.

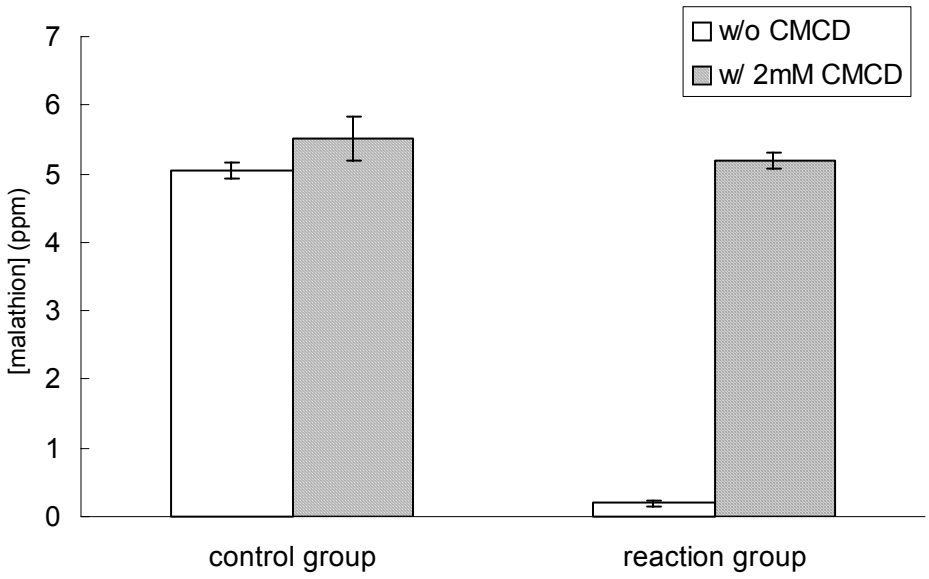

Figure 2.5 Degradation of malathion in the absence and presence of CMCD at near neutral pH condition. Degradation conditions were: $[Fe^{2+}]$=2mM, $[H_2O_2]$=0.5mM, [CMCD]= 2mM and pH=5~6.

Similar results were obtained from degradation of the other four compounds. The degradation data of all five compounds are listed in Table 2.3. These data suggest that CMCD acted as a hydroxyl radical scavenger and not as a degradation enhancement factor.

Table 2.3 The degradation percentage of the five pollutants under various conditions

Compounds	In the absence of extra scavengers*		In the presence of extra scavengers**	
	Without CMCD	With CMCD	Without CMCD	With CMCD
Linuron	63% ± 47%	0% ± 38%	42% ± 4%	43% ± 4%
Monuron	75% ± 7%	4% ± 6%	0% ± 6%	9% ± 6%
Diuron	92% ± 11%	27% ± 8%	52% ± 5%	60% ± 2%
Malathion	96% ± 7%	6% ± 6%	60% ± 3%	56% ± 3%
Demeton-S	100% ± 4%	46% ± 1%	~	~

*: Degradation conditions: pH=5~6, $[H_2O_2]$=0.25~5mM, $[Fe(ClO_4)_2]$=2 or 4mM, [CMCD]=1 or 2mM
**: Degradation conditions: pH=2.5, $[H_2O_2]$=5 or 10mM, $[Fe(ClO_4)_2]$=2 or 4mM, [CMCD]=1mM, [PrOH]=67 or 10mM.

In the degradation experiments, it was also found that CMCD inhibited the decomposition of hydrogen peroxide. The decomposition of hydrogen peroxide vs. time was plotted in Figure 2.6. The result could be due to the coordination of iron to CMCD, which changed the Fe^{2+}/Fe^{3+} cycles in the Fenton reactions. This inhibition might also be a contribution to the decreased degradation efficiency in the presence of CMCD.

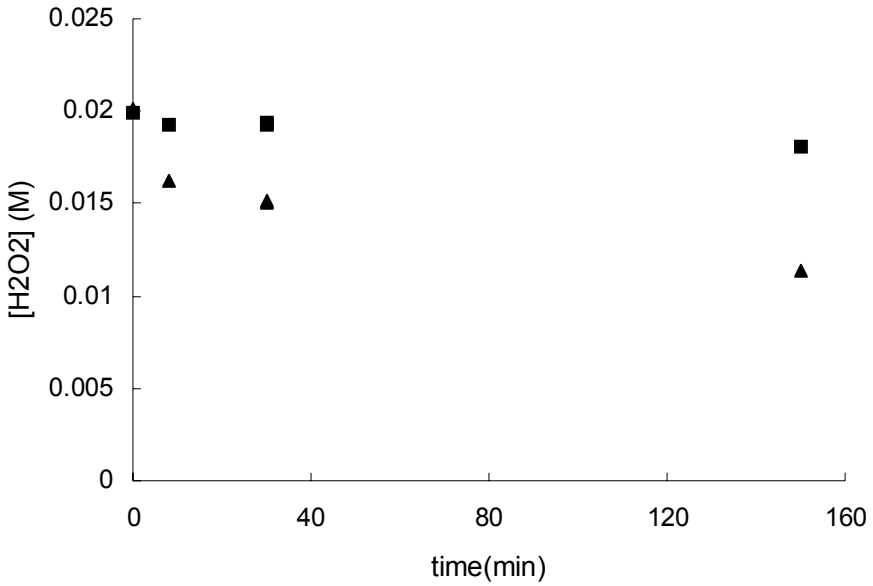

Figure 2.6 Decomposition of H_2O_2 (with 1mM Fe^{2+}) with time in the presence of CMCD (■) and in the absence of CMCD (▲).

From all above results, it seems that CMCD played a negative role in the Fenton degradation. However what made it improve the degradation of PAHs, PCBs and TNT? To answer this question, further investigation of the function of CMCD in Fenton system was carried out and discussed in Chapter 3.

2.4 References

1. Lindsey, E. M.; Xu, G.; Lu, J.; Tarr, A. M. *Sci. Tot. Environ,* 2003, 307, 215-229.
2. "Fenton and Modified Fenton Methods for Pollutant Degradation," M. A. Tarr in *Chemical Degradation Methods for Wastes and Pollutants* Tarr, M. A., Editor., Marcel Dekker, New York, 2003.
3. Goldstein, S.; Meyerstein, D. and Czapske, G. Free Radical Biology & Medicine 1993, Vol.15, 435-445.

4. Szejtli, Jäozsef *Cyclodextrins and Their Inclusion Complexes* Akadémiai Kiadó, Budapest, 1982.
5. Bender, M. L.; Komiyama, M. *Cyclodextrin Chemistry,* Springer-Verlag Berlin Heidelberg, New York, 1978.
6. Santra, S.; Zhang, P.; Tan, W. *J. Phys. Chem.* A 2000, 104, 12021.
7. Liu, J.; Castro, R.; Abboud, A. K.; Kaifer, E. A. *J. Org. Chem*. 2000, 65, 6973.
8. Nau, M. W.; Zhang, X. *J. Am. Chem. Soc*. 1999, 121, 8022.
9. Breslow, R.; Dong, S.D. *Chem. Rev*. 1998, 98, 1997.
10. Wenz, G. *Angew. Chem., Int. Ed. Engl.* 1994, 33, 803.
11. Ikeda, H.; Nakamura, M.; Ise, N.; Oguma, N.; Nakamura, A.; Ikeda, T.; Toda, F.; Ueno, A. *J. Am. Chem. Soc.* 1996, 118, 10980.
12. Borovkov, V.V.; Lintuluoto, M. J.; Sugeta, H.; Fujiki, M.; Arakawa, R.; Inoue, Y. *J. Am. Chem. Soc.* 2002, 124, 2993.
13. Liu, Y.; You, C.; Chen, Y.; Wada, T.; Inoue, Y. *J. Org. Chem*. 1999, 64, 7781.
14. Liu, Y.; Chen, Y.; Li, L.; Zhang, H.; Liu, S.; Guan, X. *J. Org. Chem*. 2001, 66, 8518.
15. Venema, F.; Rowan, E.A.; Nolte, J.M.R. *J. Am. Chem. Soc.* 1996, 118, 257.
16. Herráez-Hernández, R. and Campíns-Falcó, P. *Analytica Chimica Acta* 2001, 434, 315-324.
17. Armstrong, D.W.; Ward, T.J.; Armstrong, R.D. and Beesley, T.E. *Science* 1986, 232, 1132-1135.
18. Jae Wook Ryu; Hae Sung Chang; Young Kwan Ko; Jae Chun Woo; Dong Wan Koo and Dae Whang Kim *Microchemical Journal* 1999, 63, 168-171.
19. Bates, P.S.; Kataky, R. and Parker, D. *J. Chem. Soc. Perkin Trans. 2* 1994, 669-765.

20. Köhler, J.E.H.; Hohla, M.; Richters; M.; and König, W.A. *Angew. Chem. Int. Ed. Engl.* 1992, 31, 319-320.

21. Guy Hembury, Mikhail Rekharsky, Asao Nakamura, and yoshihisa Inoue *Org. Lett.* 2000, 2, 3257-3260.

22. Redondo, J.; Frigola, J.; Torrens, A. and Lupón, P. *Magnetic Resonance In Chemistry* 1995, 33, 104-109.

23. Mikhail V. Rekharsky; Hatsuo Yamamura; Masao Kawai; and Yoshihisa Inoue *J. Org. Chem.* 2003, 68, 5228-5235.

Chapter 3. Investigation of ternary complexes of iron, carboxymethyl-β-cyclodextrin and hydrophobic pollutants in Fenton degradation system

3.1 Introduction

Carboxymethyl-β-cyclodextrin has been found to improve Fenton degradation of certain pollutants such as PAHs, PCBs and TNT. However, the successful application of the method to some other pollutants such as malathion and linuron (Chapter 2) was not achieved. The goal of this chapter is to investigate the mechanisms lying behind the observed phenomena.

The improvement of degradation is proposed to be due to the formation of ternary complexes among iron, pollutants and CMCD. In the ternary complexes, the Fenton catalyst is located closer to the pollutant target so the attack of hydroxyl radical is more efficient. NMR and optical spectroscopy which are two powerful techniques to study the structure of complexes in aqueous solution have been employed in this investigation. Several concepts and methods related to the two techniques are introduced below. The reasons of unsuccessful application in Chapter 2 are discussed more at the end of this chapter.

3.1.1 Continuous variation method—measuring binding stoichiometry

Binding stoichiometry is usually an important parameter for people to understand the interaction between two compounds. To measure the binding stoichiometry, continuous variation method (also called Job's method) is commonly used[1].

Considering binding between two species, S (substrate) and L (ligand), the complex could be in the form of SL, SL_2, SL_3… as in the equilibrium of:

$$S + nL \rightarrow SLn \qquad (3.1)$$

If one complex (eg. n=1) predominates, the continuous variation method will be able to identify the stoichiometry of the predominant complex.

In the method, the total concentration of S plus L keeps constant while the fraction of the two changes (eg. [S] : [L] = 9:1, [S] : [L] =8:2…[S] : [L] =1:9, while [S] + [L] = 0.5M in all fractions). If UV-vis absorbance is the characteristic of the system that is monitored during the experiment, we will see the corrected absorbance reaches the maximum when the composition of S and L is equal to the stoichiometry of the predominant complex. Corrected absorbance is defined as:

$$\text{corrected absorbance} = \text{measured absorbance} - \varepsilon_S b[S]_T - \varepsilon_L b[L]_T \qquad (3.2)$$

where ε_S and ε_L are the molar absorptivities of S and L, b is the sample pathlength, and $[S]_T$ and $[L]_T$ are the total concentrations of S and L in the solution.

3.1.2 NMR titration – measuring binding constant

Binding constant is an important parameter for people to understand the stability of the complex. There are many methods to measure binding constant such as NMR, UV-vis absorbance, fluorescence, solubility measurement[2]… NMR and fluorescence methods are two main methods used in this study to determine the binding constants. In this chapter, NMR titration method is introduced while the fluorescence titration method will be introduced in next chapter.

In NMR measurement, the chemical shifts of protons are very sensitive to their local chemical environment. Upon binding to another species, the chemical environment of certain protons or all the protons of the substrate or ligand is changed. The change will cause a difference in the energy absorption and therefore in the chemical shift.

Considering a 1:1 binding system as shown in below equilibrium,

$$S + L \rightarrow SL \qquad (3.3)$$

the species S is generally in two sites: S or SL and it can exchange between these two sites. If the lifetime of the S in each site is very long, a proton in site S or SL can precess many times before it leaves one site to enter another. There is enough time for the proton to absorb energy from the radiofrequency field and thus two resonance peaks at different frequencies will appear in the NMR spectrum. This situation is called slow exchange. If the lifetime of the S in each site is very short, the proton can not precess to a significant extent before it leaves S to enter SL, the proton is essentially stationary from the point of view of rotation frame in NMR concept. Only one resonance peak at the mean frequency (mean of frequencies at site S and SL) will be observed. This situation is called fast exchange. The situation lies in between of the above two is called moderately slow exchange in which a broad resonance peak is usually observed.

In fast exchange situation, if the binding stoichiometry is 1:1 ratio, the binding constant can be calculated from the equation (1:1 binding isotherm) below:

$$\Delta = (\Delta_{11}K[L]) / (1 + K[L]) \qquad (3.4)$$

where Δ is the difference in observed chemical shift and chemical shift of S, Δ_{11} is the difference in chemical shift of SL and S, K is the binding constant, and [L] is the concentration of ligand. The equation will usually show a hyperbolic curve. In practice, it has been linearized as the form:

$$1 / \Delta = (1 / \Delta_{11}K[L]) + 1/ \Delta_{11} \qquad (3.5)$$

The linear plot of $1/\Delta$ versus 1/[L] is called double-reciprocal plot. Obviously, the binding constant K can be calculated from the slope and intercept (K = intercept / slope). Other linearized equations from equation (3.4) include the y-reciprocal form:

$$[L] / \Delta = ([L] / \Delta_{11}) + (1/ \Delta_{11}K) \qquad (3.6)$$

and the x-reciprocal form:

$$\Delta / [L] = -K\Delta + \Delta_{11}K \qquad (3.7)$$

The binding constants of the complexes that have stoichiometry other than 1:1 may also be measured[2]. However, the binding isotherm will be much more complicated than equation (3.4). Since most complexes studied in this dissertation had 1:1 ratios, only the 1:1 binding isotherm is introduced here.

3.1.3 Fluorescence quenching

Fluorescence is a phenomenon of light emission by certain molecules during their energy release from the first excitation state to the ground state. Fluorescence quenching is a process that decreases the fluorescence intensity of a given species. Many processes can cause fluorescence quenching such as energy transfer, excited state reactions, excited state collisions and complex formation[3]. Among these processes, excited state collisions and complex formation are two largely observed quenching mechanics which are called collisional quenching (or dynamic quenching) and static quenching respectively. In collisional quenching, the quencher must collide with the fluorophore during the lifetime of its excited state. Upon contact the excited fluorphore returns to the ground state without emission of a photon. In static quenching, the quencher and the fluorophore form a complex that is not fluorescent. An important character in both processes that needs to be noted here is that the fluorophore and the quencher must be in contact to introduce the quenching.

The theory of fluorescence quenching has been extensively studied. Collisional quenching can be described by the Stern-Volmer equation:

$$F_0 / F = 1 + k_q\tau_0[Q] = 1 + K_D[Q] \qquad (3.8)$$

where F_0 is the fluorescence intensity in the absence of quencher, F is the observed fluorescence intensity when the quencher is added, k_q is the bimolecular quenching constant, τ_0 is the lifetime of the fluorophore in the absence of quencher, [Q] is the concentration of quencher, and $K_D = k_q\tau_0$ is the Stern-Volmer quenching constant. The plot of F_0/F versus [Q] (Stern-Volmer plot) is expected to be linear. In static quenching, the quenching behavior can be described by the equation:

$$F_0 / F = 1 + K_s[Q] \qquad (3.9)$$

where K_s is the association constant of the complex and the other symbols have the same meanings as in equation 3.8. The plot of F_0/F versus [Q] is also expected to be linear. Therefore a linear Stern-Volmer plot is not an indication of collisional quenching or static quenching. However, it suggests that only one type of quenching occurs.

In practice, the Stern-Volmer plot sometimes deviates from linearity. The deviation indicates that either more than one fluorophore population is present in the system or more than one quenching mechanism occurrs. The former situation usually causes a downward curvature, concave towards the x axis while the later one causes an upward curvature, concave toward the y axis. In many cases the fluorophore can be quenched by collision with the quencher and at the same time, by the formation of the nonfluorescent complex with the same quencher. In such combined collisional-static quenching, an upward curvature is usually observed. However the upward curvature can also generated from a phenomenon called sphere of action. This phenomenon is often observed when the extent of quenching is large. It is caused by a close location of the quencher to the fluorophore during the lifetime of its excitation. Within the sphere of action, the probability of quenching is unity. The Stern-Volmer equation is modified to describe this situation:

$$F_0 / F = (1 + K_D[Q])\exp([Q]\upsilon N / 1000) \qquad (3.10)$$

where υ is the volume of the sphere, N is Avogadro's number. Under such a circumstances, the distance of the quencher and the fluorophore is usually only a slightly larger than the sum of the radii of the two.

3.1.4 NMR measurements in the presence of paramagnetic species

Paramagnetic species are often used in NMR measurements to deduce the conformational structure of biomolecules. We transferred this method to our ternary complex study to probe the distance of the metal ion to the guest/host complex.

The presence of paramagnetic species in NMR system will greatly change the relaxation times and chemical shifts of the nuclear resonance[4]. In a paramagnetic system, the nuclear spins relax mainly through electron-nuclear interactions. Although the nature of electron-nuclear spin interactions is similar to nuclear-nuclear interactions, the magnitudes are much larger since the electronic magnetic moments are a thousand times larger than nuclear magnetic moments. The relaxation time is significantly reduced due to the paramagnetic influence which further results in the broadening of the resonance peaks. Meanwhile the unpaired electrons introduce an extra magnetic field into the local fields which makes the effective magnetic field at the nuclear as[5]:

$$H_{eff} = H_0 + (4/3\pi - \alpha)M + qM \qquad (3.11)$$

where H_0 is the externally applied field; the second term is the contribution to the local field from the magnetization of the sample outside a spherical cavity around the nucleus under consideration, α being the demagnetizing factor and depending on the shape of the sample; and the third term is the contribution to the local field from the paramagnetic ions inside a small sphere around the nucleus. Accordingly, the chemical shifts of the nucleus change. Since both above effects are introduced by electronic magnetic moments of the unpaired electrons and the

moments drop fast with the distance, these effects are dependent on the distance between the paramagnetic species and the nucleus. The relaxation time (T) is proportional to the sixth power of the distance ($T \propto r^6$)[6,7]. As a result, only when the paramagnetic species is very close to the nucleus can we observe resonance changes in the NMR spectra.

3.1.5 Fluorescence resonance energy transfer (FRET)

FRET is a widely used method to measure the distance between two molecules or two sites on a macromolecule, especially in biosystem[8-11]. It is a phenomenon in which energy is transferred from an excited donor molecule to an acceptor molecule. Usually, two fluorophores are used as donor and acceptor. With this energy transfer, the originally excited donor gets back to the ground state without emitting a photon while the acceptor is excited and emits a photon. In FRET, energy transfer is through long-range dipole-dipole interactions between the donor and the acceptor. It is dependent on the distance of the two species.

For FRET to occur, first, the emission band of the donor must have an overlap with the excitation band of acceptor. Then, the distance between the two species must be close enough. The distance at which 50% energy is transferred is called the Forster distance (R_0). Typically, the Forster distance is in the range of 20-60Å. It can be calculated through the equation (3.12)[12]:

$$R_0^6 = [9000(\ln 10)\kappa^2\Phi_D J] / (128\pi^5 n^4 N_{AV}) \qquad (3.12)$$

where κ^2 is the orientation factor, Φ_D is the donor quantum yield in the absence of acceptor molecules, J is the overlap integral, n is the refractive index of the medium, and N_{AV} is Avogadro's number.

The rate of energy transfer (k_T) is inversely proportional to the sixth power of distance between the donor and acceptor (r^6)[8]:

$$k_T = (1/\tau_D)(R_0/r)^6 \qquad (3.13)$$

where τ_D is the decay time of the donor in the absence of acceptor. This relationship shows that the energy transfer is very sensitive to the donor-acceptor distance. That is one reason why the method is good for distance measurement.

Although FRET is similar to the fluorescence quenching in the observation of decrease in the donor's fluorescence intensity, they are two different procedures. In FRET, the energy transfer is through space and the effective distance is much longer. The interaction is mostly independent of the intervening solvent and/or macromolecule. Fluorescence quenching, on the other hand, is caused by interactions of the fluorophore with the quencher in the surrounding solvent shell. Furthermore, if the acceptor in FRET is also a fluorophore, an enhanced or sensitized acceptor emission is often observed.

3.2 Experimental

3.2.1 Attempted preparation of crystal of βCD with iron ions, and βCD with both iron ions and hydrophobic compounds

βCD was obtained from Cerestar. Biphenyl, 3-phenylphenol (90%), 4-phenylphenol (99%) and ferrous perchlorate (anhydrous) were obtained from Aldrich. Ferric nitrate was obtained from J.T.Baker.

In an attempt to grow crystals of βCD with Fe(II), solutions that contained βCD and $Fe(ClO_4)_2$ in different ratio (βCD: Fe(II) = 1:8, 1:4, 1:2, 1:1, 2:1) were prepared under acidic condition (pH=2, pH adjusted with $HClO_4$). Using acidic condition is to avoid oxidation of Fe(II). These solutions were shaken on an orbital shaker (VWR) overnight. Then they were sat quietly with a filter paper as a cover for evaporation of the solvent. In an attempt to grow crystal of βCD with Fe(II) and hydrophobic compounds (biphenyl, 3-phenylphenol or 4-phenylphenol),

excess (above solubility) of each compound was added into βCD and $Fe(ClO_4)_2$ solutions (βCD : Fe(II) = 1:2). After the mixtures were shaken overnight, the supernatant of each solution was transferred into clean vials and sat for solvent evaporation. However, it was found Fe(II) is not stable enough for crystal growth under our acidic condition. The slow oxidation of Fe(II) could disturb the growing of crystal. So Fe(III) was used to displace it. The preparation of crystal with Fe(III) followed the same procedures as described above. $Fe(NO_3)_3$ was used as Fe(III) source and HNO_3 was used for pH adjustment. Before the crystal was taken for analysis, it was rinsed several times by distilled water and acetone.

3.2.2 UV, fluorescence and NMR measurements

Anthracene (99+%), $EuCl_3 \bullet 6H_2O$ (99.99%) and cadmium chloride (99+%) were obtained from Aldrich. Ferrous sulfate heptahydrate and calcium chloride were obtained from J.T. Baker. Carboxymethyl-β-cyclodextrin(average substitution degree = 3) was obtained from Cerestar. 2-naphthol (99+%) was obtained from EM Science. Potassium bromide (99%) was obtained from Mallinckrodt. Deuterated water (99.9%) was obtained from Cambridge Isotope Laboratories Inc. All reagents were used as received. Purified water for the preparation of aqueous solutions was obtained from a Barnstead NanopureUV water treatment system.

To prepare aqueous anthracene solutions, a more concentrated anthracene stock solution was first prepared in hexane. A small aliquot of this stock solution was transferred into a clean dry volumetric flask and the solvent was evaporated. Water (pH adjusted with H_2SO_4) was then used to fill the flask to the mark. The solute was dissolved by low-energy (60W) sonication in a bath sonicator (Branson 1510) for about half an hour. The final concentration of aqueous anthracene was 0.1 μM. Naphthol aqueous solutions were prepared by dissolving solid 2-naphthol in pH adjusted water or deuterated water. A more concentrated stock solution was

prepared first, then it was diluted to the concentrations in the range 10 μM to 5 mM. To prepare samples containing cyclodextrins, solid CMCD was added to the aqueous anthracene or 2-naphthol solutions, making the final CD concentration 2 mM to 10 mM. These samples were shaken on an orbital shaker from several hours to several days before analysis in order to allow the CD and PAH to equilibrate.

UV spectra were recorded with a Cary 500 UV-vis-near IR spectrophotometer. The stoichiometry of iron(II)/cyclodextrin complexes were determined from spectra of iron-cyclodextrin mixtures using the continuous variation method[1]. The total concentration of Fe(II) + CMCD was kept at 5mM.

Fluorescence spectra were recorded with a Photon Technology International QM-1 fluorometer. Aliquots (3mL) of aqueous anthracene or 2-naphthol solutions were placed in a quartz cuvette and were subsequently modified by consecutive additions of 5 or 10 μL aliquots of $FeSO_4$ (aq) or KBr (aq). The sample was stirred by a magnetic stirring bar throughout the whole period of measurement. In total 30-60 μL of quencher solution was added for each experiment. Compared to the 3 mL sample volume, these additions caused negligible decreases in the fluorescence due to dilution. To evaluate the possible interference of O_2, which is also a fluorescence quencher, some quenching experiments were carried out under low O_2 conditions. Sample preparation and transfer were undertaken under a nitrogen stream or in an argon box. The samples were sealed using rubber stoppers and kept under nitrogen atmosphere prior to measurement. During quenching experiments, $FeSO_4$ or KBr was injected into a septum sealed quartz cuvette using a syringe. In the Cd^{2+} or Ca^{2+} substitution experiments, aliquots (10-30 μL) of concentrated Cd^{2+} or Ca^{2+} stock solution was added to each sample.

^{1}H NMR spectra were recorded using Varian Unity 400 and 500 spectrometers operating at 400 or 500 MHz. D_2O was used as the solvent and the trace H_2O served as an internal standard. In NMR titration experiment, aliquots (10-20μL) of concentrated CMCD (7.5mM-100mM) was added to 2-naphthol sample each time and shaken heavily to get the solution mixed well. Then NMR analysis was followed by each addition.

All experiments were repeated two to three times in order to determine precision.

3.3 Results and discussion

3.3.1 Temptation to grow crystal of binary complexes: βCD-iron ions, and ternary complexes: βCD-iron ions-hydrophobic compounds

To investigate the structure of a possible binary or ternary complex in aqueous solution, one good way is to study the crystal structure of the intended complexes. X-ray crystallography can provide very detailed structural information about the complexes. Although the solid structure is usually different from the structure in solution, it could provide people with a good guess about the structure in solution.

In our study, CMCD is the main interest. However, CMCD is a mixture with carboxymethyl groups substituting in different hydroxyl group positions. This impurity could make the complexes difficult to crystallize, or even if they were crystallized the analysis by X-ray would be more complicated. Therefore, we used pure βCD which has similar cavity size as CMCD. Following the procedures described in the experimental section, transparent crystals were obtained from solution 1βCD-2Fe(III)-saturated biphenyl. A small piece of the crystal was used to test the existence of Fe(III). The test is based on the reaction:

$$Fe^{3+} + 5\ NH_4SCN \rightarrow Fe(SCN)_5^{2-}\ (red) + 5\ NH_4^+ \qquad (3.14)$$

Appearance of red color in the solution of dissolved crystal indicates the existence of Fe(III). It is a very sensitive method and trace Fe(III) can be detected this way. However, no red color was showed in the test. It suggests that Fe(III) was not crystallized with the other components. It explained why the crystal is transparent instead of having any yellowish color. Another piece of the crystal was dissolved in D_2O to get NMR analysis. The spectrum illustrates the same character as that of pure βCD. It indicates that no biphenyl was crystallized with βCD or the amount of crystallized biphenyl was not large enough for NMR to detect. Therefore the crystal is either pure βCD or βCD with small amount of biphenyl.

No crystals were found in other samples. As can be seen, crystal growth was not fruitful. However it does not mean that the binary or ternary complexes were not formed in the aqueous solution. It is probably just due to the difficulty of crystallization of the intended complexes. Therefore other methods need to be employed to investigate the structure of cyclodextrin, iron and hydrophobic compounds.

3.3.2 Binding stoichiometry between Fe^{2+} and CMCD

Continuous variation method[1] was used to determine the binding stoichiometry between Fe(II) and CMCD in aqueous solution (pH=3.1). The UV absorbance spectra of Fe(II), CMCD and Fe(II) + CMCD are shown in Figure 3.1. The Fe(II) + CMCD system exhibits maximum absorbance at 200nm. However at the wavelength near 200nm range a lot of species absorb light, which leads to a serious interference. Therefore the absorbance at 250nm was chosen for analysis. At 250nm, the Fe(II)/CMCD complex shows a moderate absorbance while Fe(II) or CMCD have only a very small absorbance. In such case the maximum corrected absorbance at this wavelength should occur when the greatest amount of complex is formed. The result is presented in Figure 3.2. The corrected absorbance reached a maximum at approximately 0.5

mole fraction of Fe(II), which indicates that a 1:1 binding stoichiometry was predominant for the Fe(II)/CMCD complex.

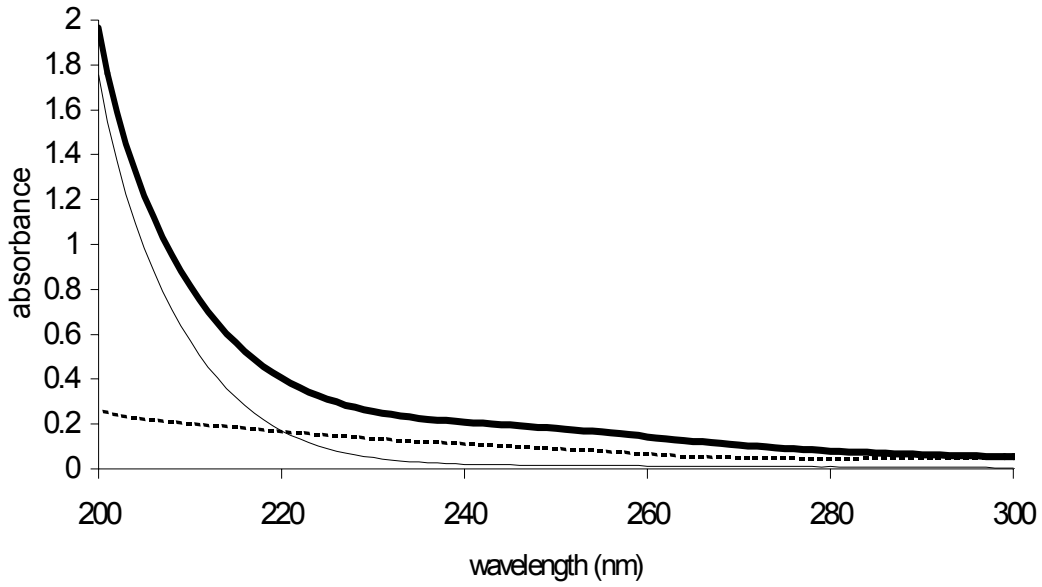

Figure 3.1 UV absorbance spectra of 2.5mM Fe(II) (---), 2.5mM CMCD (─) and 2.5mM Fe(II) + 2.5mM CMCD (▬) in aqueous solution (pH=3.1)

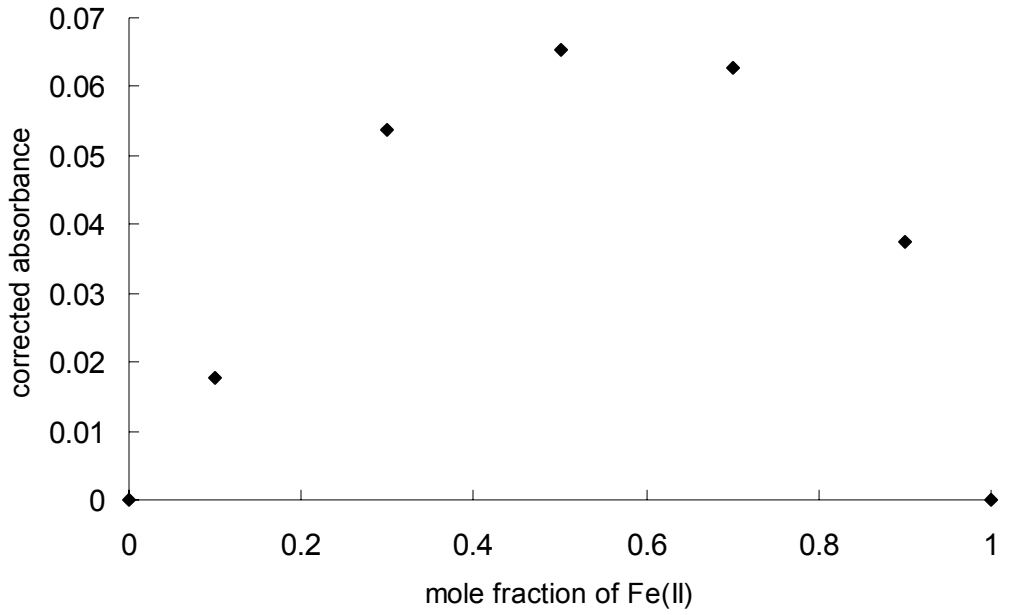

Figure 3.2 Corrected absorbance at 250nm vs mole fraction of Fe(II) in mixtures with CMCD. Solution pH was 3.1.

3.3.3 Fluorescence quenching of anthracene and 2-naphthol by Fe^{2+}, Br^- and Eu^{3+}

Fluorescence quenching results usually provide the structure information in the solvent shell of the fluorophore.[3] So this technique was employed here to study the structure of CMCD, Fe(II) and certain hydrophobic fluorophores (anthracene and 2-napthol) in aqueous solution. Anthracene (see Figure 1.1) and 2-naphthol (see Figure 3.11) were selected as study interests because firstly, they are members of PAH and PAH analogues. Anthracene and naphthalene (an analogue of 2-naphthol) have been successfully degraded by Fenton chemistry with addition of CMCD. Secondly, their sizes match the dimension of the cavity of CMCD. The encapsulation of the two species by βCD has previously been proven and studied[13-16]. Although CMCD has been modified from βCD by substitution of some secondary hydroxyl groups with carboxymethyl groups, the size and shape of the cavity likely remains the same. Consequently, CMCD is expected to bind with these two compounds. Thirdly, most PAH members have very limited

solubility in aqueous solution including anthracene. This property greatly hindered the investigation of their interactions with other species in water. 2-Naphthol, on the other hand, has a much higher water solubility. It enabled us to use other powerful structure investigation techniques such as NMR.

3.3.3.1 Different quenching effect of Fe^{2+} and Br^-

Fe^{2+} is a good fluorescence quencher for anthracene and 2-naphthol. Br^- is also a quencher for the two species. Figure 3.3 shows the Stern-Volmer plot for anthracene fluorescence quenching by Fe^{2+} and Br^- in the presence or absence of CMCD at pH = 3.1 (to avoid the precipitation of iron, all quenching experiments were carried out under acidic conditions, pH ~ 1-4). As can be seen in Figure 3.3a, the quenching efficiency of Fe^{2+} is significantly higher in the presence of CMCD, and the Stern-Volmer plot deviated significantly from linearity with CMCD present. In the case of Br^- (Figure 3.3b), the quenching efficiency decreased in the presence of CMCD, and linear Stern-Volmer plots were obtained (R^2 = 0.991 with CMCD and 0.999 without CMCD). The linear relationship indicates that only one quenching mechanism is involved. Since the negative charge on Br^- makes it unlikely to bind with either anthracene or cyclodextrin, Br^- quenching is considered to occur via a collisional mechanism. Less efficient quenching by Br^- in the presence of CMCD is the result of a protecting effect by CMCD.

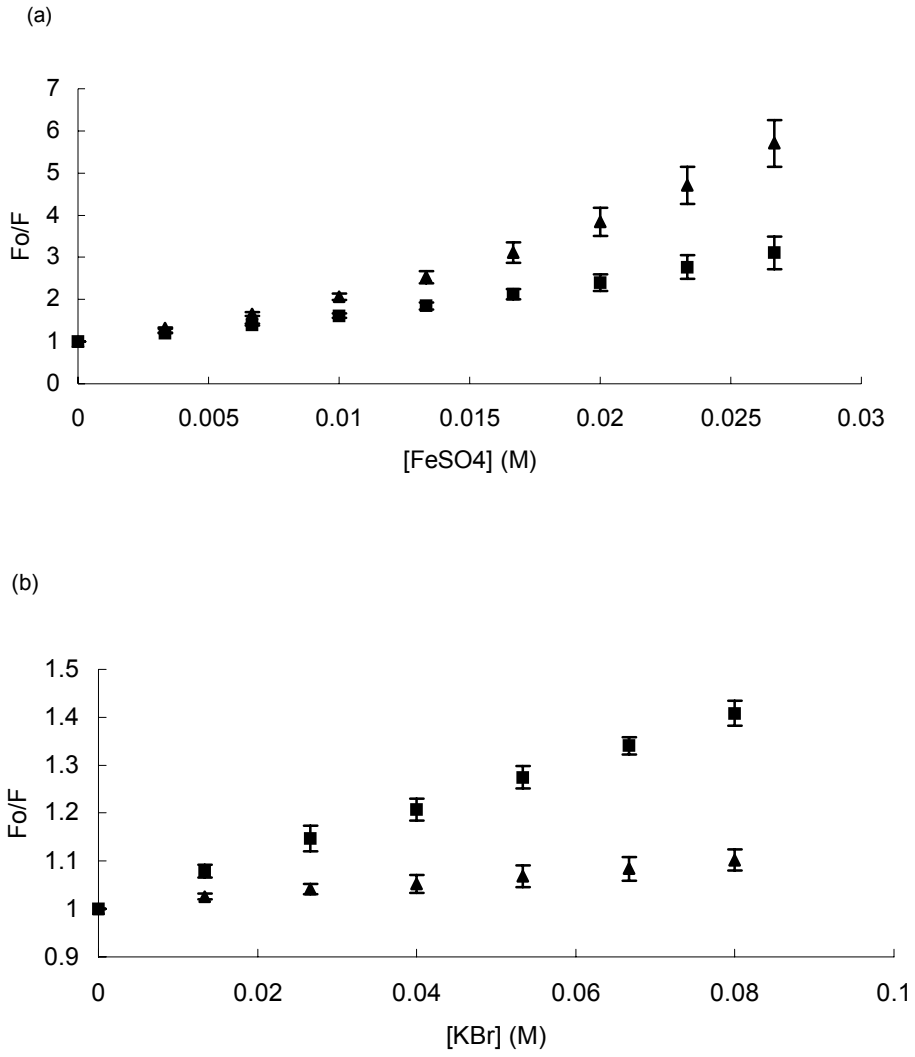

Figure 3.3 Stern-Volmer plot of anthracene (0.1 μM) quenched by (a) Fe^{2+} and (b) Br^- in aqueous solution (pH = 3.1) in the presence (▲) and absence (■) of CMCD (2 mM).

Because of electrostatic repulsion between the bromide anion and the partially negative carboxyl groups on CMCD, the bromide ion is unlikely to have close contact with the CMCD or any species included within the hydrophobic cavity. Therefore collisional quenching is decreased. A number of studies have shown that ionic species could not quench the fluorescence of aromatic compounds which were encapsulated into micelles having the same charge as the quencher[17-20]. On the contrary, the positive charge of Fe^{2+} and the metal coordinating ability of carboxylic acid groups makes it likely that iron can bind to the rim of CMCD. Such binding would lead to a higher local concentration of Fe^{2+}, and therefore result in a higher quenching efficiency. Furthermore, the non-linear result for Fe^{2+} quenching in the presence of CMCD is an indication of mixed collisional and static quenching mechanisms; the static mechanisms are only likely in the case of ternary pollutant/CMCD/Fe^{2+} complexes.

Molecular oxygen quenches almost all known fluorophores[3]. To test its interference, additional anthracene quenching experiments were carried out under low O_2 concentrations (Figure 3.4). The results were the same as those under air-equilibrated conditions, indicating that oxygen effects were not significant in these studies.

The Fe^{2+} quenching experiments were repeated with 2-naphthol (Figure 3.5). Although Fe^{2+} quenching efficiency of 2-naphthol is lower than for anthracene, the general quenching behavior in the presence and absence of CMCD were similar to that of anthracene.

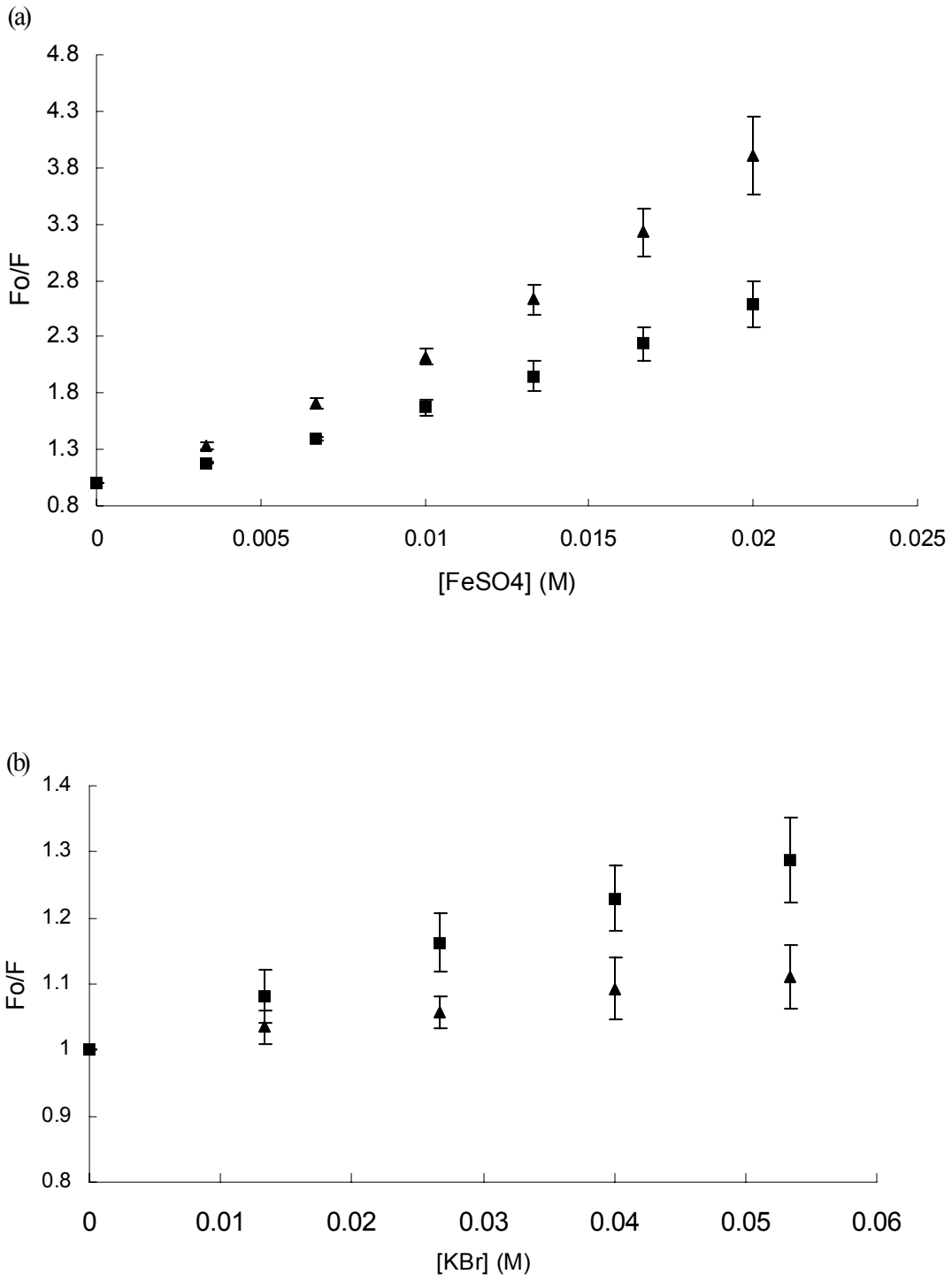

Figure 3.4 Stern-Volmer plot of anthracene (0.1 μM) quenched by (a) Fe^{2+} and (b) Br^- in aqueous solution (pH = 3.1) under low O_2 condition in the presence (▲) and absence (■) of CMCD (2 mM).

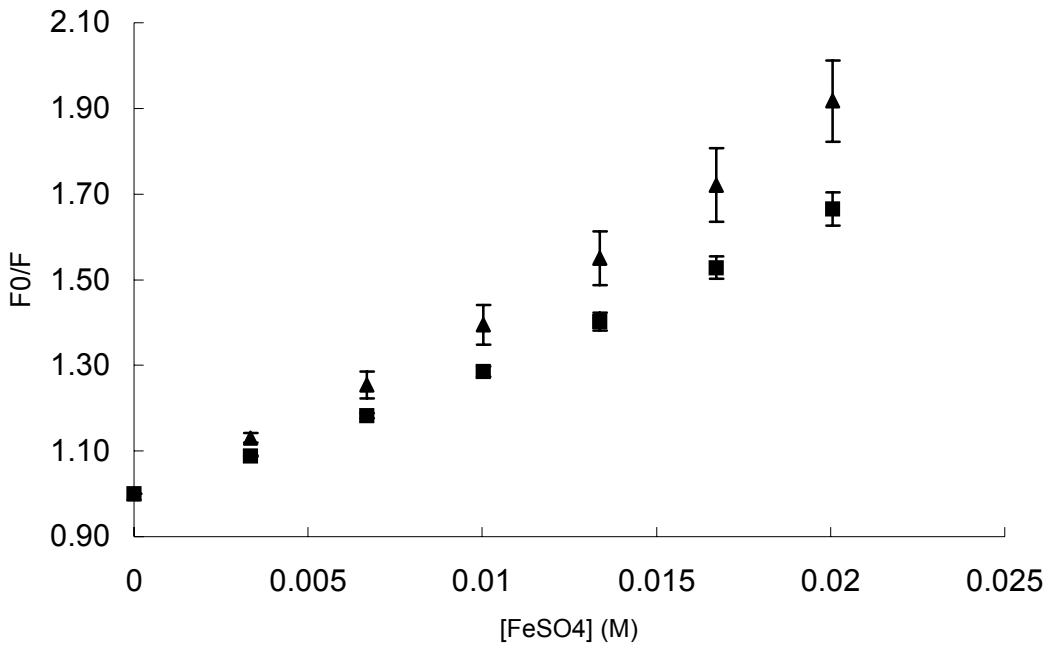

Figure 3.5 Stern-Volmer plot of 2-naphthol (10 μM) quenched by Fe^{2+} in aqueous solution (pH = 3.1) in the presence (▲) and absence (■) of CMCD (2 mM).

3.3.3.2 pH effect

Acidity of the solution affected the quenching efficiency of Fe^{2+} in the presence of CMCD. Figure 3.6 shows anthracene fluorescence quenching in pH = 1.9, 3.1, and 4.1 solutions. At pH = 1.9 the quenching was reduced compared to higher pH systems. This effect is caused by protonation of the CMCD carboxyl groups (whose pKa is assumed ~3.75 from an analog of CMCD[21]), which makes them less likely to bind iron. Furthermore, the pH = 1.9 system gave a linear Stern-Volmer plot ($R^2 = 0.995$), indicating that only a single quenching mechanism (most likely collisional) was occurring. The same pH effect was also observed in 2-naphthol fluorescence quenching studies (Figure 3.7).

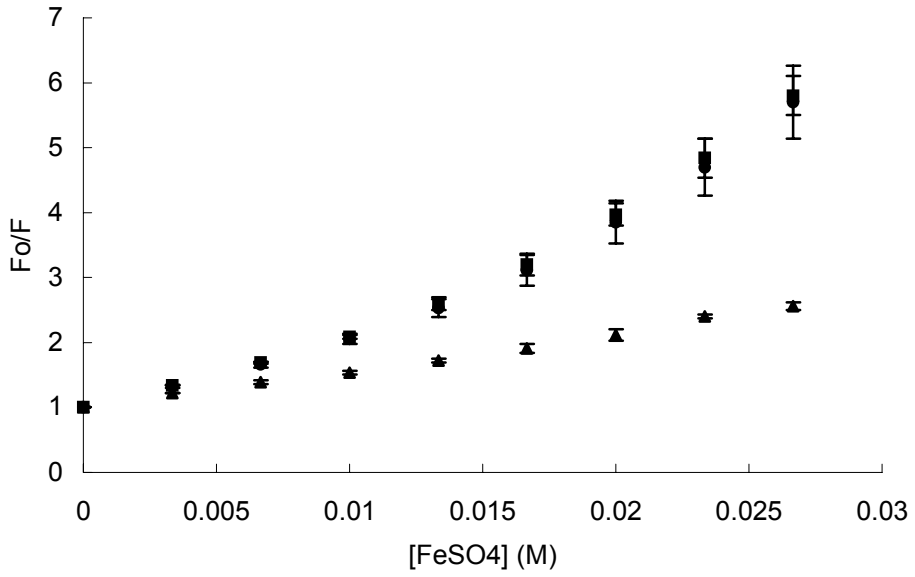

Figure 3.6 Stern-Volmer plot of anthracene (0.1 μM) quenched by Fe^{2+} in pH = 1.9 (▲), 3.1 (●), and 4.1 (■) solutions in the presence of CMCD (2 mM).

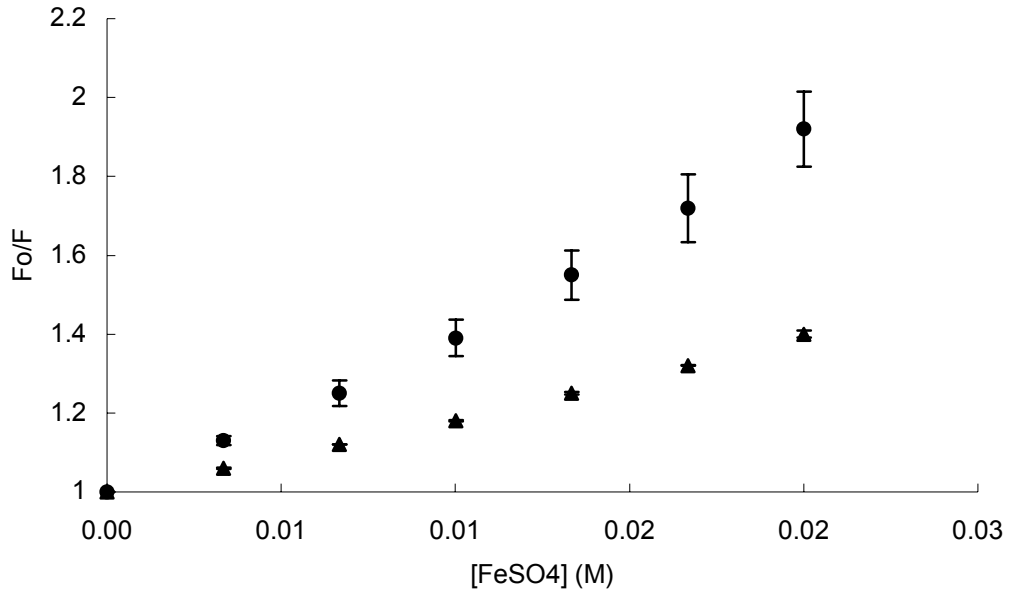

Figure 3.7 Stern-Volmer plot of 2-naphthol (10 μM) quenched by Fe^{2+} in pH = 1.2 (▲) and 3.1 (●) solutions in the presence of CMCD (2 mM).

3.3.3.3 Fluorescence quenching by Eu^{3+}

Europium (III) was also used as a fluorescence quencher in the present work. Similar to the results for iron, anthracene quenching by Eu^{3+} was significantly enhanced in the presence of CMCD (Figure 3.8). The effect for europium was more pronounced than for iron. These results are consistent with the formation of a ternary pollutant/CMCD/Eu^{3+} complex analogous to the iron containing complex.

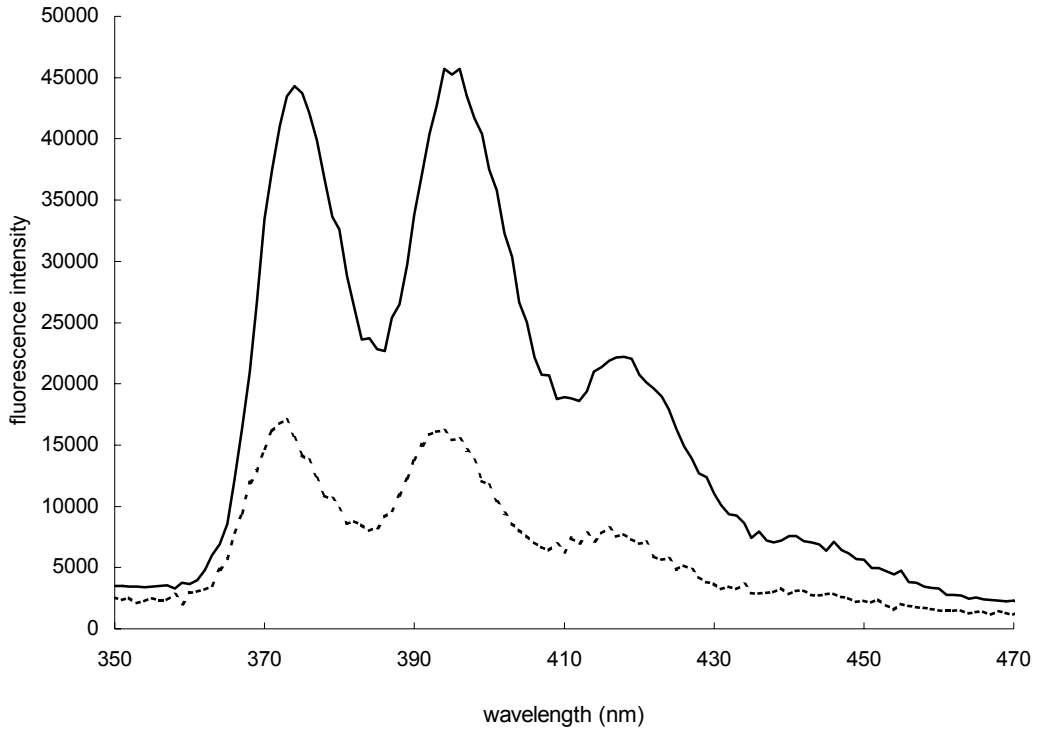

Figure 3.8 Eu^{3+} (5mM) quenching of anthracene (0.1μM) in aqueous solution (pH=3.1) in the presence (---) and absence(—) of CMCD.

3.3.4 Ca^{2+} and Cd^{2+} substitution of Fe^{2+} in fluorescence quenching experiment

For the fluorophores used in this study, Ca^{2+} and Cd^{2+} are less efficient fluorescence quenchers than Fe^{2+}. When Ca^{2+} was added to an anthracene + CMCD + Fe^{2+} solution, the fluorescence was restored by a small but statistically significant amount (Figure 3.9a). In the absence of CMCD (anthracene + Fe^{2+} solution), addition of Ca^{2+} resulted in greater quenching (Figure 3.9b). The substitution experiment was repeated with Cd^{2+} and similar results were observed (data not shown). Without CMCD, the addition of Ca^{2+} and Cd^{2+} increased the total concentration of quenchers, which resulted in greater quenching of anthracene fluorescence. In the presence of CMCD, Ca^{2+} and Cd^{2+} competed with Fe^{2+} for the binding sites on CMCD. Consequently, some of the bound Fe^{2+} was displaced by Ca^{2+} or Cd^{2+}. Since Ca^{2+} and Cd^{2+} are poorer quenchers than iron, displacement of the iron resulted in an increase in fluorescence. These effects were small, so a statistical test for Ca^{2+} substitution was used to confirm that there was a significant difference. Results of a t-test yielded $t_{calc} = 5.9$ ($n_1 = n_2 = 3$; $t_{table} = 5.598$ at 99.5% confidence and 4 degrees of freedom), indicating that the fluorescence for the anthracene + CMCD + Fe^{2+} solution before and after addition of Ca^{2+} were statistically different. To ensure the validity of these results, the intensity of fluorescence at two separate wavelengths (378 nm, 400 nm) were compared and both indicated statistical differences. (At 378 nm: $\Delta F = -2900 \pm 1400$ without CMCD and $\Delta F = +2700 \pm 800$ with CMCD; at 400nm: $\Delta F = -4379 \pm 2069$ without CMCD and $\Delta F = +1646 \pm 937$ with CMCD; ΔF is the fluorescence difference in the presence and absence of Ca^{2+}.) These results further indicate that Fe^{2+} binds in a ternary pollutant/CMCD/Fe^{2+} complex, and also indicate that iron binding to the complex is reversible.

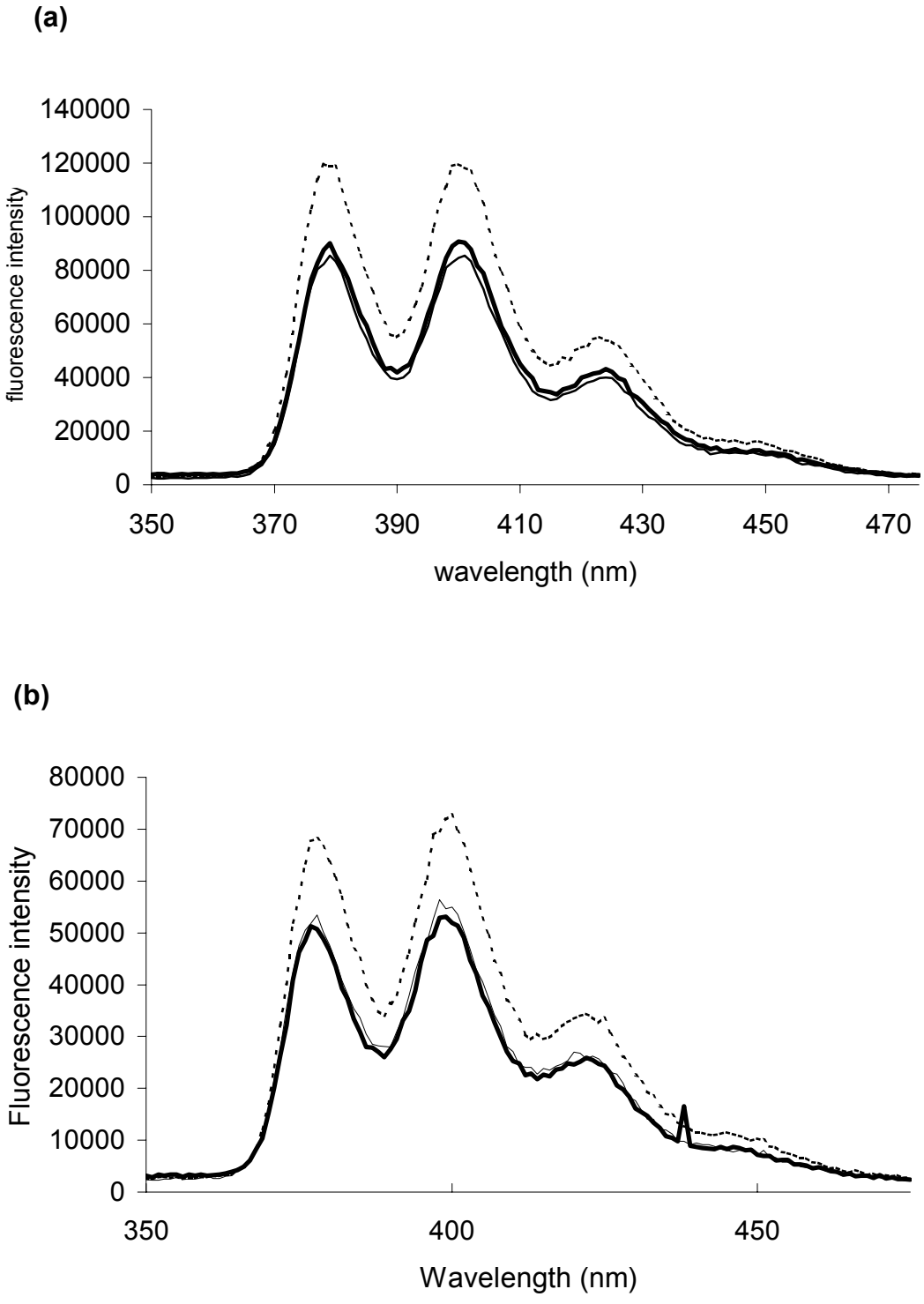

Figure 3.9 Fluorescence spectra of anthracene (---), anthracene + Fe^{2+} (—) and anthracene + Fe^{2+} + Ca^{2+} (▬) (a) in the presence of CMCD (2mM) and (b) in the absence of CMCD.

3.3.5 NMR study of interactions among 2-naphthol, CMCD and Fe^{2+}

3.3.5.1 NMR measurement of binding constant between 2-naphthol and CMCD

The binding constant between 2-naphthol and CMCD in aqueous solution was determined by a NMR titration method. To get a better understanding of the spectrum of 2-naphthol, a COSY experiment was carried out beforehand (Figure 3.10). 2-Naphthol peaks were assigned mainly according to the COSY spectrum. At the mean time, other reference has been considered too [www.aist.go.jp RIODB db004 img/hsp/W/WHSP40229.gif]. The spectrum of 2-naphthol with peak assignment was illustrated in Figure 3.11.

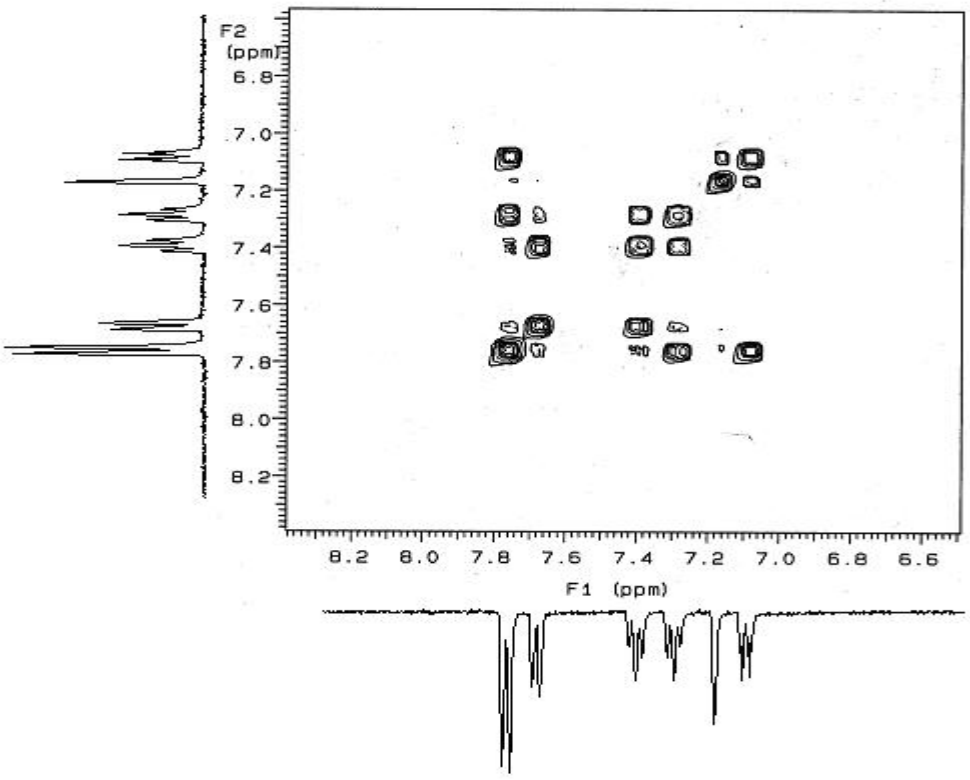

Figure 3.10 COSY NMR spectrum of 2-naphthol (2 mM).

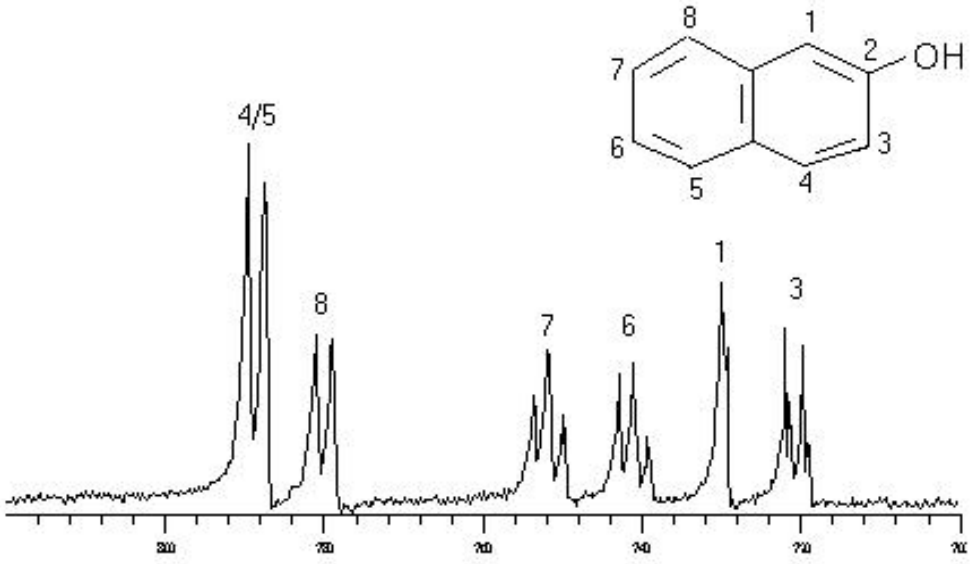

Figure 3.11 ^{1}H NMR spectrum of 2-naphthol (2mM) with peak assignment (the insert is 2-naphthol molecule structure).

In NMR titration experiments, it was found that upon addition of CMCD, the hydrogens of 2-naphthol at positions 3, 6, and 7 shifted toward high field while hydrogens at positions 1, 4, 5, and 8 shifted toward low field. These shifts indicate that the 2-naphthol molecules were binding with CMCD. A binding constant of 224 ± 10 M^{-1} was obtained. The proton shifts at position 7 on addition of CMCD were shown in Figure 3.12a. Figure 3.12b is the double-reciprocal plot for the data in Figure 3.12a, and from it the binding constant was calculated. CMCD protons also exhibited a shift in the presence of 2-naphthol (data not shown). However, due to the complex NMR spectrum of CMCD, which is a mixture with different numbers of carboxymethyl substitutions on each molecule, it is difficult to determine which CMCD protons were involved in interactions with 2-naphthol.

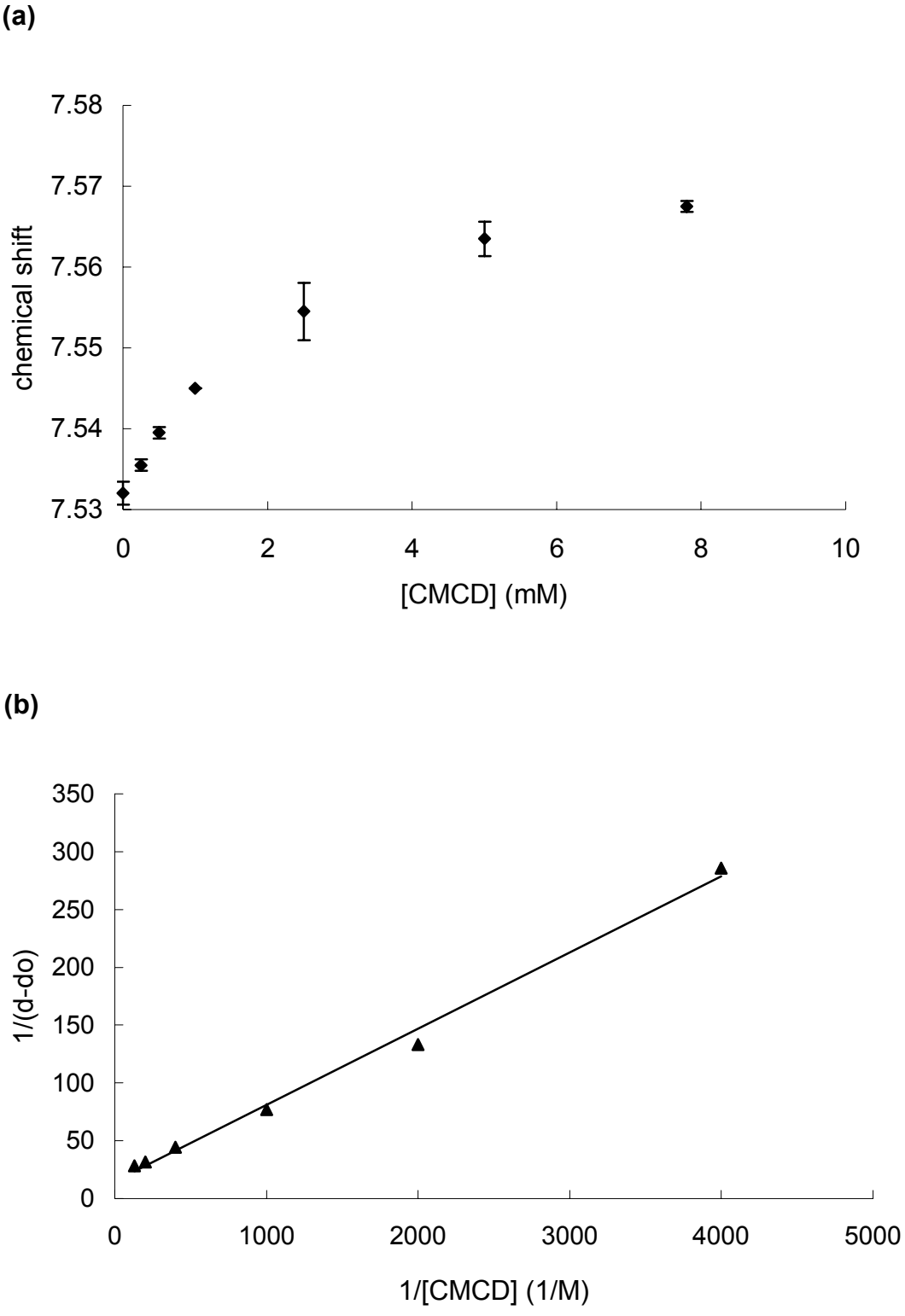

Figure 3.12 (a) Chemical shift of proton 7 in 2-naphthol on addition of CMCD and (b) double-reciprocal plot of (a) [1/(d-do) = 1/ Δ].

3.3.5.2 NMR spectra in the presence of Fe^{2+}

Fe^{2+} is paramagnetic when it coordinates with water molecules (Figure 3.13). Therefore, the peak of the protons in close proximity to it will be broadened and the chemical shift of the protons may also be changed[22-25]. Since both effects are highly dependent on the distance between Fe^{2+} and the protons, the phenomena have been employed to investigate the distance between Fe^{2+} and hydrophobic compound (2-naphthol) in the presence and absence of CMCD.

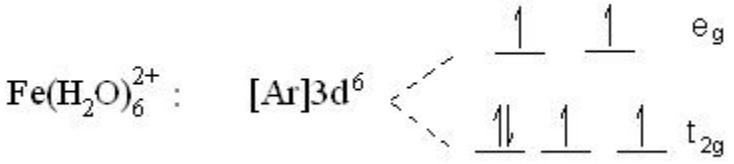

Figure 3.13 Electron distribution of Fe^{2+} when it coordinates with H_2O.

In aqueous solution of 10 mM Fe^{2+}, 2-naphthol peaks were not broadened and did not show changes in chemical shift (Figure 3.14). The apparent peak shift in this spectrum compared to Figure 3.11 is an artifact caused by a shift in the water signal used for calibration. The shift in the water signal was caused by interaction with the Fe^{2+} present in solution. Note that all the peaks in Figure 3.14 are shifted to the same extent due to an offset in the reference peak. The lack of broadening of 2-naphthol peaks indicates that Fe^{2+} is not close enough to the 2-naphthol molecules to induce such a change. In other words, the iron and 2-naphthol do not exhibit noticeable interaction.

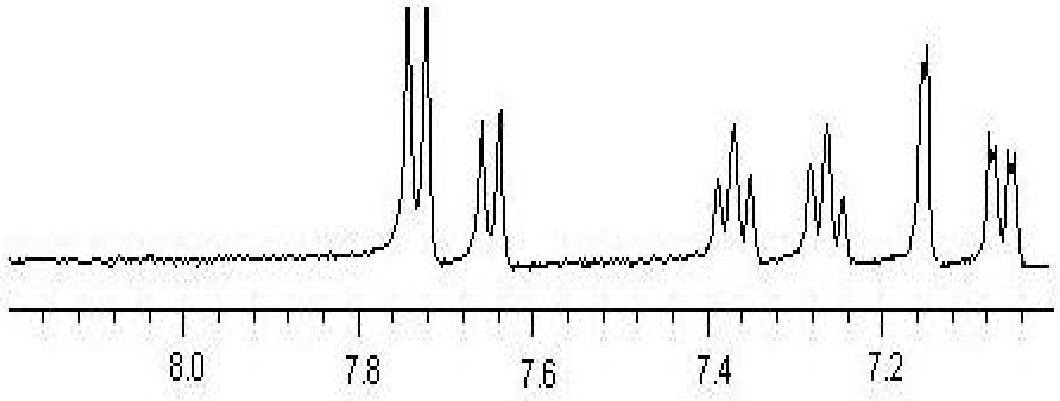

Figure 3.14 ^{1}H NMR spectrum of 2-naphthol (2mM) in the presence of Fe^{2+}(10mM).

In the presence of CMCD, 2-naphthol peaks were significantly broadened when Fe^{2+} was also present (Figure 3.15). Although there were no significant chemical shift changes, the observed broadening in peak width suggests that iron and 2-naphthol are in close proximity in this system. In the measurement, peak broadening of CMCD was also observed (Figure 3.16). Therefore, iron must be close to both species.

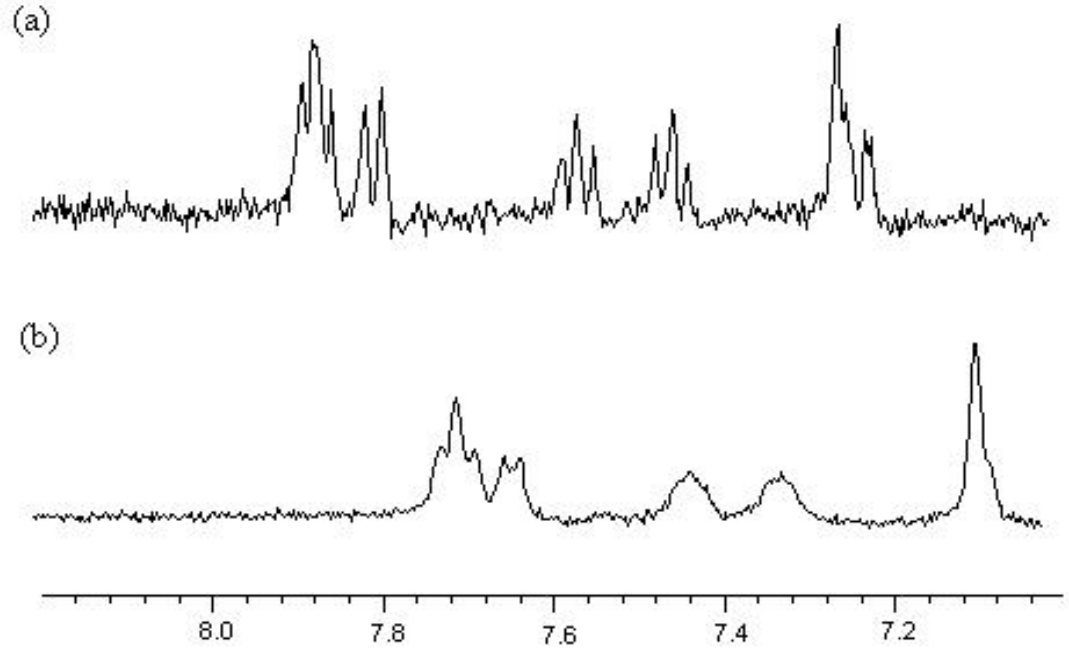

Figure 3.15 ^{1}H NMR spectra of (a) 2-naphthol (0.5mM) in the presence of CMCD (5mM) and (b) 2-naphthol (2mM) in the presence of CMCD (10mM) and Fe^{2+} (10mM).

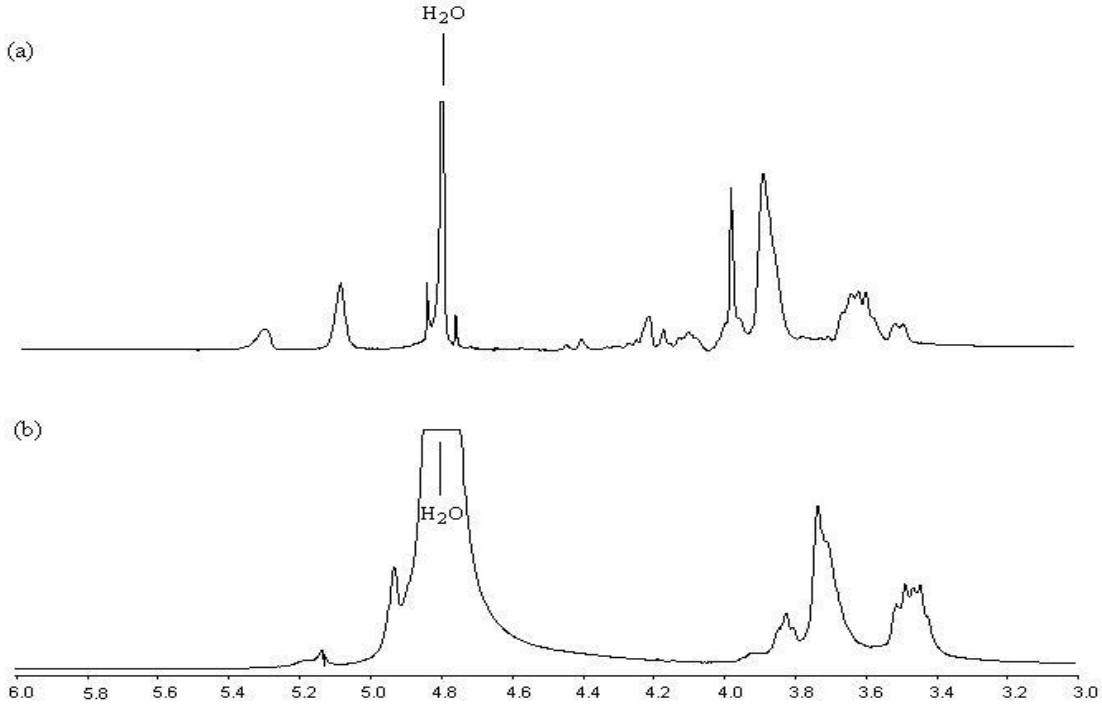

Figure 3.16 ^{1}H NMR spectra of (a) CMCD (5mM) in the presence of 2-naphthol(0.5mM) and (b) CMCD (10mM) in the presence of 2-naphthol (2mM) and Fe^{2+} (10mM).

3.3.5.3 Cd^{2+} and Ca^{2+} substitution of Fe^{2+} in NMR measurement

Ca^{2+} and Cd^{2+} are diamagnetic cations. The electronic structure of Ca^{2+} is [Ar] and that of Cd^{2+} is $[Kr]4d^{10}$. They were used to displace Fe^{2+} from CMCD binding sites. Both of these ions have been proven to bind with CMCD by the fluorescence experiments discussed above, and binding of Cd^{2+} was further proven by ^{113}Cd NMR[26-29] measurements (Table 3.1). If Fe^{2+} was displaced by Ca^{2+} or Cd^{2+}, the peak broadening effect caused by it should be weakened.

Table 3.1 Chemical shift of Cd^{2+} (0.1M) in ^{113}Cd NMR with addition of CMCD

[CMCD] (M)	0	0.01	0.05	0.1	0.5
Chemical shift of Cd^{2+}	2.356	18.337	44.869	62.911	77.052

The narrowing of 2-naphthol peaks was observed upon addition of Cd^{2+} or Ca^{2+} to the 2-naphthol + CMCD + Fe^{2+} solution. Figure 3.17 shows the spectrum of 2-naphthol in the presence of CMCD, Fe^{2+} and Cd^{2+}. Compared to Figure 3.15b (2-naphthol + CMCD + Fe^{2+}), the data in Figure 3.17 exhibit considerably less peak broadening. Ca^{2+} displacement has a similar effect (Figure 3.18), although the peak narrowing of 2-naphthol is not as significant as that in Cd^{2+} displacement. These data clearly indicate that a ternary 2-naphthol/CMCD/Fe^{2+} complex must exist in solution. Furthermore, this complex must exist in an arrangement that allows direct interaction of iron and 2-naphthol.

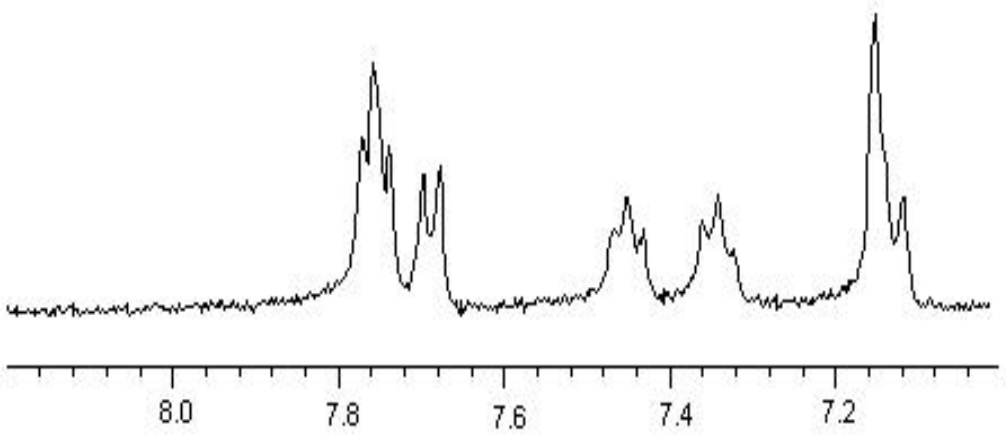

Figure 3.17 ^{1}H NMR spectra of 2-naphthol (2mM) in the presence of CMCD (10mM), Fe^{2+} (10mM) and Cd^{2+} (90mM).

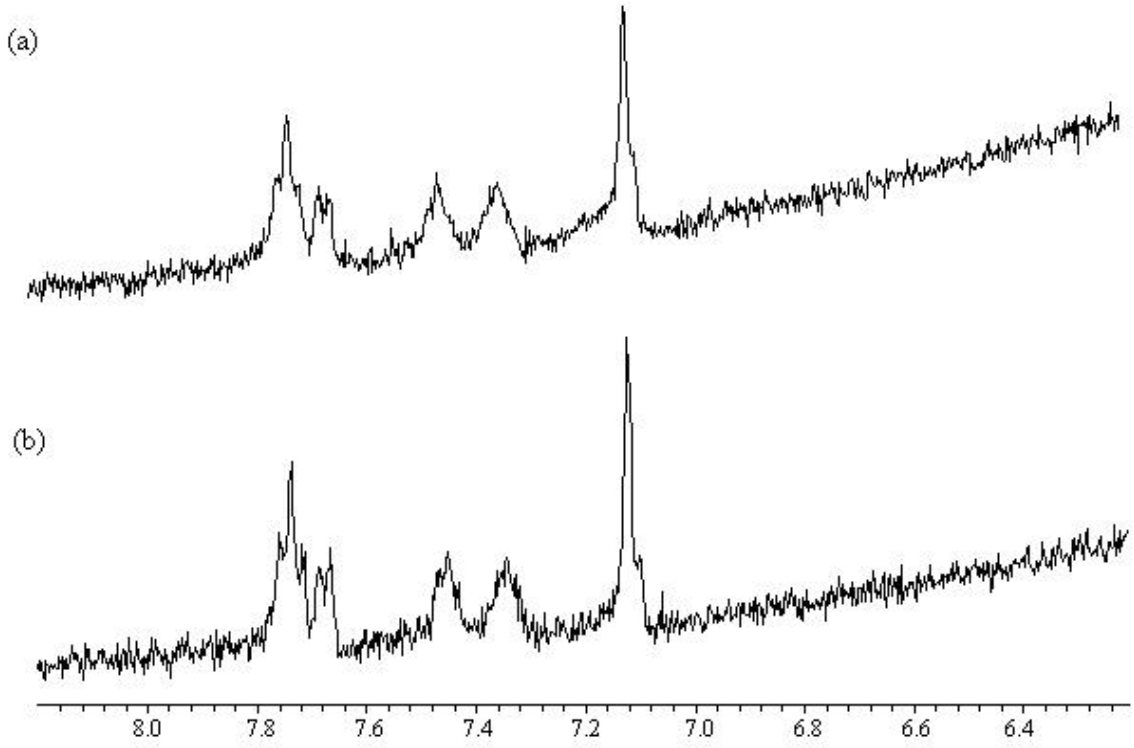

Figure 3.18 ^{1}H NMR spectra of 2-naphthol (0.5mM) (a) in the presence of CMCD (8mM) and Fe^{2+} (10mM); (b) in the presence of CMCD (8mM), Fe^{2+} (10mM) and Ca^{2+} (90mM).

As additional control experiments, NMR spectra were recorded for the ternary systems using Ca^{2+} or Cd^{2+} instead of Fe^{2+} as the binding cations. Because Ca^{2+} and Cd^{2+} are diamagnetic, they cannot cause NMR peak broadening due to paramagnetic effects. The NMR spectra of 2-naphthol + CMCD + Cd^{2+} (Figure 3.19) and 2-naphthol + CMCD + Ca^{2+} (data not shown) did not exhibit any observable peak broadening or shift in 2-naphthol peak positions. The peak broadening observed with Fe^{2+} is therefore believed to be due to an interaction between the paramagnetic iron and the naphthol molecule. Since this interaction was only observed in the presence of CMCD, the CMCD must play a substantial role in mediating the iron-naphthol interaction.

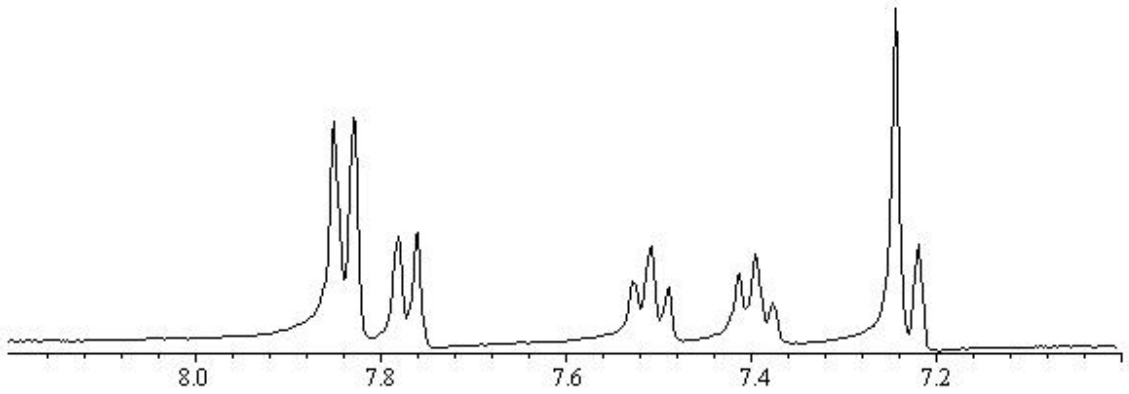

Figure 3.19 ^{1}H NMR spectra of 2-naphthol (2mM) in the presence of CMCD (10mM) and Cd^{2+} (50mM).

3.3.5.4 2D NMR ─ NOESY and ROESY experiments

To get more detailed information about the structure of the ternary complex CMCD/Fe^{2+}/hydrophobic compound, NOESY 2D NMR experiment with βCD and 2-naphthol was carried out. The use of βCD instead of CMCD is to make the spectra easier to interpret. To avoid peak broadening, Fe^{2+} was not added at first. However, the NOESY spectrum did not show any interactions between 2-naphthol and βCD (data not shown). This result is not due to the lack

of interaction between the two because it has been determined that the binding constant of the two is about $600M^{-1}$.[30] The result could be due to the NOESY technique itself. In NOESY experiment, NOE (nuclear overhauser effect) will be zero if the product of frequency of the applied magnetic field (ω) and the rotational correlation time of the molecule (τ_c) equals 1.12 ($\omega\tau_c = 1.12$)[31]. The rotational correlation time can be roughly estimated by equation 2.12 (Stokes-Einstein-Debye model)[32]:

$$\tau_c = (V\eta) / (kT) \qquad (3.15)$$

where V is the volume of the host molecule, η is the viscosity of the solvent, k is Boltzman constant, and T is the temperature. If βCD is treated as a spherical molecule, the volume of it can be calculated using:

$$V = 4/3\ (\pi r^3) \qquad (3.16)$$

The radii (r) of βCD is about 7.6 Å. In the magnetic field of 500 MHz, under temperature 295K and in the solvent D_2O, the calculated product of ω and τ_c is about 1.43. This result is very close to 1.12, which means that the NOE of the system is very small. If the interaction between 2-naphthol and βCD is not strong enough, little interaction signal between the two can be detected.

ROESY experiment which gives similar information as NOESY does not have such a limitation. Therefore, ROESY NMR was carried out with 2-naphthol and βCD. However, again, the spectrum showed no evidence of interaction between the two. This result has been partly attributed to the fact that the interaction of 2-naphthol with βCD is not very strong. 1D NMR of the binary complex shown in Figure 3.20 illustrates that the binding of the two is in a moderately slow exchange range. The exchange speed of two species between their complexed state and free state is probably too fast for ROESY NMR to detect. Therefore, the further plan of 2D NMR with ternary complex (addition of metal ion) was given up.

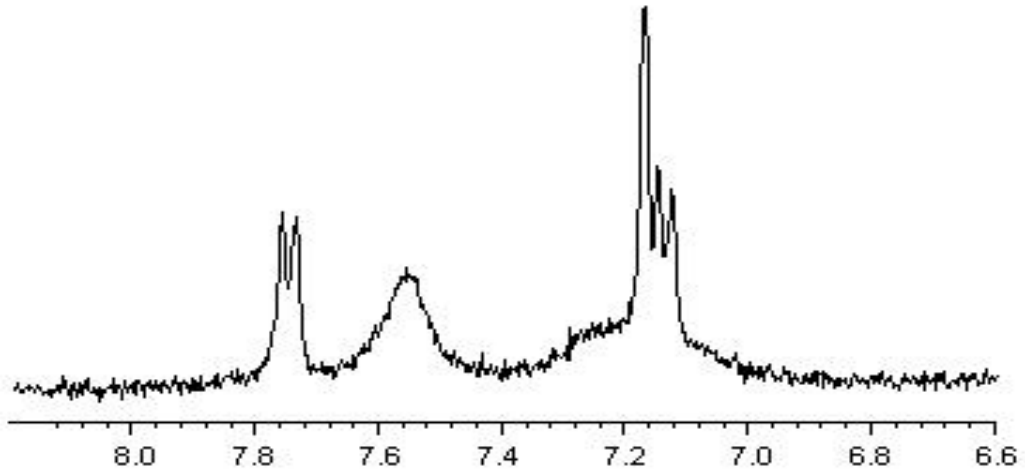

Figure 3.20 ^{1}H NMR spectra of 2-naphthol (2mM) in the presence of βCD (4mM).

3.3.6 Intended FRET experiment

FRET is another method that had been intended to get more structure information about the ternary complex — estimate the distance between Fe^{2+} and hydrophobic molecule in the presence of CMCD. The donor molecule chosen was anthracene and the acceptor was Eu^{3+}. The selection of these two species to be donor and acceptor pair is because that the excitation of Eu^{3+} overlaps the emission of anthracene and the maximum excitation and emission of Eu^{3+} are far separated (Figure 3.21). Additionally, Eu^{3+} is also a metal ion. It could coordinate with CMCD as Fe^{2+}. The similarity between the two ions makes it reasonable to estimate anthracene-Fe^{2+} distance from anthracene-Eu^{3+} distance. Although Eu^{3+} quenches the fluorescence of anthracene, resonance energy transfer between the two species can still be detected if the fluorescence emission of Eu^{3+} was enhanced by the excitation of anthracene.

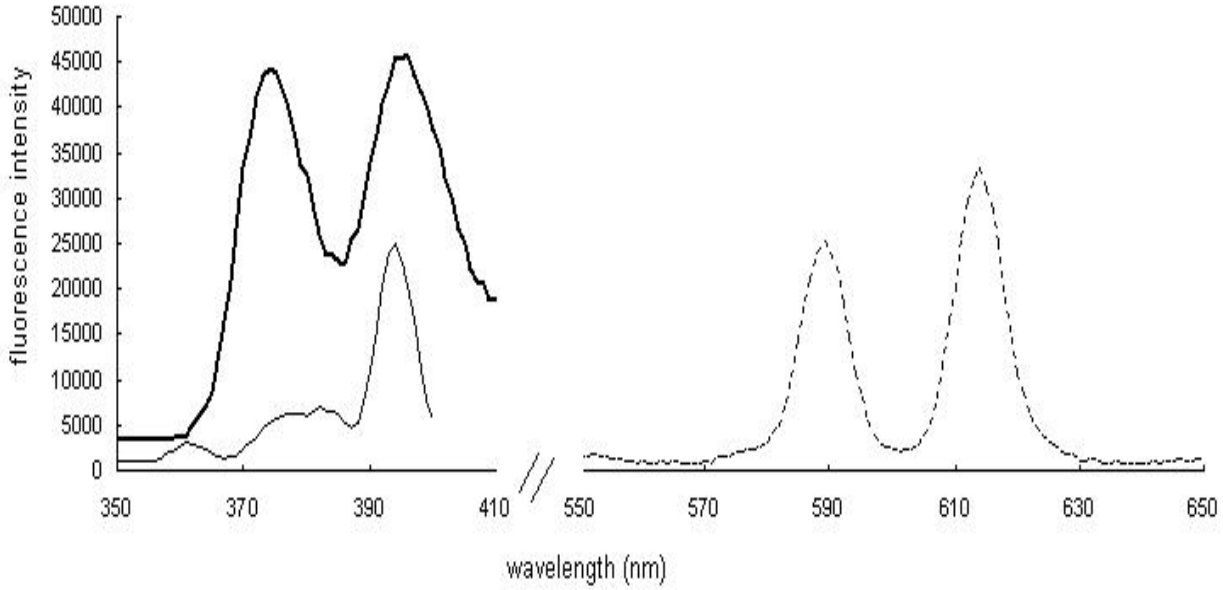

Figure3.21 Fluorescence emission spectrum of anthracene (—), excitation spectrum of Eu^{3+}/CMCD (—) and emission spectrum of Eu^{3+}/CMCD (---).

However, the results show that by excitation of anthracene at 250nm, no fluorescence emission of Eu^{3+} was observed in the presence of CMCD (data not shown). It indicates that FRET does not occur between anthracene and Eu^{3+} or the energy transfer efficiency is quite low between the two species. In addition, Eu^{3+} quenches the fluorescence of anthracene which makes resonance energy even less available for transferring.

3.3.7 More discussion on degradation results observed in Chapter 2

From the investigation in this chapter, we understand that ternary complexes — CMCD/Fe^{2+}/certain hydrophobic compounds, were formed in aqueous solution. The formation of the complexes improved Fenton degradation by pulling the pollutants and catalyst closer. In CMCD enhanced PAHs degradation, the geometry of the ternary complexes must be favorable in order to enhance the interaction of hydroxyl radical with PAH molecules. The proposed

mechanics is shown in Figure 3.22a. As a result, CMCD improved the degradation efficiency even though it could act as a scavenger and inhibit the decomposition of hydrogen peroxide.

In the degradation of malathion etc. that was discussed in Chapter 2, however, addition of CMCD did not enhance the degradation. A possible reason is that CMCD did not function as a bridge to bring the pollutants and Fe^{2+} together in such a system. On the contrary, it could isolate the two species. All five compounds investigated in Chapter 2 bear hetero atoms such as S, P and N. These atoms have lone electron pairs therefore they have potential to coordinate with Fe^{2+}. If the pollutants contacted the catalyst directly, the degradation would be most favored. The addition of CMCD, under such circumstances, would disturb the binding between pollutants and Fe^{2+}. CMCD became a binding competitor with the pollutants and therefore inhibited the degradation. This situation is illustrated in Figure 3.22b. The results of degradation under different pH support above arguments (section 2.3). When pH of the degradation system was raised from 2.5 to about 6, the degradation in the presence of CMCD was less significant while that in the absence of CMCD was not influenced. In the solution with a higher pH value, carboxymethyl groups on CMCD dissociated more so they have a higher coordination potential to Fe^{2+}. As a result, less Fe^{2+} was available to the pollutant molecules. The degradation was thus reduced.

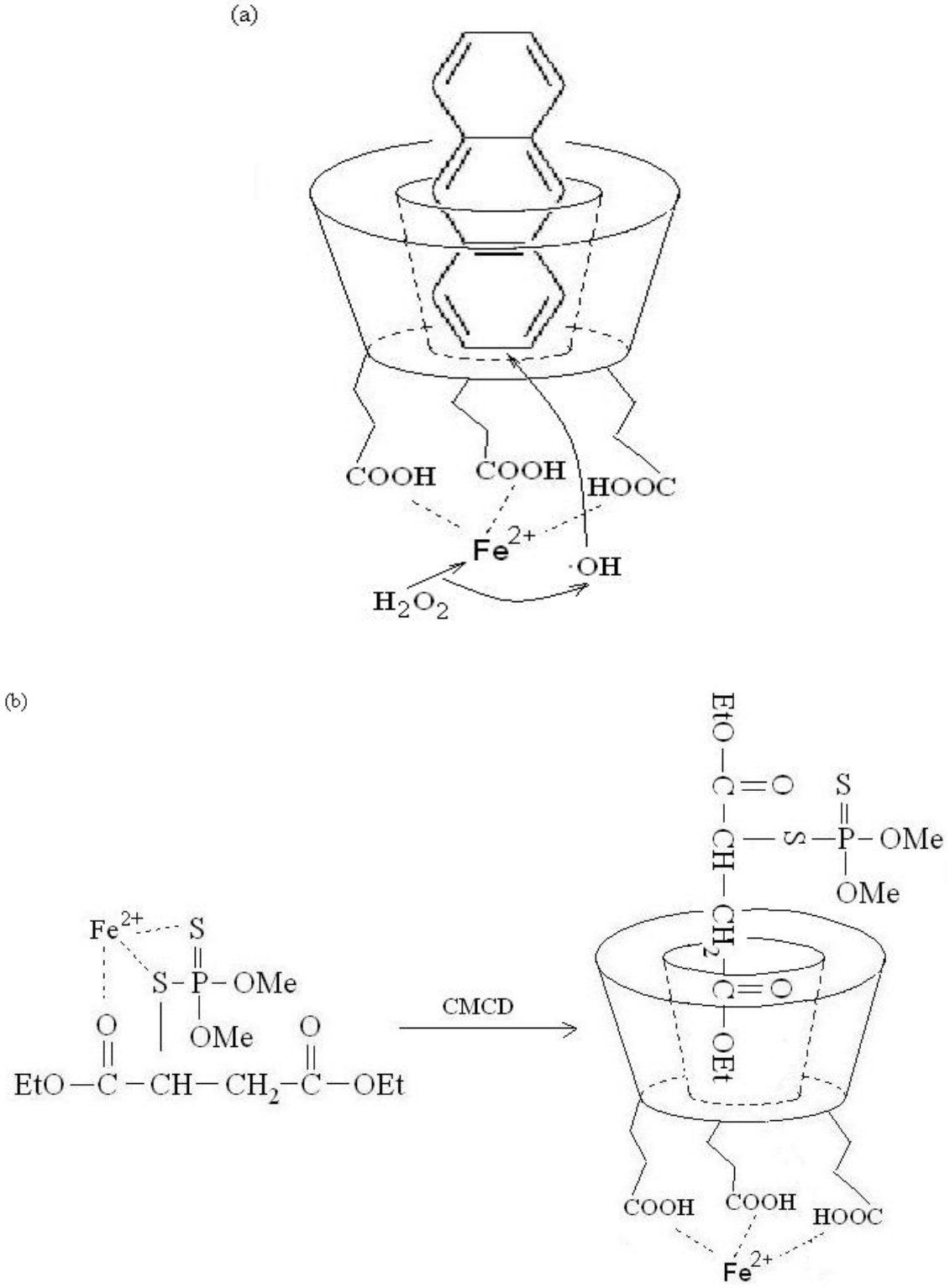

Figure 3.22 (a) Proposed mechanics of CMCD enhanced Fenton degradation and (b) possible inhibition mechanics of CMCD in malathion degradation.

3.4 References

1. Harris, D.C. *Quantitative Chemical Analysis*, 5th ed.; Freeman: New York, 1999, pp 550-554.
2. Kenneth A. Connors *Binding Constants: The Measurement of Molecular Complex Stability,* John Wiley & Sons, 1987.
3. Joseph, R. L. *Principles of Fluorescence Spectroscopy*, Plenum Press*,* New York, 1983*,* pp 258-275.
4. Govil, G. and Hosur R.V. "*Conformation of Biological Molecules*" in *NMR Basic Principles and Progress*, edited by Diehl, P.; Fluck, E.; and Kosfeld, R., vol.20, pp 30-34.
5. Bloembergen, N. *Phys. Rev*. 1950, 79, 179.
6. Bloembergen, N. *J. Chem. Phys*. 1957, 27,572.
7. Solomon, I. *Phys. Rev*. 1955, 99, 559.
8. Joseph, R. L. *Principles of Fluorescence Spectroscopy*, Plenum Press*,* New York, 1983*,* pp 367-390.
9. Selvin, P.R.; Rana, T.M.; and Hearst, J.E. *J. Am. Chem. Soc*. 1994, 116, 6029-6030.
10. Sueda, S.; Yuan, J. and Matsumoto, K. *Bioconjugate Chem.* 2000, 11, 827-831.
11. Cooper, M.E. and Sammes, P.G. *J.Chem. Soc.,Perkin Trans. 2*, 2000, 1695-1700.
12. Uwe Schobel; Hans-Joachim Egelhaaf; Andreas Brecht; Dieter Oelkrug; and Günter Gauglitz *Bioconjugate Chem.* 1999, 10, 1107-1114.
13. Park, H.; Mayer, B.; Wolschann, P.; Kőhler, G. *J. Phys. Chem*. 1994, 98, 6158.
14. Yorozu, T.; Hoshino, M.; Imamura, M.; Shizuka, H. *J. Phys. Chem*. 1982, 86, 4422.
15. Blyshak, L; Dodson, K.Y.; Patonay, G.; Warner, I.M.; May, W.E. *Anal.Chem*. 1989, 61, 955.
16. Agbaria, A. R.; Uzan, B.; Gill, D. *J. Phys. Chem.* 1989, 93, 3855.

17. Hautala, R. R.; Schore, E. N.; Turro, J. N. *J. Am. Chem. Soc.* 1973, 95, 5508.

18. Pownall, J. H.; Smith, C. L. *Biochemistry,* 1974, 13, 2594.

19. Quina, H. F.; Toscano, G. V. *J. Phys. Chem*. 1977, 81, 1750.

20. Eftink, R. M.; Ghiron, A. C. *J. Phys. Chem*. 1976, 80, 486.

21. Uekama, K.; Horiuchi, Y.; Irie, T.; Hirayama, F. *Carbohydrate Research* 1989, 192, 323.

22. Cohn, M.; Hughes, R. T. *J. Biol. Chem*. 1962, 237, 176.

23. Edited by Waugh, S. J. *Advances in Magnetic Resonance* volume 1, Academic Press: New York, 1965, pp 103-148.

24. Dickinson, C. W. *Phys. Rev.* 1951, 81, 717.

25. Phillips, D. W.; Looney, E. C.; Ikeda, K. C. *J. Chem. Phys.* 1957, 27, 1435.

26. Otto, W.H.; Carper, W. R. and Larive, C. K. *Environ. Sci. Technol.* 2001, 35, 1463-1468.

27. Otto, W.H.; Burton, S.D.; Carper, W. R. and Larive, C. K. *Environ. Sci. Technol.* 2001, 35, 4900-4904.

28. Li, J.; Perdue, E. M. and Gelbaum, L.T. *Environ. Sci. Technol.* 1998, 32, 483-487.

29. Larive, C. K.; Gogers, A.; Morton, M.; and Carper, W.R. *Environ. Sci. Technol.* 1996, 30, 2828-2831.

30. H. Park, B. Mayer, P. Wolschann and G. Koehler, *J. Phy. Chem.,* 1994, 98, 6158.

31. Neuhaus, D.; and Williamson, M. *The Nuclear Overhauser Effect in Structural and Conformational Analysis* VCH publishers Inc., 1989.

32. René T. Boeré and R. Garth Kidd *Ann. Rep. NMR Sepc.* Vol 13, pp 319-337.

Chapter 4. Assessment of ternary complexes of iron, hydrophobic pollutants and several other cyclodextrins in aqueous solution

4.1 Introduction

Since it has been proven that ternary complexes can be formed in aqueous solution among iron, certain hydrophobic pollutants and CMCD[1], the next step is to explore some other cyclodextrins as potential additives to enhance the Fenton degradation. The different sizes and modifications in cyclodextrins could change their association behavior with the iron and pollutants, thus further influencing their degradation enhancing effect. In this chapter, four more cyclodextrins have been examined: hydroxypropyl-β-cyclodextrin (HPCD), sulfated- β-cyclodextrin (SCD), underivitized β-cyclodextrin (βCD) and underivitized α-cyclodextrin (αCD). Anthracene and 2-naphthol were kept as the hydrophobic pollutant models. The techniques employed are mostly the same as those in Chapter 3 except for that fluorescence titration has been used as a substitution method for NMR titration in deterimining binding constants.

In fluorescence titration, addition of ligands could lead to enhancement or reduction of fluorescence intensity of the solution. The intensity change is due to the fact that the interaction between the substrate and the ligand changes the quantum yields of the fluorophore. Under the condition of 1:1 binding equilibrium, in which the complex and the substrate are fluorescent, the increase or decrease in intensity can be expressed by the equation[2]:

$$F_0 / F = (1 + K[L]) / (1 + aK[L]) \qquad (4.1)$$

where F_0 and F are the fluorescence intensity in the absence and presence of ligands respectively; [L] is the concentration of free ligands (non-bound); K is the binding constant; $a = \varepsilon_{CX}\varphi_{CX} / \varepsilon_S\varphi_S$ (ε_{CX} and ε_S are the absorptivities of the substrate in its complexed and free forms, φ_{CX} and φ_S are

the quantum yields of the substrate in its complexed and free forms). This equation can be linearized to:

$$1 / (F_0/F - 1) = a / (1 - a) + 1 / [(1 - a)K[L]] \qquad (4.2)$$

When the amount of added ligand is much larger than the substrate in the solution, [L] ≈ total concentration of L. Under these conditions, the plot of $1 / (F_0/F - 1)$ versus 1/[L] is a straight line. The binding constant can be calculated from the slope and the intercept: K = (intercept + 1) / slope.

4.2 Experimental

Sulfated-β-cyclodextrin (average degree of substitution = 9) and anthracene (99+%), were obtained from Aldrich. Hydroxypropyl-β-cyclodextrin (average degree of substitution = 5) and β-cyclodextrin were obtained from Cerestar. α-cyclodextrin was obtained from Sigma. Ferrous sulfate heptahydrate was obtained from J.T. Baker. 2-naphthol (99+%) was obtained from EM Science. All reagents were used as received. Purified water for the preparation of aqueous solutions was obtained from a Barnstead NanopureUV water treatment system.

Aqueous solutions of anthracene and 2-naphthol with and without cyclodextrins were prepared in the same way described in the experimental section of Chapter 3.

Fluorescence spectra were recorded with a Photon Technology International QM-1 fluorometer. Aliquots (3mL) of aqueous anthracene or 2-naphthol solutions were placed in a quartz cuvette and were subsequently modified by consecutive additions of 10 μL aliquots of $FeSO_4$ (aq) or cyclodextrins (aq). The sample was stirred by a magnetic stirring bar throughout the whole period of measurement. In total 60-80 μL of iron or cyclodextrin solution was added for each experiment.

^{1}H NMR spectra were recorded using Varian Unity 400 and 500 spectrometers operating at 400 or 500 MHz. D_2O was used as the solvent and trace H_2O served as an internal standard.

4.3 Results and discussion

4.3.1 Hydroxypropyl-β-cyclodextrin

The binding constant of HPCD and 2-naphthol was measured by the fluorescence titration method[2]. Figure 4.1a shows the fluorescence enhancement of 2-naphthol upon addition of HPCD. Figure 4.1b is the linearized plot of data in 4.1a according to equation (4.2). The good linear fit ($R^2 = 0.9973$) of the data shows that the binding between HPCD and 2-naphthol was in a 1:1 ratio. The calculated binding constant was 173 ± 28 M^{-1}. The measurement of binding constant between HPCD and anthracene was also carried out. However the increase of fluorescence was not observed upon addition of the cyclodextrin. On the contrary, a small fluorescence quenching was observed. Due to the sensitivity of anthracene to many fluorescence quenchers such as O_2, the fluorescence quenching was attributed to quenchers in the solution. Although HPCD may also quench the fluorescence of anthracene, the interference of other quenchers makes this method difficult to give an accurate binding constant between anthracene and cyclodextrins. However, we still assume that anthracene has a binding with HPCD according to the same reason described in Chapter 3.

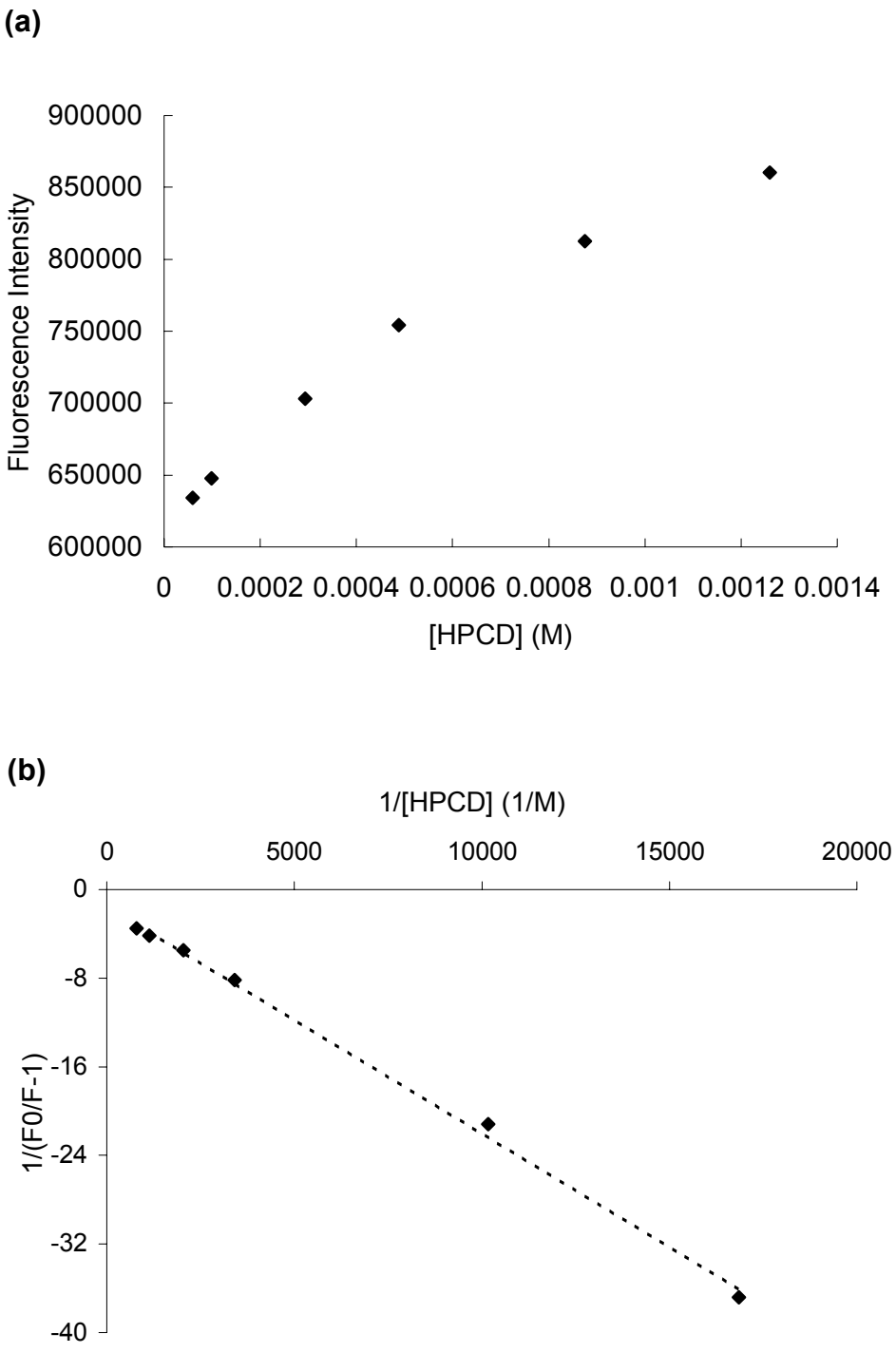

Figure 4.1 (a) Fluorescence titration of 2-naphthol (50 μM) with HPCD in aqueous solution (excitation at 326 nm and emission at 360 nm). (b)The linear plot obtained from (a) using Equation 4.2.

Fluorescence quenching experiments were carried out to investigate the geometry of the three species: HPCD, anthracene or 2-naphthol and Fe^{2+} in aqueous solution. Figure 4.2 and 4.3 show the Stern-Volmer plots of Fe^{2+} quenching of anthracene and 2-naphthol in the presence and absence of HPCD respectively. As clearly shown in the figures, the quenching efficiencies of both species were not influenced by the presence of HPCD. This result suggests minimal binding of Fe^{2+} with HPCD. The most reasonable binding sites are the hydroxyl groups located on the ends of the cavity. Metal binding by hydroxyl groups has been reported for mono- and disaccharides[3,4]. Since hydroxyl groups have a very small pKa, we assume that lowering the pH of solution would not change the quenching behavior of Fe^{2+}(Figure 4.4), contrary to the observation in the similar experiments with CMCD (Chapter 3). The stability of the quenching as a function of HPCD concentration suggests that HPCD does not effectively alter the accessibility of iron to the anthracene and 2-naphthol.

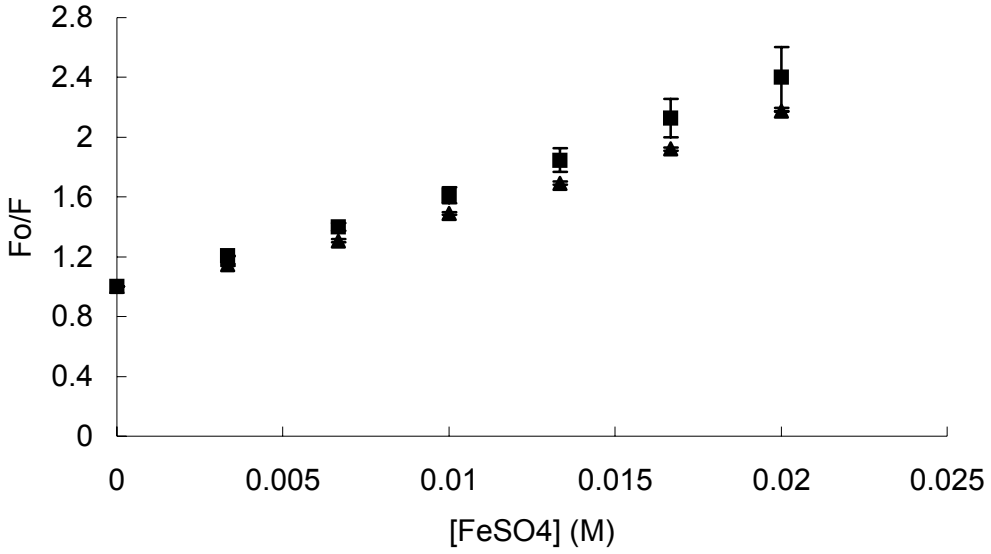

Figure 4.2 Stern-Volmer plot of anthracene (0.1 μM) quenched by Fe^{2+} in aqueous solution (pH = 3.1) in the presence (▲) and absence (■) of HPCD (2 mM).

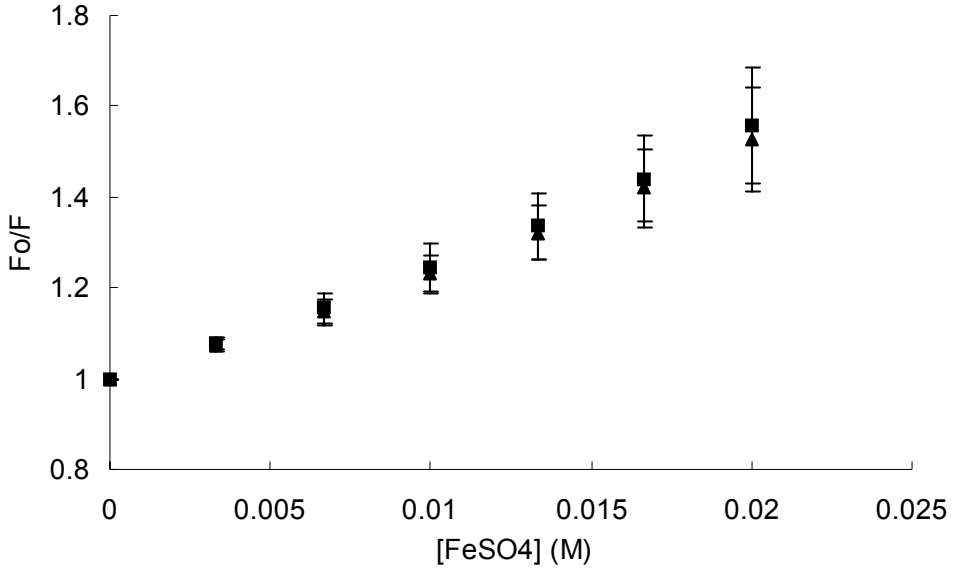

Figure 4.3 Stern-Volmer plot of 2-naphthol (50 μM) quenched by Fe^{2+} in aqueous solution (pH = 3.1) in the presence (▲) and absence (■) of HPCD (2.5 mM).

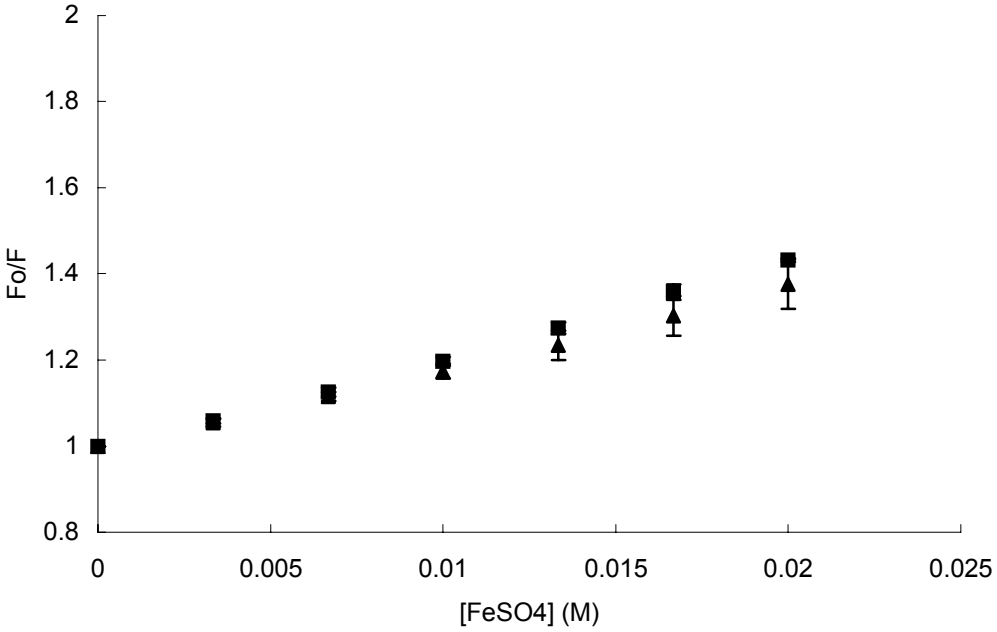

Figure 4.4 Stern-Volmer plot of 2-naphthol (50 μM) quenched by Fe^{2+} in aqueous solution (pH = 1.2) in the presence (▲) and absence (■) of HPCD (2.5 mM).

To further confirm the above observations, NMR measurements of 2-naphthol + HPCD solutions were carried out in the presence of Fe^{2+}. In aqueous solutions of 10 mM Fe^{2+}, 2-naphthol peaks (7-8 ppm) and HPCD peaks (1-5 ppm) were not broadened and did not show changes in chemical shift (Figure 4.5). The apparent peak shift in spectrum 4.5b is an artifact caused by a shift in the water signal used for calibration (see Chapter 3). The lack of broadening of 2-naphthol and HPCD peaks indicates that Fe^{2+} is not close enough to either species to induce such changes. This observation is in agreement with the fluorescence quenching results.

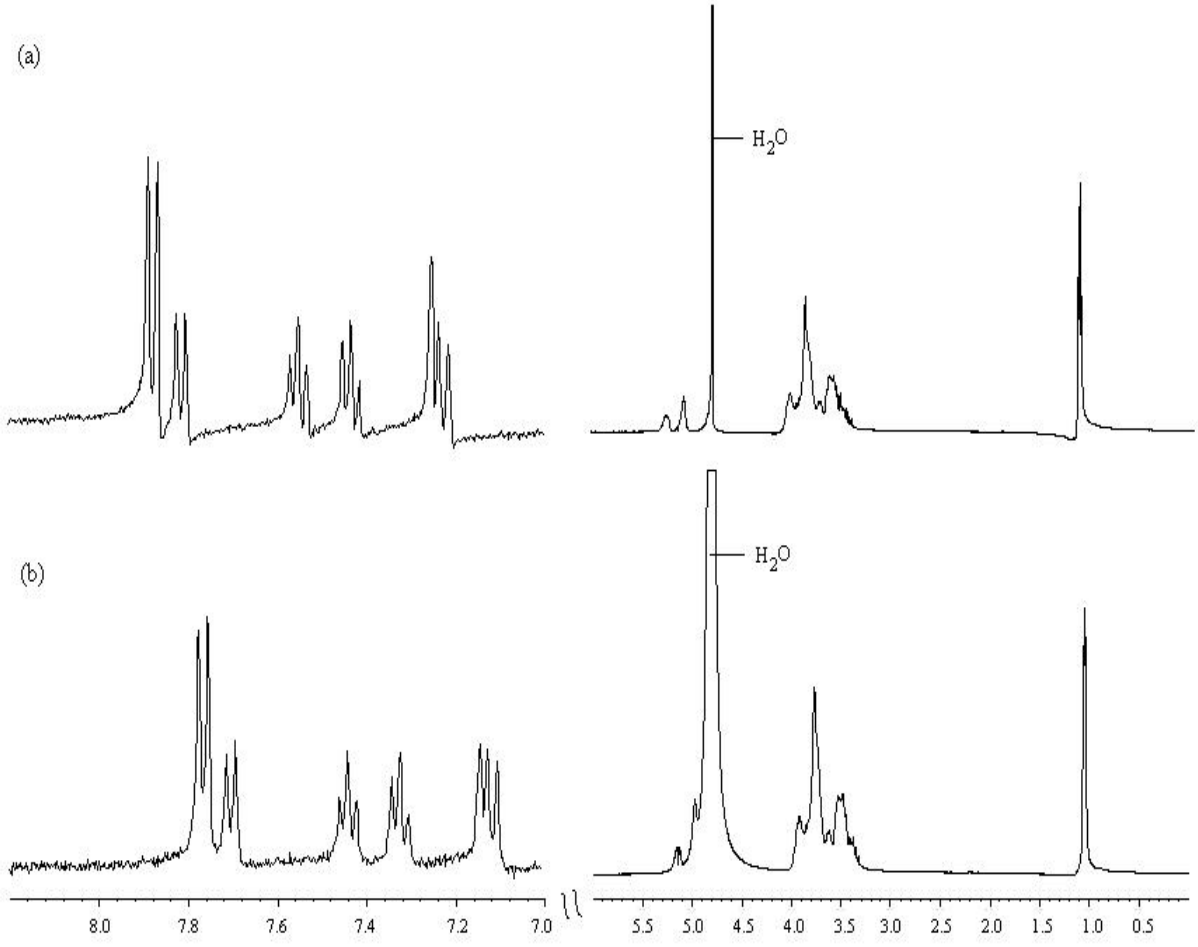

Figure 4.5 ^{1}H NMR spectra of 2-naphthol (1 mM) + HPCD (10 mM) (a) in the absence and (b) in the presence of Fe^{2+} (10 mM).

4.3.2 Sulfated-β-cyclodextrin

The measurement of the binding constant of SCD and 2-naphthol was attempted using the fluorescence titration method as used for HPCD. However, the fluorescence intensity of the solution did not change with addition of SCD. This result indicates that there is no significant interaction between 2-naphthol and SCD. The possible reason lies in the high substitution degree of the cyclodextrin. With an average 9 sulfate groups substituted on each cyclodextrin, the entrances to the cavity are very likely blocked because the sulfate groups are much more bulky than the hydroxyl groups present in the underivatized cyclodextrin. Furthermore, the presence of multiple charged groups at the rim of the cyclodextrin could contribute to a decrease in the hydrophobicity of the cavity.

In agreement with above observations, the fluorescence quenching efficiency of Fe^{2+} on anthracene (Figure 4.6) or 2-naphthol (Figure 4.7) fluorescence was neither enhanced nor decreased in the presence of SCD.

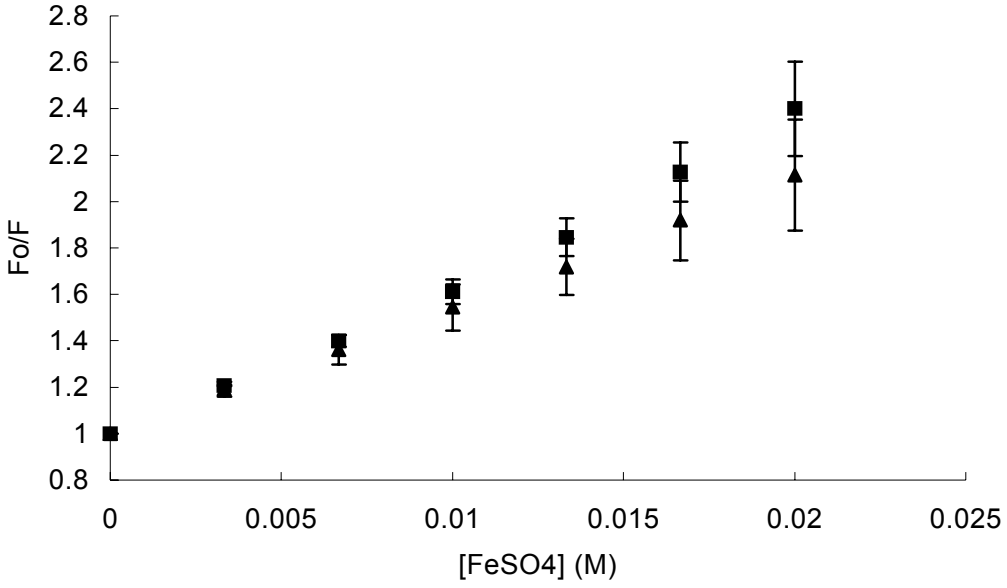

Figure 4.6 Stern-Volmer plot of anthracene (0.1 μM) quenched by Fe^{2+} in aqueous solution (pH = 3.1) in the presence (▲) and absence (■) of SCD (2 mM).

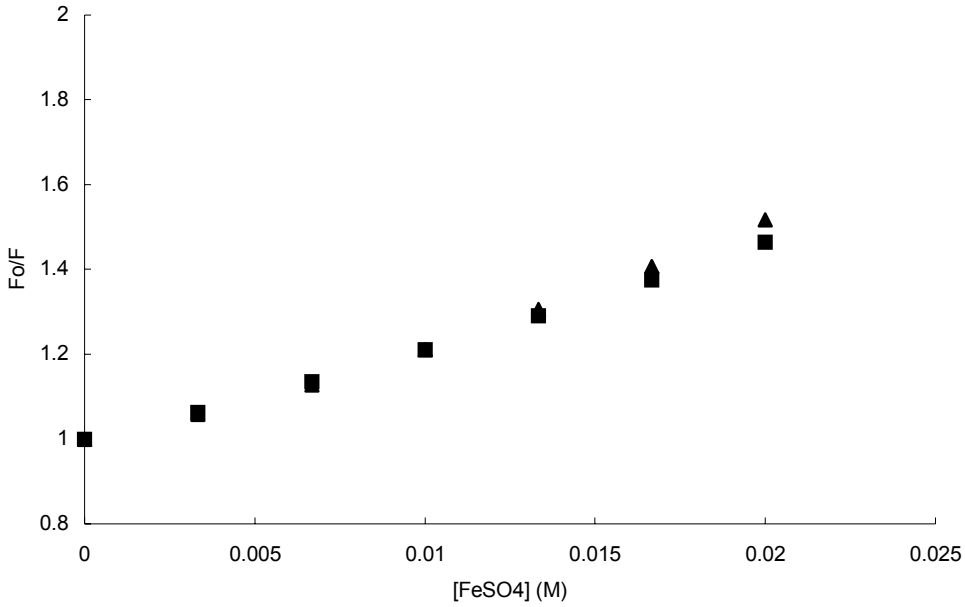

Figure 4.7 Stern-Volmer plot of 2-naphthol (50 μM) quenched by Fe^{2+} in aqueous solution (pH = 3.1) in the presence (▲) and absence (■) of SCD (2.5 mM).

However, NMR measurement of SCD in the presence of Fe^{2+} showed a peak broadening effect which indicates that Fe^{2+} has a significant interaction with SCD (Figure 4.8). At the same time, NMR spectra of 2-naphthol in the presence of SCD + Fe^{2+} did not show any peak broadening effect (data not shown). These NMR results suggest close location of Fe^{2+} to SCD molecules but not to 2-naphthol molecules. These data agree with the fluorescence results and also indicate that 2-naphthol was not encapsulated inside the SCD. Therefore, we can conclude that little if any ternary complex of SCD, Fe^{2+} and 2-naphthol was formed in aqueous solution.

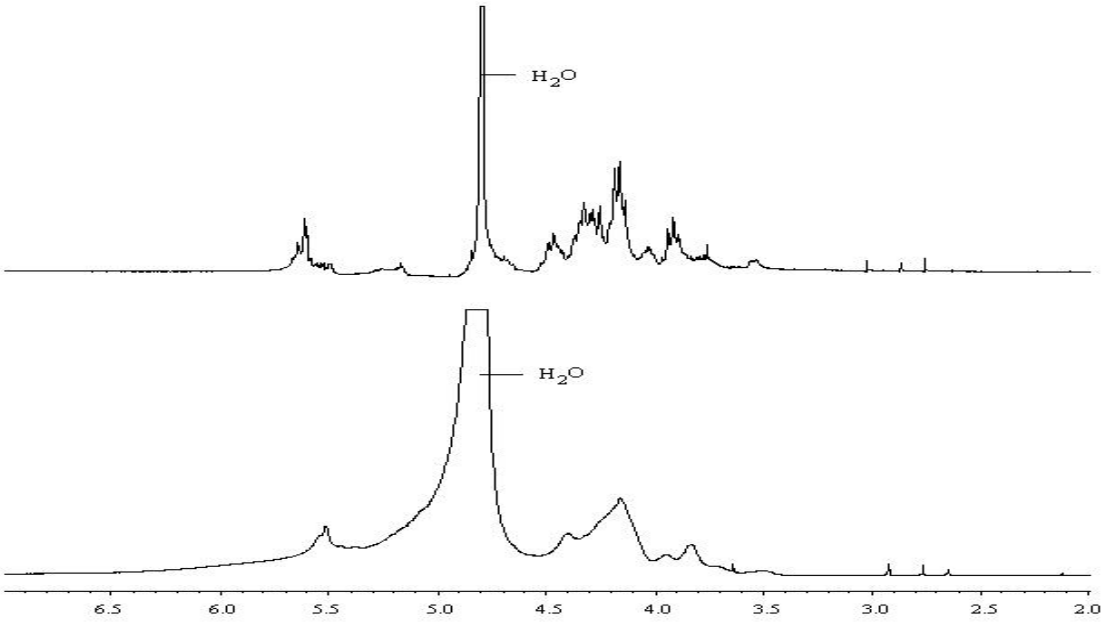

Figure 4.8 ^{1}H NMR spectra of SCD in the solution of (a) 1 mM 2-naphthol + 10 mM SCD and (b) 1 mM 2-naphthol + 10 mM SCD + 10 mM Fe^{2+}.

4.3.3 β-cyclodextrin

The binding constants of β-CD with anthracene, and β-CD with 2-naphthol have been reported as about 3000 M^{-1} and 600 M^{-1} respectively[5,6]. The binding ratio is 1:1 for each binary complex. The Fe^{2+} coordination sites on β-CD are hydroxyl groups, just as in HPCD. Therefore, only weak binding between Fe^{2+} and β-CD was expected. Fe^{2+} quenching data for 2-naphthol fluorescence in the presence of β-CD were similar to that for HPCD (Figure 4.9). Fe^{2+} quenching data for anthracene in the presence of β-CD (Figure 4.10) showed that β-CD had a protecting effect on anthracene. It is probably due to the fact that β-CD has a higher binding ability to anthracene. With more anthracene molecules inside β-CD and a minimal binding of Fe^{2+} to β-CD, less anthracene was available to the quencher. Both quenching results indicate that β-CD did not induce a strong interaction between Fe^{2+} and the two hydrophobic compounds.

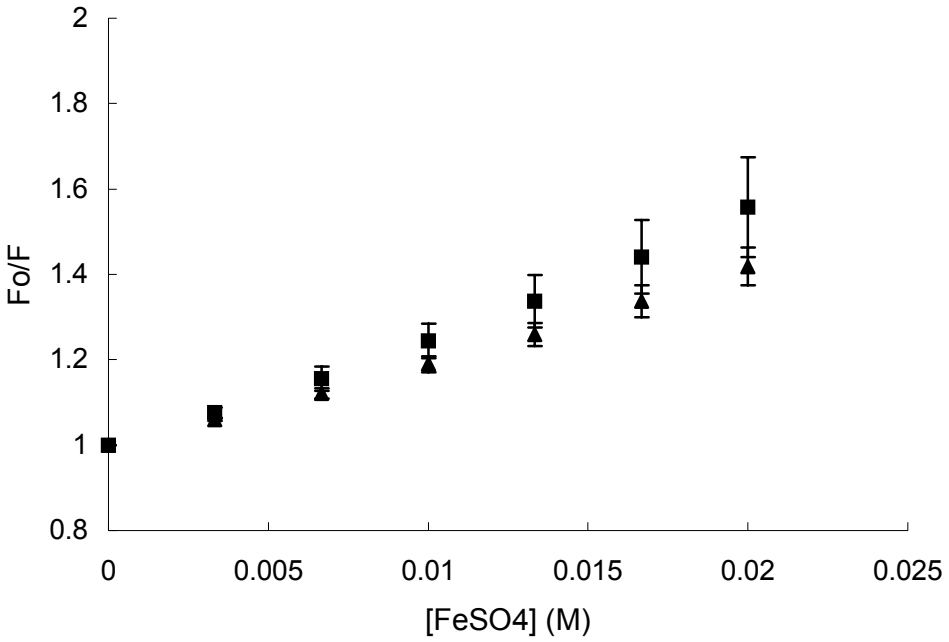

Figure 4.9 Stern-Volmer plot of 2-naphthol (50 μM) quenched by Fe^{2+} in aqueous solution (pH = 3.1) in the presence (▲) and absence (■) of β-CD (2.5 mM).

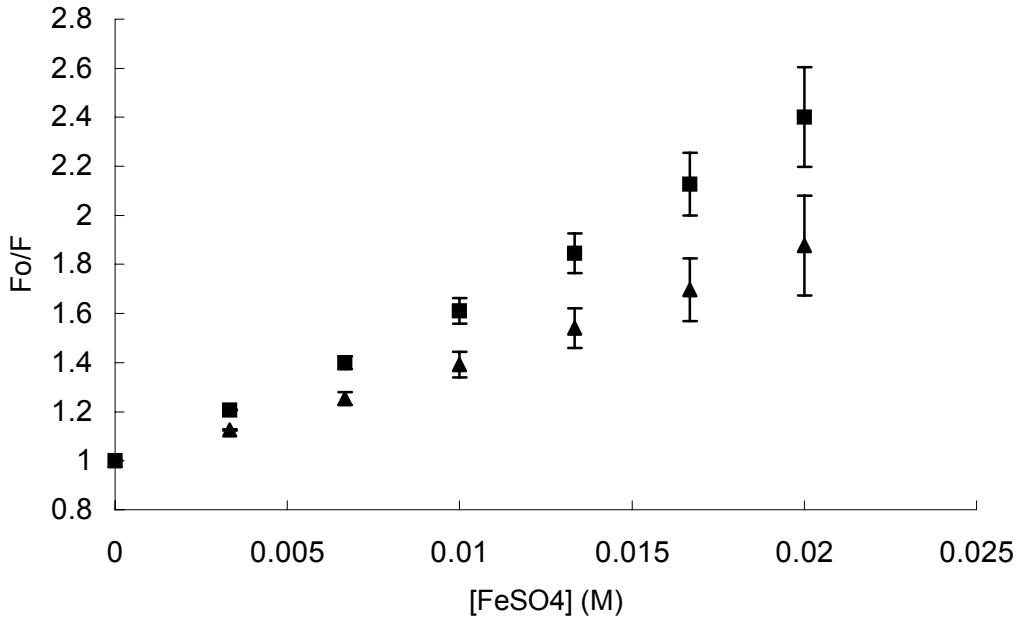

Figure 4.10 Stern-Volmer plot of anthracene (0.1 μM) quenched by Fe^{2+} in aqueous solution (pH = 3.1) in the presence (▲) and absence (■) of β-CD (2 mM).

Furthermore, NMR measurements of 2-naphthol + βCD in the presence of Fe^{2+} showed no significant peak broadening effect (Figure 4.11). Comparing 2-naphthol spectra in Figure 4.11 and those in Figure 4.5, we see a significant peak broadening in the presence of βCD. This peak broadening, of course, is not caused by paramagnetic effect, but due to a moderately slow exchange process. With increasing temperature, the broadened peaks became narrower and the missing peaks reappeared (Figure 4.12). At 55°C the spectrum of 2-naphthol in the binary complex looks similar to that of free 2-naphthol (Figure3.11). It is a result of increased exchange rate between the complexed state and free state of the two species with increased temperature. The peak shifts in the figure is caused by water shift which is influenced by temperature. Also, from the figure, we see that 30°C temperature increase can make the exchange rate of the two species from a moderately slow one to a very fast one. It suggests that the interaction between 2-naphthol and βCD is not very strong. It confirms the argument in Chapter 3 explaining why the ROESY experiment did not show interaction between 2-naphthol and βCD.

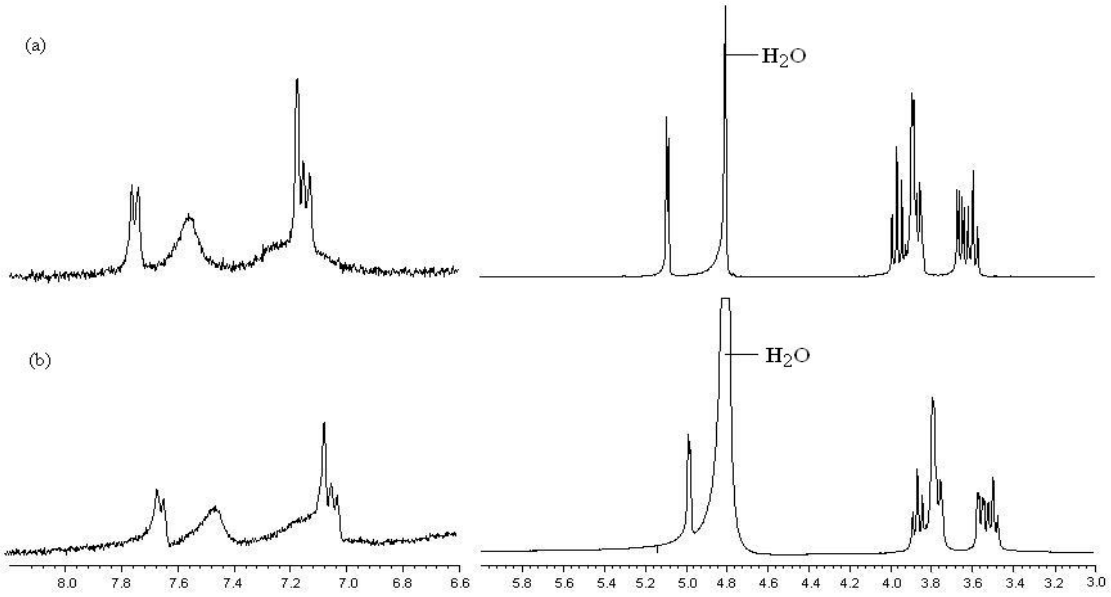

Figure 4.11 ^{1}H NMR spectra of 1 mM 2-naphthol (7-8 ppm) + 8 mM βCD (3-6 ppm) (a) in the absence and (b) in the presence of 10 mM Fe^{2+}.

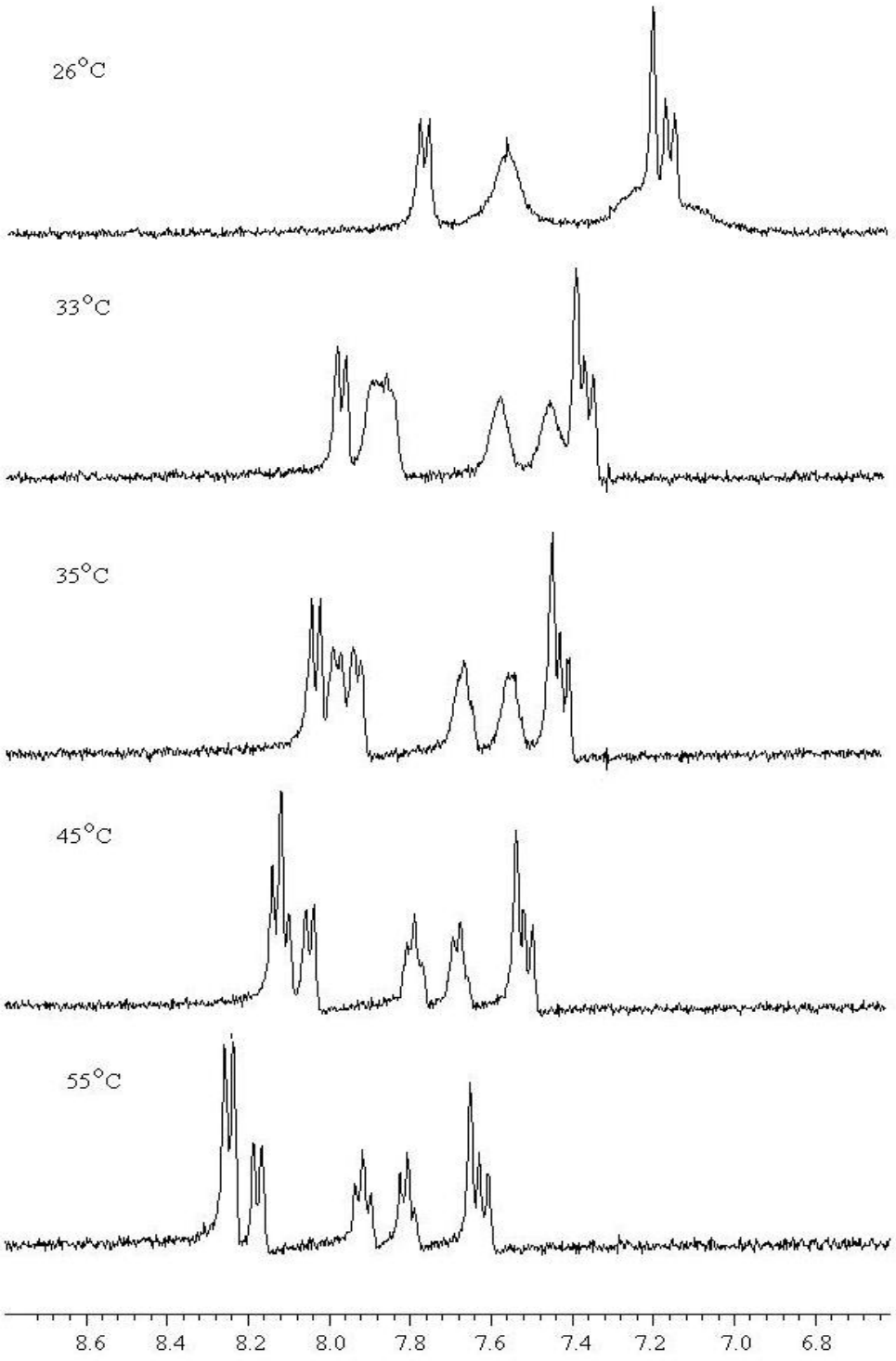

Figure 4.12 ^{1}H NMR spectra of 2-naphthol (2 mM) in the presence of βCD (2 mM) under different temperatures.

4.3.4 α-cyclodextrin

The cavity of αCD is smaller than that of β-CD[7]. However, there is still enough room to encapsulate one aromatic ring. The reported binding constant of α-CD and 2-naphthol (1:1 ratio) is 18 ± 3 M^{-1} in basic solution (pD=11) [8]. NMR titration method was used in an attempt to determine the binding constant of 2-naphthol and αCD in neutral condition. The chemical shift of each proton in 2-naphthol upon addition of αCD was plotted in Figure 4.13. The changes in chemical shift indicate an interaction between the two species. However, the data could not be fit to the linear equation (3.3), which means the binding is not a 1:1 ratio. Since 2-naphthol has two aromatic rings, binding by more than one αCD can occur. Unlike the other cyclodextrins studied here, binding between αCD and 2-naphthol takes two days. The binding between the other cyclodextrins and 2-naphthol only takes a few seconds. For anthracene, it is too bulky to get into αCD. The binding between the two can not be found in the literature. Therefore we did not make it a study object here.

Fluorescence quenching of 2-naphthol with Fe^{2+} showed a decreased efficiency in the presence of α-CD (Figure 4.14). This result indicates that the 2-napthol was protected from interaction with iron, most likely through the ability of αCD to bind 2-napthol but not Fe^{2+}. Since αCD can only accommodate one aromatic ring in each cavity, there must be more than one αCD binding with 2-naphthol. If not, 2-naphthol should be still quite available to the Fe^{2+} with one aromatic ring intruding outside αCD. Decreased quenching efficiency suggests that α-CD isolates the 2-napthol from Fe^{2+}.

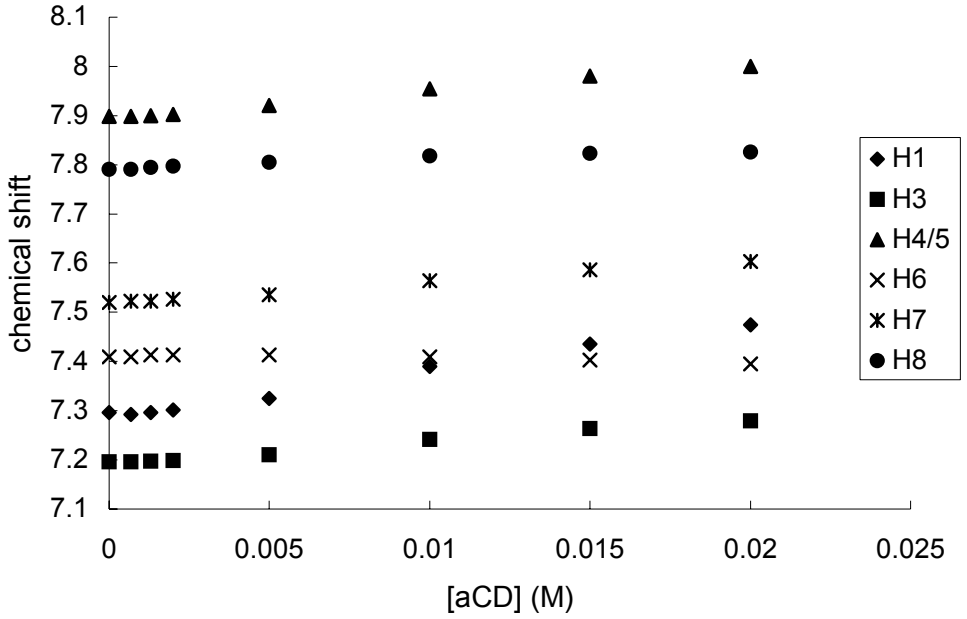

Figure 4.13 Chemical shift of protons in 2-naphthol in the solutions with different concentration of αCD. (For the positions of the protons, please see Figure 3.11 in Chapter 3).

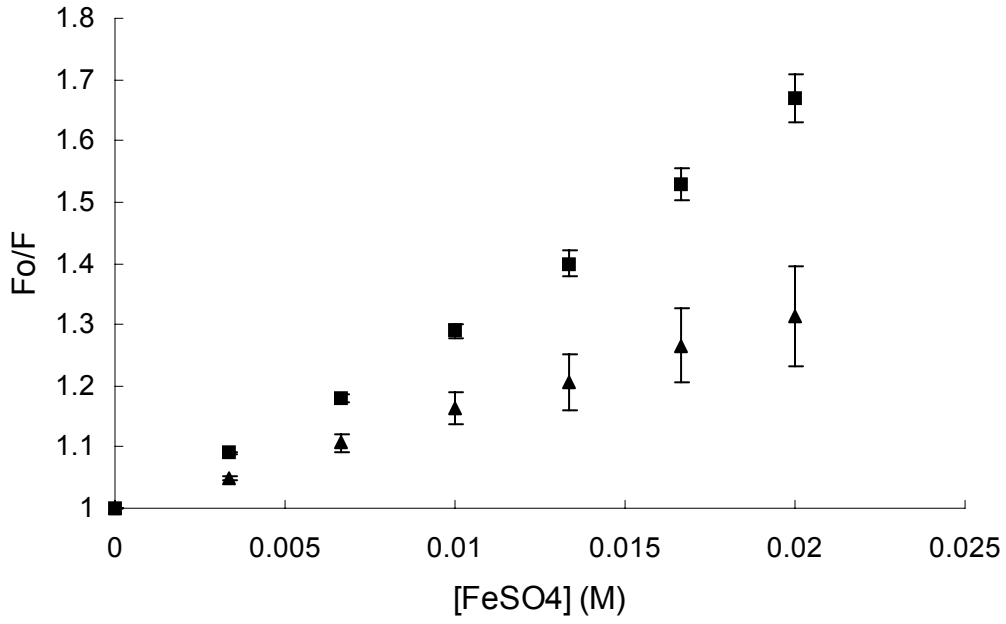

Figure 4.14 Stern-Volmer plot of 2-naphthol (50 μM) quenched by Fe^{2+} in aqueous solution (pH = 3.1) in the presence (▲) and absence (■) of αCD (2.5 mM).

This argument was confirmed by NMR measurements of aqueous 2-naphthol + α-CD in the presence of Fe^{2+}, which showed no peak broadening effect (Figure 4.15).

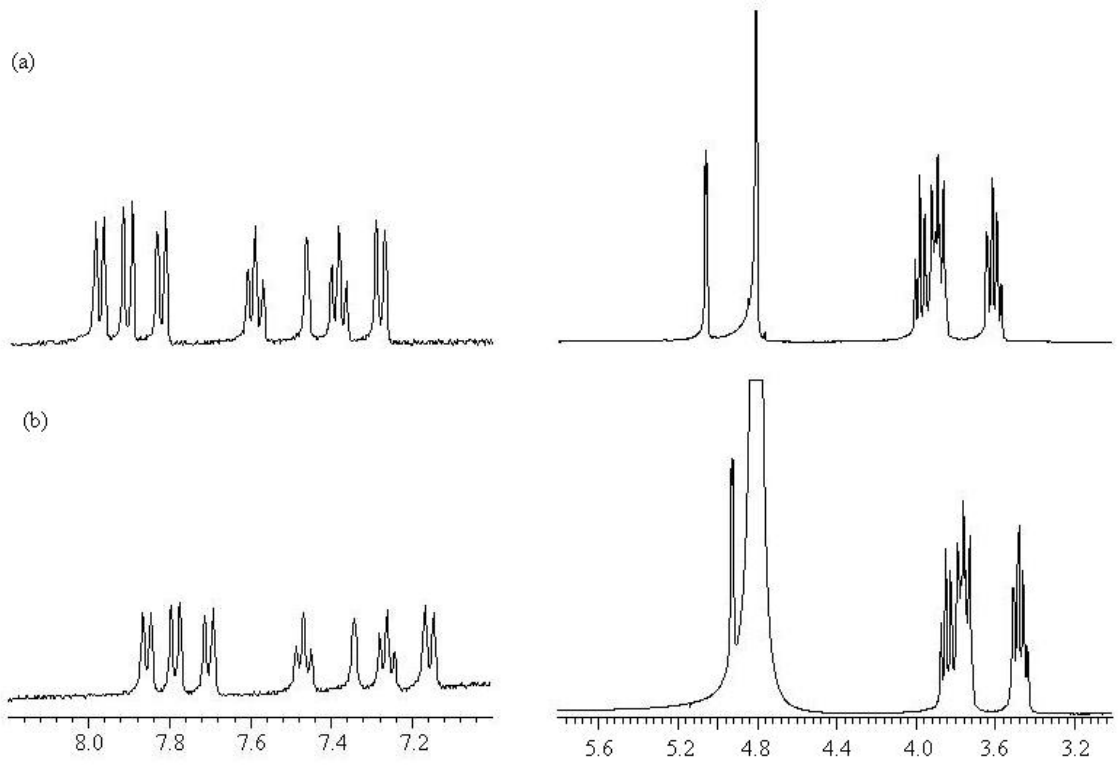

Figure 4.15 ^{1}H NMR spectra of 2 mM 2-naphthol (7-8 ppm) + 20 mM αCD (3-6 ppm) (a) in the absence and (b) in the presence of 10 mM Fe^{2+}.

4.4 References

1. Zheng, W. and Tarr, M.A. *J. Phys. Chem. B,* 2004, 108, 10172-10176.
2. González-Gaitano, G.; Guerrero-Martínez, A.; Núnez-Barriocanal, J.L.; Montoro, T. and Tardajos, G. *J. Phys. Chem. B,* 2002, 106, 6069
3. Kaiwar, S.P.; Bandwar, R.P.; Raghavan, M.S.S.; Rao, C.P. *Proc Indian Acad Sci (Chem Sci),* 1994, 106, 743 –752.
4. Geetha, K.; Raghavan, M.S.S.; Kulshreshtha, S.K.; Sasikala, R.; Rao, C.P. *Carbohydr Res.,* 1995, 271(2), 163 –175.

5. Blyshak, L; Dodson, K.Y.; Patonay, G.; Warner, I.M.; May, W.E. *Anal.Chem*. 1989, 61, 955.

6. Park, H.; Mayer, B.; Wolschann, P.; Kőhler, G. *J. Phys. Chem*. 1994, 98, 6158.

7. Szejtli, Jäozsef *Cyclodextrins and Their Inclusion Complexes*, Akadémiai Kiadó, Budapest, 1982.

8. Vecchi, C.; Naggi, A.; Torri, G. *Proceedings of the Fourth International Symposium on Cyclodextrins,* Munich, Germany, April 20-22, 1988.

Chapter 5. Enhancement of sonochemical degradation of phenol using hydrogen atom scavengers

5.1 Introduction

In sonochemistry, ultrasound is used as an energy source to achieve various chemical processes. Ultrasound was first produced about 100 years ago by F. Galton who studied the threshold levels of hearing in animals and humans[1]. He found that the normal limit of human hearing is about 16kHz. So ultrasound was defined as the sound of a frequency that is beyond human hearing, i.e. above 16 kHz. The piezoelectric effect is the basis of the production of ultrasound. When some crystalline materials such as quartz experience a sudden compression, a potential difference will be produced across the opposite faces. The reverse effect – a rapidly alternating potential placed across the faces of a piezoelectric crystal will produce a dimensional change and thus convert electrical energy into vibrational or sound energy.

The ultrasound energy has been divided into two distinct ranges in chemistry: power (16-1000 kHz) and diagnostic (above 1000 kHz). Diagnostic ultrasound is nondestructive when operating at medium intensities. So it can be used in fetal imaging in medical field. It is also used in material flaw detection and remote sensing in flow systems. Power ultrasound is the one that used in sonochemistry and industry. Its applications in industry include cleaning and degreasing of surfaces, crystallization, homogenization, welding of thermoplastics, filtration, degassing, and etc.

5.1.1 Cavitation phenomenon

The application of power ultrasound in sonochemistry is based on a phenomenon called cavitation[2-4]. Ultrasound is transmitted through a solution as a wave. It superimposes an

acoustical pressure (P_a) on the hydrostatic ambient pressure (P) of the fluid. The total pressure (P_t) is:

$$P_t = P + P_a \qquad (5.1)$$

As ultrasound passes through, the acoustic pressure compresses some part of the fluid, which is called compression; and pulls apart some other portion of the fluid, which is called rarefaction (Figure 5.1). The rarefaction and compression cycle consecutively at all points in the acoustic field.

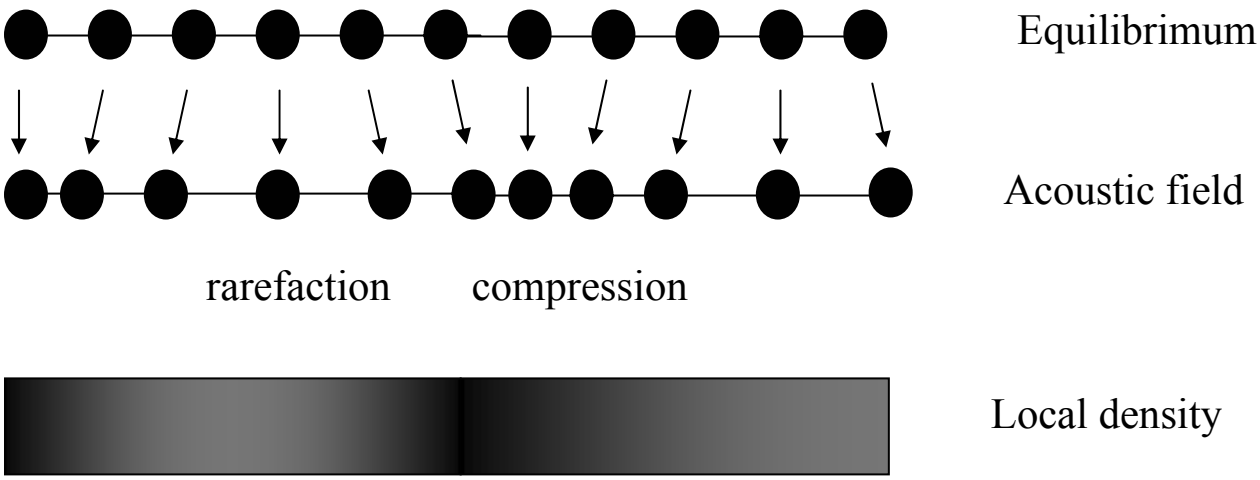

Figure 5.1 The effect on the solution of ultrasound as it goes though[2].

During rarefaction, if the negative pressure is strong enough to overcome the intermolecular forces binding the fluid, a cavitation bubble is generated. These bubbles will disappear on the next compression cycle if the radius is smaller than the critical value. However, if the radius is large enough, the bubbles will undergo oscillatory growth and shrinking during the subsequent acoustical cycles.

There are two kinds of cavitation: stable cavitation or transient cavitation. In stable cavitation, a bubble oscillates about the equilibrium radius with the acoustical field for several cycles (Figure 5.2a). In this case, the bubble does not experience a dramatic size change and the evaporation and condensation processes of the solvent are quasi-reversible. Therefore, stable cavitation is of little use in sonochemistry. It is the transient cavitation that is useful. In transient cavitation, the bubble grows slowly from a very small radius. After a few oscillation cycles, it experiences a huge size increase, from tens to hundreds of times the equilibrium radius (Figure 5.2b). The wall can not hold the bubble anymore and the bubble collapses. During this collapse, an extreme situation is created. The temperature could go as high as several thousand Kelvin and the pressure could reach up to a thousand atmousphere[1,5-7]. Under this condition, many chemical changes will take place.

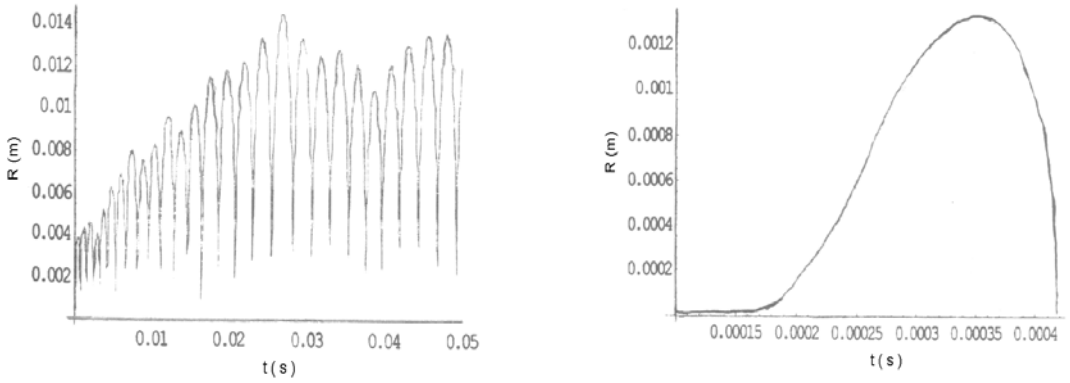

P_0 = 2.7 bar
ν= 20 kHz
R_0 = 2 mm

P_0 = 2.7 bar
ν= 20 kHz
R_0 = 20 μm

Figure 5.2. (a) Stable and (b) transient cavitation. Examples under the listed conditions[2].

5.1.2 Chemical processes in transient cavitation

One important chemical change in the solution under transient cavitation is the thermal dissociation of water[8-12]:

$$H_2O\ (g) \rightarrow \cdot H\ (g) + \cdot OH\ (g) \quad (5.1)$$

Other species[13,14] such as dissolved O_2, N_2 and volatile solutes can also undergo thermal dissociation. Once the radicals are produced, they will further react with other compounds either in the liquid bulk or in the bubble phase. One main reaction of these radicals is recombination reaction. In the case of hydroxyl and hydrogen radicals, either water, hydrogen peroxide or hydrogen are generated through the reactions:

$$\cdot H + \cdot OH \rightarrow H_2O \quad (5.2)$$

$$\cdot OH + \cdot OH \rightarrow H_2O_2 \quad (5.3)$$

$$\cdot H + \cdot H \rightarrow H_2 \quad (5.4)$$

If hydrogen peroxide does not react with other solutes, it will disproportionate into water and oxygen:

$$H_2O_2 \rightarrow H_2O + \tfrac{1}{2}\ O_2 \quad (5.5)$$

Since the hydrogen and hydroxyl radicals are in present relatively large amounts in aqueous solutions that are irradiated by ultrasound, and they are close to each other, the main products of the system are hydrogen, hydrogen peroxide and oxygen. The reactions of these radicals with other compounds are always secondary from the energy balance point of view.

5.1.3 Some effects that influence the cavitaion and chemical processes

Many effects have influences on cavitation and therefore on chemical processes[1,4,13,15-17]. The frequency of ultrasound determines the critical size of the cavitation bubbles. The change in the number of excited bubbles will have an effect on the rate of chemical reactions. The intensity

of ultrasound also matters. Usually, the reaction rates increase with the enhancement of power intensity. Temperature plays a more complicated role in the reaction. For the volatile species whose reactions occur in the bubble phase, higher temperature will increase the concentration of such species inside the bubbles, therefore increasing their reaction rates. However, for the nonvolatile species, sometimes the increased temperature could decrease the reaction rates. This is due to the condensation of water vapor inside the cavity during its collapse, which reduces the amount of energy available to the reactions. Different gases dissolved in the solution could change the physical properties of the bubble. Accordingly, the temperature or pressure during the collapse changes. Some of the background gases can even provide new reaction species in the gas phase (e.g. ozone). The sample matrix is another important influence on the reactions. Its effect is complicated and difficult to predict. In many cases, the matrix has a competition with the reactant of interest for certain radicals. Therefore, the reaction of interest could be inhibited. The influence of the matrix also depends on its volatility and other physical properties.

5.1.4 Drawback and possible improvement of the method in application of pollutant degradation

A major drawback of sonochemistry used in pollutants degradation is the fact that a large amount of the major reactive transients (e.g. hydroxyl radical) are consumed by the predominate recombination reactions. This phenomenon makes the degradation efficiency low. One reasonable way to improve the degradation efficiency is to inhibit the recombination reaction of hydroxyl radical, especially with hydrogen atoms, which regenerates water. The recombination of hydroxyl radical itself, which produce hydrogen peroxide, is fine since hydrogen peroxide is active too. The goal can be achieved by scavenging the hydrogen atoms. With less hydrogen atoms, more hydroxyl radical will be available for the degradation.

There are a few species that are more reactive with hydrogen atoms than with hydroxyl radical. Carbon tetrachloride is one of them.

$$CCl_4 + \cdot H \rightarrow HCl + \cdot CCl_3 \qquad (5.6)$$

$$CCl_4 + \cdot OH \rightarrow \text{no reaction} \qquad (5.7)$$

The rate constant of equation (5.6) is 3.8×10^7 $M^{-1}s^{-1}$.[18] In contrast, it has no reaction with hydroxyl radical (5.7). Iodate is another compound that reacts faster with hydrogen atoms.

$$IO_3^- + \cdot H \rightarrow \cdot OH + IO_2^- \qquad (5.8)$$

$$IO_3^- + \cdot OH \rightarrow \qquad (5.9)$$

The rate constant of equation (5.8) is 1.2×10^7 M^{-1} s^{-1} in pH = 4.6 solution while the rate constant of equation (5.9) is less than 10^5 M^{-1} s^{-1} in pH = 5.2 solution.[19] Perfluorohexane (C_6F_{14}) is the third possible choice. It is fully oxidized so it is expected to be a poor hydroxyl radical scavenger. However, it could probably be reduced by strong reducing agent such as hydrogen atom (standard reduction potential for $H^+ + e \rightarrow \cdot H$ = -2.3 V [18]). Both iodate and perfluorohexane are much less toxic to animals and plants than carbon tetrachloride. Perfluorohexane is also photostable in the atmosphere.[20] It seems iodate and perfluorohexane are better choices as additives to improve the degradation of the pollutants. However, if carbon tetrachloride was initially presented in the waste solutions, it probably could increase the degradation efficiency of co-existing pollutants while the carbon tetrachloride would also be degraded during sonication.

5.2 Experimental

Phenol (biotech grade) and acetonitrile (HPLC grade) were purchased from Acros. Carbon tetrachloride (spectroanalyzed), methanol (HPLC grade), and hexanes (pesticide grade) were purchased from Fisher. Perfluorohexane (99%) and hydroquinone (99%) were purchased

from Aldrich. Potassium iodate was purchased from EM Science. p-Hydroxyphenyl acetic acid and peroxidase (type VI-A) were purchased from Sigma. All the chemicals were used as received. Purified water was obtained from a Barnstead NanopureUV water treatment system.

A concentrated stock solution of phenol was prepared by dissolving phenol in water, and dilute (~ 25 μM) aqueous phenol samples were prepared from the stock solution. To avoid photodegradation, all phenol samples were kept in the dark before and after sonication. Saturated aqueous CCl_4, perflurohexane, or hexane solutions were prepared by adding more than the soluble amount of these agents into water and stirring overnight using a magnetic stirring bar. These solutions were prepared freshly every day. The final concentration of CCl_4 in phenol solution was ~150 μM, that of hexane was ~14 μM, that of perfluorohexane was less than 1.5 μM, and that of potassium iodate was 150 μM or 1 mM. All samples were sonicated using an ACE Glass (Vineland, NJ) 600W sonochemical apparatus operating at 20 KHz (Figure 5.3). A ½ in. diameter titanium probe was used with the power supply set to 50% amplitude, which resulted in coupling of ~ 75-90 W of acoustic power into the solution. Two probes were used, probe 1 and probe 2. Probe 2 introduced more energy into the system due to a better connection between it and the rest of sonochemical apparatus. Sonication was carried out with a 50% duty cycle (sonication on for 1s, off for 1s); this duty cycle helped to minimize bulk temperature increases. Samples were contained in an all-glass, water jacketed reaction vessel. The sonication was done with 20ºC water circulating through the jacket of the reaction vessel. The vessel was sealed with O-rings and glass stoppers during sonication. Solutions were air equilibrated and were sonicated under a headspace of air. The volume of sonicated samples was 50 mL. At regular time intervals, 1 mL aliquots were removed and analyzed by HPLC (Hewlett Packard

1090). The tip of the titanium probe was polished by sandpaper (#800 and #320) on a regular basis to maintain a smooth surface.

Sonication products were analyzed by HPLC. Samples were injected using a 100 μL loop into an Econosphere C18 column (length = 25cm, id = 4.6mm). The mobile phase was 50/50 acetonitrile/water at 1 mL min^{-1}. Analytes were detected by absorbance at 254nm.

Hydrogen peroxide produced by sonication of pure water or water containing ~150 μM CCl_4 was measured using the p-hydroxyphenyl acetic acid dimerization method[21].

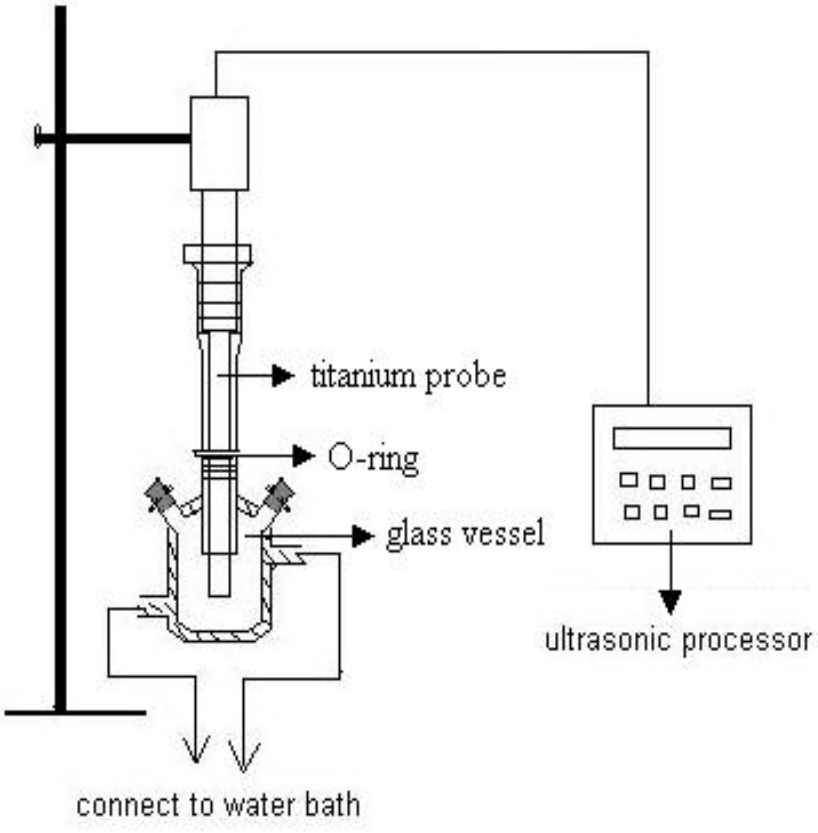

Figure 5.3 Schematic plot of sonication apparatus used in this study.

5.3 Results and discussion

5.3.1 Phenol degradation in the presence and absence of CCl_4

Sonolysis of phenol in aqueous solution in the presence and absence of CCl_4 with probe 1 was shown in Figure 5.4a. The degradation can be fitted to a pesudo first order reaction model as shown in Figure 5.4b (the plot is linear with R^2= 0.97-0.99). The rate constants were calculated from the slope of the regression line. With probe 1, the degradation rate constant was 0.014 min^{-1} in the absence of CCl_4 and 0.031 min^{-1}in the presence of CCl_4. The sonolysis was repeated with probe 2 and it was found that the rate constants in the absence and presence of CCl_4 were 0.022 min^{-1} and 0.061 min^{-1} respectively. As can be seen, by addition of a small amount of CCl_4, the phenol degradation efficiency was enhanced by about 2.2 ~ 2.8 times.

Hydroquinone was identified as a major intermediate in phenol sonolysis in the presence and absence of CCl_4. Hydroquinone was identified by comparison of HPLC retention time with an authentic standard. The appearance of hydroquinone, a product of hydroxylation of phenol, indicates that the hydroxyl radical oxidation is an important degradation pathway in phenol degradation (equation 5.10).

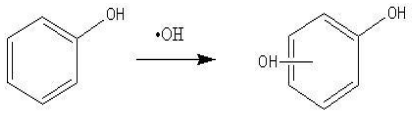

(5.10)

In the presence of CCl_4, a substantial increase in the observed hydroquinone concentration at short sonication times was observed. At later times, the hydroquinone concentration decreased rapidly in the presence of CCl_4, indicating that its further degradation was facile. On the contrary, in the absence of CCl_4, the amount of hydroquinone produced was small at short sonication times and increased with longer sonication time. Figure 5.5 illustrates the

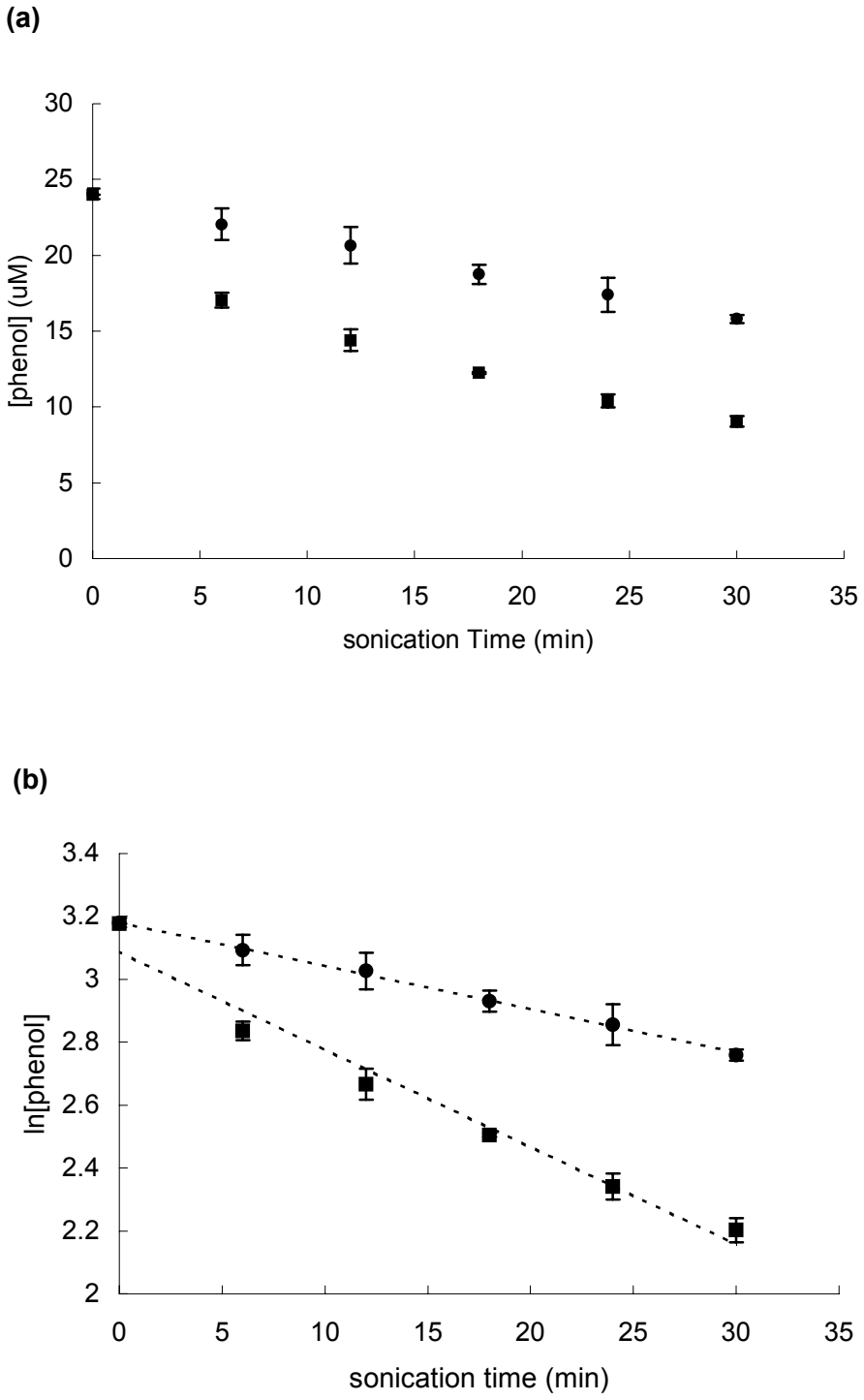

Figure 5.4 (a) Degradation of phenol by sonication in the presence (■) and absence (●) of CCl_4 (initially ~ 150μM) and (b) pesudo first order reaction model fitting with data in (a).

hydroquinone concentration as a function of sonication time (with probe 1) in the presence and absence of CCl_4. For both phenol and hydroquinone, the observed degradation is significantly faster in the presence of dissolved CCl_4. The observed increased degradation rates indicate that the CCl_4 enhances sonochemical degradation of dissolved organics. Although sonolysis of CCl_4 likely results in the formation of Cl and CCl_3 radicals[22,23], the data presented here suggest that these radicals are not the predominant cause of increased degradation rates. The substantial increase in initially formed hydroquinone upon phenol sonolysis in the presence of CCl_4 suggests that increased concentrations of hydroxyl radical are present. During sonochemical processes a major sink of hydroxyl radical is recombination with hydrogen atom to reform water[3]. Such recombination reactions are very likely since the two species are close to each other after their initial formation.

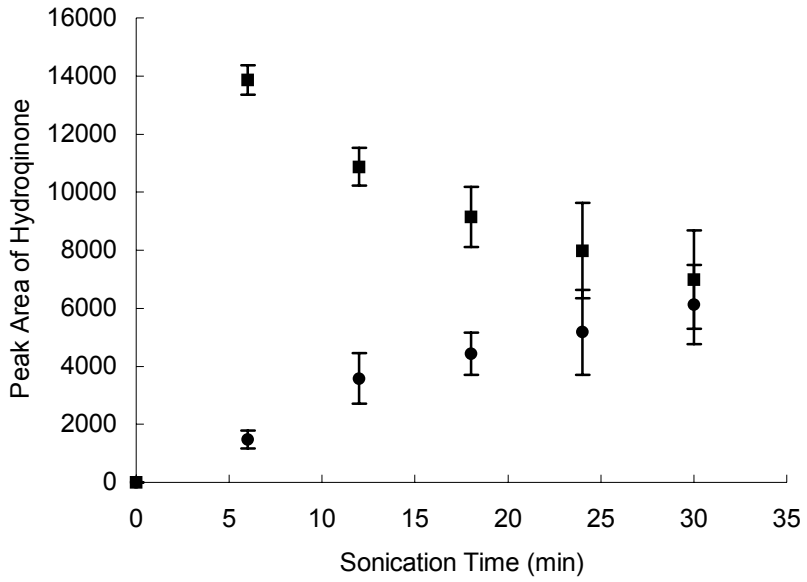

Figure 5.5 Hydroquinone levels as a function of sonication time in the presence (■) and absence (●) of CCl_4 (initially ~ 150μM).

Addition of CCl_4, however, traps hydrogen atoms so that they cannot recombine with hydroxyl radical. The expected result of this trapping would be an increase in hydroxyl radical concentration. The observed hydroquinone concentrations support the theory that more hydroxyl radical is available in solution in the presence of CCl_4.

Methanol is a good hydroxyl radical scanvenger ($k = 1 \times 10^9\ M^{-1}s^{-1}$).[19] To further confirm that hydroxyl radical oxidation is a major degradation pathway, phenol sonolysis was repeated in the presence of 0.01M of methanol (Figure 5.6). Compared to Figure 5.4a, phenol degradation was inhibited in the presence of methanol, regardless of the presence or absence of CCl_4. The enhancement effect of CCl_4 is largely eliminated by addition of methanol. This result indicates that the reaction of phenol with hydroxyl radical is an important pathway that is enhanced in the presence of CCl_4.

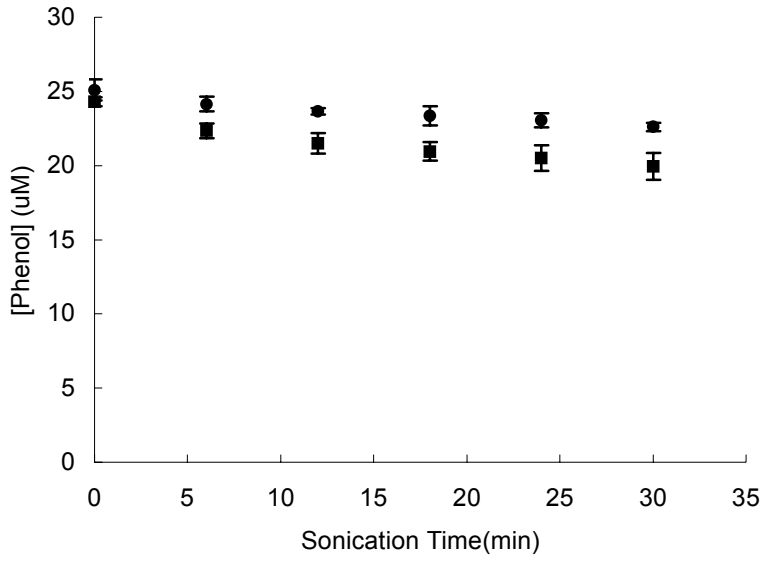

Figure 5.6 Degradation of phenol with methanol by sonication in the presence (■) and absence (●) of CCl_4 (initially ~ 150μM).

In the presence of CCl_4 and methanol, the hydroquinone production (Figure 5.7) was diminished compared to the results without CCl_4 alone (Figure 5.5). It further supports the conclusion that methanol effectively scavenged much of the increased hydroxyl radical resulting from added CCl_4.

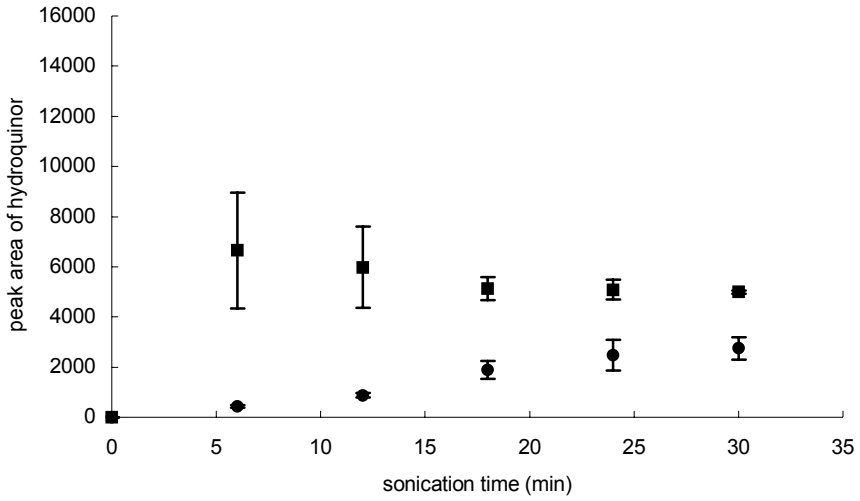

Figure 5.7 Hydroquinone levels as a function of sonication time in the presence (■) and absence (●) of CCl_4 (initially ~ 150μM) with methanol presented in solution.

5.3.2 Measurement of H_2O_2 produced in the sonolysis process

A more direct probe of hydroxyl radical concentration in the solution is measurement of hydrogen peroxide. Two hydroxyl radicals can combine to produce hydrogen peroxide. With more hydroxyl radical in the solution, we assumed more hydrogen peroxide would be produced. Measurement of hydrogen peroxide was performed according to the p-hydroxyphenyl acetic acid (POHPAA) dimerization method. The proposed mechanism of this method is illustrated in Figure 5.8[19]. Firstly, hydrogen peroxide oxidizes the peroxidase (3+) to peroxidase (5+). Then POHPAA reduces peroxidase (5+) to peroxidase (4+) and another POHPAA reduces peroxidase (4+) to peroxidase (3+). In the mean time two POHPAA radicals are obtained. Thirdly, the two

POHPAA radicals combine to produce a fluorescent dimer. The overall reactions of the method are:

$$H_2O_2 + 2\ POHPAA \rightarrow 2\ POHPAA\cdot + H_2O \qquad (5.11)$$

$$2\ POHPAA\cdot \rightarrow (POHPAA)_2 \qquad (5.12)$$

The stoichiometry between H_2O_2 and POHPAA dimmer is 1:1. Therefore, the concentration of H_2O_2 is proportional to the intensity of fluorescence observed.

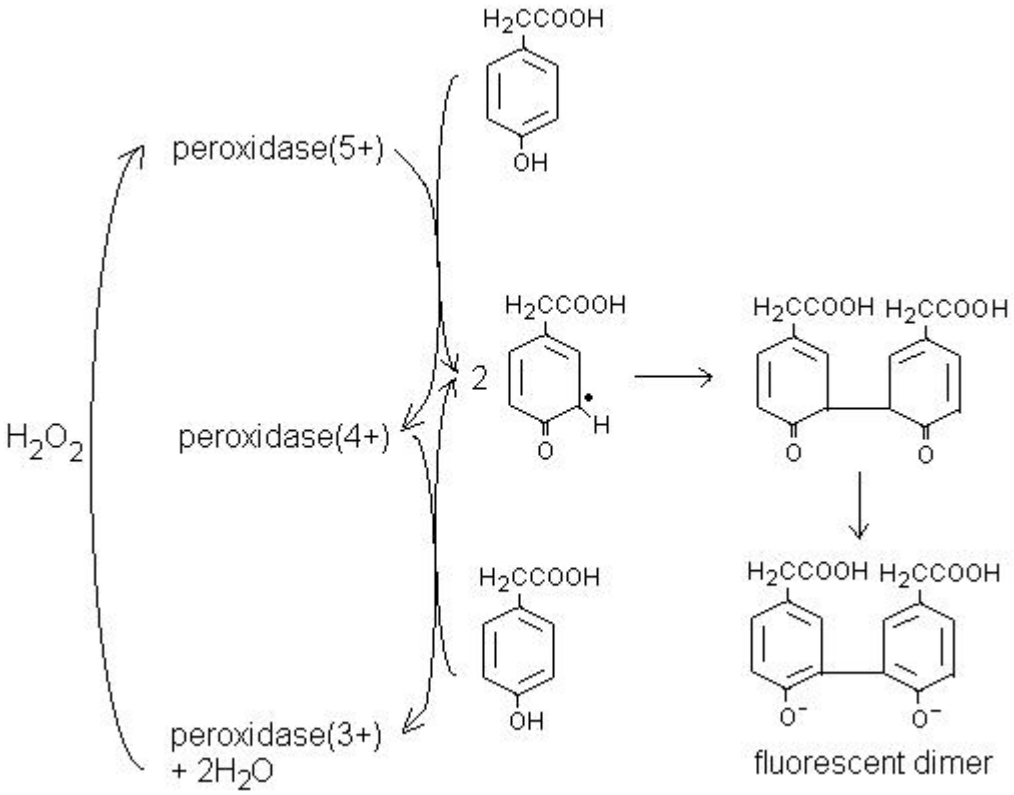

Figure 5.8 Schematic plot of proposed mechanism of p-hydroxyphenyl acetic acid dimerization method for measuring the concentration of hydrogen peroxide.

Figure 5.9 shows the concentration of hydrogen peroxide in pure water and in ~150 μM CCl_4 aqueous solution after certain sonication times. More hydrogen peroxide was detected in the early stage of sonication in the presence of CCl_4. However, with longer sonication time, hydrogen peroxide decomposed by the ultrasonic energy. The data shown here is a combined result of producing and decomposing effects. This result indicated that more hydroxyl radical was produced by the presence of trace amount of CCl_4, at least in the early stage of sonication.

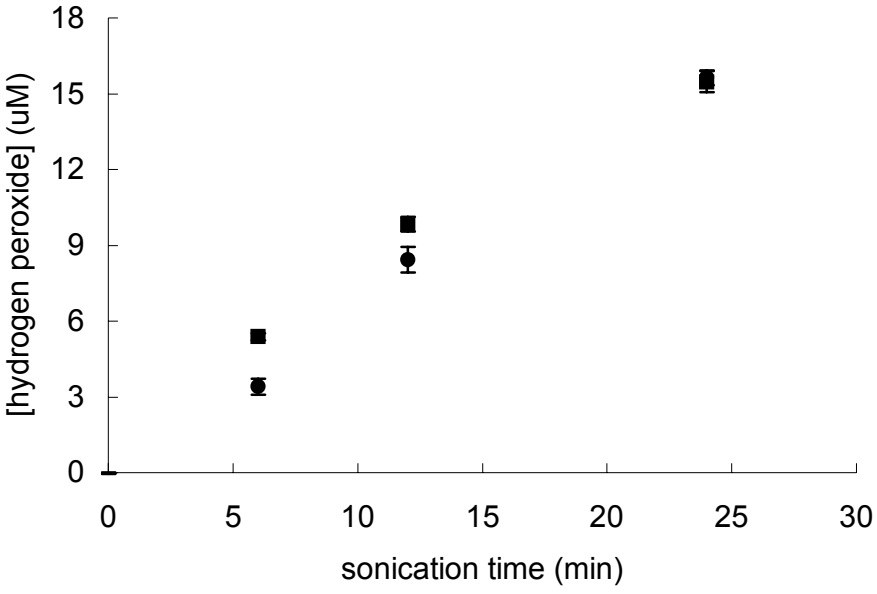

Figure 5.9 Concentration of hydrogen peroxide produced during the sonication in the presence (■)and absence (●)of CCl_4 (initially ~ 150μM).

5.3.3 Phenol degradation in the presence of perfluorohexane

Sonolysis of phenol in the presence and absence of perfluorohexane with probe 1 was shown in Figure 5.10. Similar to degradation in the presence of CCl_4, addition of perfluorohexane enhanced the sonolysis efficiency of phenol. To examine if the enhancement is due to the C-C backbone other than C-F, the experiment was repeated with hexane as an additive. The result was shown in Figure 5.11.

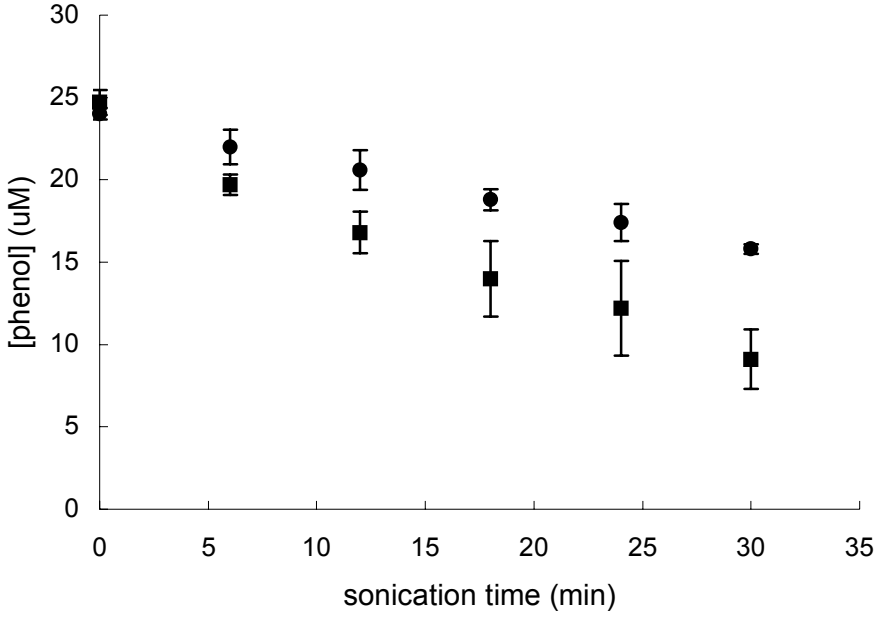

Figure 5.10 Degradation of phenol by sonication in the presence (■) and absence (●) of perfluorohexane (initially ~ 1.5μM).

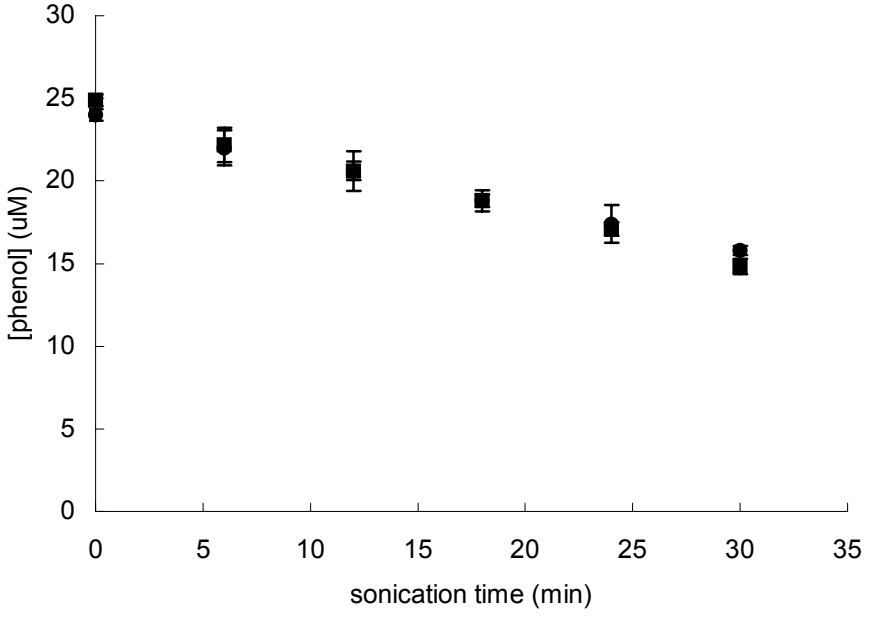

Figure 5.11 Degradation of phenol by sonication in the presence (■) and absence (●) of hexane (initially ~ 14μM).

In comparison, addition of hexane to the system did not give any observed change in the rate of phenol degradation. Therefore, it is not C-C backbone that induced the enhancement. Although perfluorohexane has a much less aqueous solubility than CCl_4, it is probably more readily volatilized into the gas phase due to its 20°C lower boiling point compared to CCl_4. Furthermore, the perfluorohexane molecule is bigger than CCl_4 so it has a higher possibility to meet hydrogen atoms. As a result, perfluorohexane had a similar enhancement effect as CCl_4 despite its lower concentration.

5.3.4 Phenol degradation in the presence of iodate

Sonolysis of phenol in the presence and absence of potassium iodate is shown in Figure 5.12. No enhancement was observed with this additive. This result is probably due to the low volatility of IO_3^-. Since water homolysis occurs predominantly in the gas phase during sonication[10,11], hydrogen atoms and hydroxyl radicals would be most likely to recombine in this region. With little gas phase IO_3^- present, this species is unlikely to be able to scavenge hydrogen atoms before they react with hydroxyl radical.

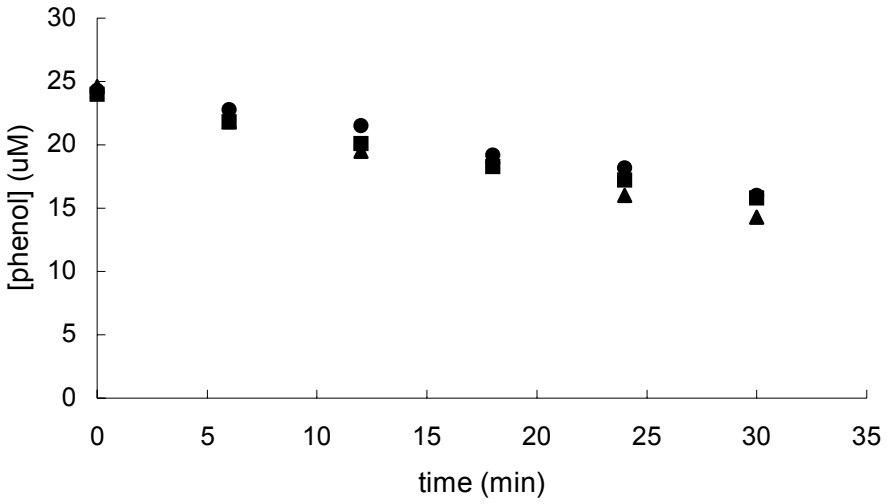

Figure 5.12 Degradation of phenol by sonication in the absence of KIO_3 (●) and under two KIO_3 concentrations: 1mM (■) and 150μM (▲).

5.4 References

1. Edited by Mason T.J. *Sonochemistry: The uses of ultrasound in chemistry*, Royal Society of Chemistry, pp 9-26.
2. Destaillants, H.; Hoffmann, M.R.; and Wallace, H.C. "Sonochemical Degradation of Pollutants" in *Chemical Degradation Methods for Wastes and Pollutants*, Tarr, M.A. ed., Marcel Dekker, Inc., New York, 2003.
3. Joseph, J.M.; Destaillats, H.; Hung, H.; Hoffmann, M.R. *J. Phys. Chem. A* 2000, 104, 301.
4. Peller, J.; Wiest, O.; Kamat, P.V. *J. Phys. Chem. A* 2001, 105, 3176.
5. Flint, E.B.; Suslick, K.S. *Science* 1991, 253, 1397.
6. Suslick, K.S.; Flint, E.B.; Grinstaff, M.W.; and Kemper, K.A. *J. Phys. Chem.* 1993, 97, 3098.
7. Suslick, K.S.; Kemper, K.A.; and Flint, E.B. *Proc. IEEE Ultrason. Symp. 2* 1993, 777.
8. Chen, Y.C.; and Smirniotis, P. *Ind. Eng. Chem. Res.* 2002, 41, 5958.
9. Suslick, K.S.; Hammerton, D.A.; and Cline R.E.Jr. *J. Am. Chem. Soc,* 1986,108, 5641.
10. Suslick, K.L. *Science* 1990, 247, 1439.
11. Misik, V.; Miyoshi, N.; and Riesz, P. *J. Phys. Chem.* 1995, 99, 3605.
12. Makino, K.; Mossoba, M.M.; and Riesz, P. *J. Am. Chem. Soc.* 1982, 104, 3537.
13. Kang, J.; Hung, H.; Lin, A. and Hoffmann, M.R. *Environ. Sci. Technol.* 1999, 33, 3199.
14. Thompson, L.H.; and Doraiswamy, L.K. *Eng. Chem.* 1999, 38, 1215.
15. Laughrey, Z.; Bear, E.; Jones, R. and Tarr, M.A. *Ultrasonics Sonochemistry* 2001, 8, 353.
16. Taylor, E.Jr.; Cook, B.B.; and Tarr, M.A. *Ultrasonics Sonochemistry* 1999, 6,175.
17. Beckett, M.A.; and Hua, I. *J. Phys. Chem. A* 2001, 105, 3796.
18. Buxton, G.V.; Greenstock, C.L.; Helman, W.P.; and Ross, A.B. *Journal of Physical and Chemical Reference Data,* 1988, 17, No 2.

19. www.rcdc.nd.edu

20. www.epa.gov/chemrtk/perfluoro/c13244rs.pdf

21. Miller, W.L.; and Kester, D.R. *Anal. Chem.* 1988, 60, 2711.

22. Hung, H.M.; and Hoffmann, M.R. *J. Phys. Chem. A* 1999, 103, 2734.

23. Chendke, P.K.; and Fogler, H.S. *J. Phys. Chem.* 1983, 87, 1362.

Conclusions

The study has shown that CMCD/Fe^{2+}/hydrophobic compound ternary complexes which have not been reported before are formed in aqueous solution. The binding ratio between CMCD and selected hydrophobic compound is 1:1 and that between CMCD and Fe^{2+} is predominantly 1:1 as well. The ternary complex likely brings the reaction catalyst closer to the pollutant molecules and thus enhances the Fenton degradation efficiency. However, in the cases where the pollutant has coordination ability to Fe^{2+}, the presence of CMCD competes with the pollutant for Fe^{2+} binding and results in reduced degradation. This result illustrates the potential of CMCD in protecting certain classes of compounds from being degraded or attacked. The protection effect may be useful in organic synthesis to keep certain compounds or certain groups of a compound intact. On the other hand, effective formation of metal-cyclodextrin-guest complexes can be used to selectively react the guest molecule with hydroxyl radical. In general, the role the cyclodextrin plays depends on the properties and interactions of all species coexisting in the solution. Therefore thorough study of the solution must be conducted in order to make a good prediction of the effect of cyclodextrin.

From similar investigation of HPCD, SCD, βCD and αCD, it was found that HPCD, βCD and αCD could bind with hydrophobic pollutants, but their binding ability to Fe^{2+} was small. SCD, on the other hand, had a relatively strong binding ability to Fe^{2+}, but it could not encapsulate the pollutant molecules due to the bulky substitution groups located at the entrance of the cavity.

In comparison, the binding ability of the five cyclodextrins to the hydrophobic compounds under investigation is in the order (from strongest to weakest): βCD > CMCD ≅

HPCD > αCD > SCD. Their binding ability to Fe^{2+} is in the order (from strongest to weakest): SCD ≅ CMCD > βCD ≅ HPCD ≅ αCD. To enhance Fenton degradation of those pollutants with little binding potential to Fe^{2+}, strong binding of both pollutant molecules and Fe^{2+} is required.

Therefore, natural cyclodextrins would not greatly enhance the Fenton degradation with their poor binding ability to Fe^{2+}. The cyclodextrins with electron rich groups such as the carboxymethyl group have the potential to increase Fenton reaction efficiency. However, the substitution should not be too extensive and the substituted group should not be too bulky. From the results obtained in this study, CMCD is expected to give the biggest enhancement for the selected pollutants in Fenton degradation.

In the study of sonochemical degradation of phenol, it was found that hydroxyl radical oxidation is a very important degradation pathway. Addition of small amounts of CCl_4 or C_6F_{14} can increase the sonolysis efficiency. The enhancement is due to the fact that CCl_4 or C_6F_{14} scavenge hydrogen atoms produced from dissociation of water. Therefore the water recombination reaction is inhibited and more hydroxyl radical becomes available for the degradation. Since the water recombination reaction mainly takes place in the bubble phase, the hydrogen atom scavenging must also occur in the bubble phase (or at least near the bubble phase) to give the enhancement. The idea of scavenging hydrogen atoms to increase concentration of hydroxyl radical could be transformed to other fields and benefit the processes where hydroxyl radical is an important intermediate.

VITA

Weixi Zheng was born in China on February 5th, 1973. She was grown up in Beijing. In 1991, she enrolled in Beijing Normal University and four years later she obtained her bachelor degree in chemistry. After graduation, she continued her graduate study in Fujian Institute of Research on the Structure of Matter, Chinese Academy of Sciences. In 1998, she obtained her master degree in physical chemistry. In 1999, she was accepted as a PhD student by the department of chemistry in University of New Orleans and came to US. Later that year, she joined Dr. Matthew A. Tarr's group and conducted research in the field of environmental chemistry under the guidance of Dr. Tarr.